2013

Computational Model of Pitting Corrosion

Muhammad Ibrahim Israr Bin
Virginia Commonwealth University

School of Engineering
Virginia Commonwealth University

This is to certify that the thesis prepared by Israr Bin Muhammad Ibrahim entitled COMPUTATIONAL MODEL OF PITTING CORROSION has been approved by his committee as satisfactory completion of the thesis requirement for the degree of Master of Science in Mechanical Engineering.

Ramana Pidaparti, Ph.D., Committee Chair, School of Engineering

Brian Hinderliter, Ph.D., Committee Member, School of Engineering

Vojislav Kecman, Ph.D., Committee Member, School of Engineering

Gary C. Tepper, Ph.D., Department Chair, Mechanical Engineering, School of Engineering

Rosalyn Hobson, Ph.D., Ph.D., Associate Dean of Graduate Studies, School of Engineering

Barbara D. Boyan, Ph.D., Dean, School of Engineering

F. Douglas Boudinot, Ph.D., Dean, School of Graduates Studies

Date

Computational Model of Pitting Corrosion

A thesis submitted in partial fulfillment of the requirements for the degree of Master of Science in Mechanical Engineering at Virginia Commonwealth University.

by

Israr B. M. Ibrahim

Bachelor of Engineering in Mechanical Engineering
Syiah Kuala University, July 2009

Director: Ramana M. Pidaparti, Ph.D.
Professor, Department of Mechanical and Nuclear Engineering

Virginia Commonwealth University
Richmond, Virginia
May, 2013

Acknowledgement

I would like to thank Dr Ramana Pidaparti for his support, advice and guidance since the beginning of my master program. His direction and encouragement has greatly helped me to take a good direction in my master program. His thoughts and ideas have given me new useful insights in research topics that I am interested in.

Next, I would like to thank Dr Brian Hinderliter for his contribution and advice for the completion of my thesis, and Dr Vojislav Kecman and late Dr David Primeaux for opening my mind for the first time to the topic of Machine Learning that I had been interested since a long time and has helped me completing my thesis. I'd also thank all my MNE teachers during my master program, and friends that have helped me with discussions and having fun. In this regard, I'd like to especially thank Trenicka Rolle, Jae Hwan Lee, Le Yang, Matthew Burnett, Ahmad Saleh and Phil Card.

Finally, I dedicate this thesis to my parents that kept encouraging me during these two years, my sister and the Pante Geulima family in my country, Indonesia. Distance don't matter for family's love to reach out for me.

Table of Contents

List Of Tables

List Of Figures

Abstract

Pitting corrosion is a form of highly localized corrosion that can lead to crack and failure of a structure. Study on pitting corrosion is necessary in order to predict and prevent the risk of failure of structure susceptible to corrosion. In this thesis, a combination of Cellular Automata (CA) and Boundary Element Method (BEM) was developed to simulate pitting corrosion growth under certain environment. It is assumed that pitting corrosion can be simplified to electrochemical corrosion cell. The distribution of potential around this corrosion cell can then be simulated by BEM. This distribution potential represents cathodic and anodic reactions around the corrosion cell. A CA model was developed that uses transition rules reflecting mechanism of pitting corrosion. The CA model has two types of cell states, one reflecting BEM simulation results and the other reflecting the status of corrosion cell (anode, cathode, and passive metal's surface). For every CA iteration, the CA decides the state of the corrosion cells (the location and size of anode, cathode) while BEM simulate the level of electrochemical activity at discrete location on the surface (represented by potential distribution). In order to demonstrate the methodology, a simple case of rectangular corrosion cell with varied dimensions and under different polarization functions is considered. Results show certain shapes tend to grow at certain type environment and these pits are comparable to commonly observed pit shapes. In addition, stress analysis was carried out to investigate the severity of corrosion pits of varying shapes and sizes. Results show that certain pits induced highly varying stress concentration as it grows over time, while others have more steady increase of stress concentration.

Chapter 1 Introduction

1.1. Motivation

Corrosion is defined as degradation of materials by chemical reaction with its environment. It reduces strength of the materials, as well as degrading the appearance. Corrosion can lead to disastrous failures. Among the most well-known ones are described in [1], including the leak of oil pipeline at Prudhoe Bay in 2006. The loss caused by corrosion is estimated as 4% of the gross national product [2], including direct and indirect losses. A particular occurrence of corrosion produces small holes or pits on the metal surfaces. It occurs on metals that are supposed to resist corrosion by having protective layer on metallic surface. But failure to maintain this layer instead lead to localized process of corrosion that dig into the depth of metals, and form pits (and hence it is called pitting corrosion). These pits then act as defects on metallic surface and become stress raisers. It has been reported that these pits are the initiation location of stress corrosion and fatigue crack [2-9]. Pits can assume various shapes and densities. Shapes and densities are two parameters that are used to measure the severity of pitting corrosion [10]. The shapes and densities consequently also affect the stress distribution on metallic surface [10-17]. Analysis of this stress distribution is necessary toward understanding the mechanism and prediction of failures that start with crack initiated in pits.

Pitting corrosion occurs electrochemically, like most metallic corrosion [18]. This means electrochemical reactions exist when pitting corrosion occurs [19]. Electrochemical corrosion simulations have been carried out in many studies, such as

[20 – 25]. In this study it is assumed that electrochemical corrosion is the main driving force in pitting corrosion process, and thus pitting growth. Pitting corrosion is assumed to be a particular electrochemical corrosion problem. In this study, pit initiation is ignored. This study is based on electrostatic potential distribution that occurs on metallic surface once electrochemical reactions of corrosion are established, and the growth of pits is stable. Because electrochemical reactions take main role, the environmental condition is incorporated in the model as polarization of potential. Simulation is used to predict the shapes and densities of pits on a specified range of metallic surface. After the shapes and densities are obtained, stress analysis can be done to get stress distribution and concentration factor that are necessary in failure analysis.

1.2. Thesis Objectives

The objective of this study is to develop a mean to predict pitting corrosion shape under different environmental condition through simulation. The method used is CA. Analysis of pitting shape growth and the effects of shape under loading condition is also considered.

The CA is a discrete-time based computational tool that has been used in various fields. CA offers broad range of way to do discrete-time simulation and usually is based on normalization of space and other parameters. In this study, in order to other kinds of information are used to drive the behavior of CA. Assuming the pitting corrosion is mainly based on electrochemical reaction, the distribution of potential over the surface of pitting corrosion is simulated by using Boundary Element Method (BEM). The BEM only uses information on the surface to do calculation and thus suitable for corrosion problem, while CA can be set to only take into consideration the boundary part of the

system. The CA-based simulation tool for pitting cavity shape prediction is developed by using combination of these two methods.

The next important thing in analyzing pitting corrosion is the loading that the area experiencing. In this study, the BEM for stress analysis is used and compared to the result from FEM.

1.3. Thesis Overview

Thesis is outlined as follow. Chapter 2 provides the theory of corrosion mechanism in general, and particularly pitting corrosion.

Chapter 3 describes the Boundary Element Method (BEM) modeling of electrochemical corrosion, the Cellular Automata (CA), and application of the CA to pitting corrosion problem that is assisted by BEM simulation of corrosion. Study cases of pitting corrosion and results of CA simulation are also given. Finally discussion on results and suggestion are given at the end of the chapter.

Chapter 4 discusses the stress analysis of pitting corrosion. Some pitting shapes modeled after results in previous chapter are carried out into stress analysis.

Chapter 6 discusses recommendation and future works.

Chapter 2 Corrosion

1.1. Metal Corrosion

1.1.1. Electrochemistry of Corrosion

Corrosion is an inevitable occurrence in metal, since metal tends to be in state of higher energy level. Processed metals has been injected an amount of energy to make it tends to react with substances in the environment around it in order to release the energy. The mechanism of corrosion in metals is mainly electrochemical. Corroding metals can be viewed as a electrochemical battery (or also called as corrosion cell). There are two reactions in a corrosion cell, cathodic and anodic reaction:

Oxidation: $M \longrightarrow M^{n+} + ne$

Reduction: $nX^{+} + ne^{-} \longrightarrow X_n$

Oxidation reaction removes electron from electrode and thus reducing its mass. The electrode where oxidation occurs is called anode. The part of electrode experiencing reduction reaction is called cathode. In a corrosion cell, the corroded metal is under oxidation, or anodic reaction. The area under oxidation reaction receives electron from anode and does not experience mass reduction. Thus corrosion occurs if there is electron and ionic flows between two areas of metal. Corrosion can occur if two metals that provide enough potential differences coupled in an electrolyte, or when different area on a metal have enough potential difference that allow the exchange of ions and electrons. The latter is called self-corrosion.

An example of corrosion cell formed in self-corrosion is illustrated in Figure 2.1. A body of metal could form potential difference on its surface because of non-uniformity of properties on its surface. The metal itself is a conductor and hence allowing the flow of electrons. When the surface of metal is in contact with electrolyte, the electrochemical reactions forming electrochemical cell are able to take place. This situation can be found everywhere, such as when metallic fence rusting. In the corrosion of reinforcing bar, the water film serves as electrolyte.

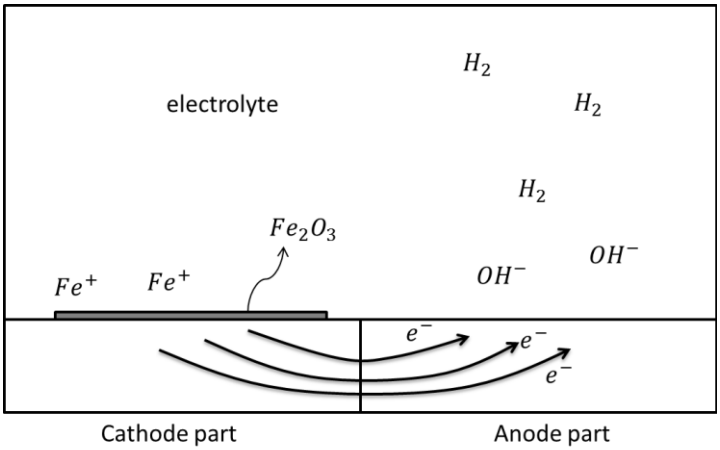

Figure 2.1: A corrosion cell formed between two metals

The electrochemical process can results in several forms of corrosion in metallic surface. Generally, corrosion occurs uniformly on a metal and can easily be found in daily life, such as rusting of fences or copper statue. The product of corrosion, which is the rust, covers the surface of fences. It makes the fences look less pleasant. Other kinds of corrosion occur locally, such as pitting and crevice corrosion.

Corrosion can be divided into five generalized categories [10], which are: general corrosion, localized corrosion, metallurgically-assisted corrosion, mechanically-assisted

corrosion and environmentally induced corrosion. Under the term general corrosion is corrosion that reduces the thickness of material uniformly. The rusting fence is an example. The rusting fences is also an example of what called as atmospheric corrosion, since the electrolyte that make the ionic exchange possible is substance in air, such as oxygen and water molecules. The thinning of metallic surface can also occur by galvanic coupling of two dissimilar metals, which happen either intentionally or unintentionally. An example of galvanic coupling that can be found in daily life is the corrosion of bolt which electrochemically coupled with the component that it is tied to. The bolt is the metal that release electron here and thus corroded. Due to this fact, some bolts are designed to protect the component by selecting the less corrosion-resistant materials for the bolt and thus making it as the corroded metal. Similar technique is used in corrosion protection method called sacrificial anode that is well known in corrosion protection for coastal structure.

General corrosion leads to uniformly reduction of mass such that it is thinning the metallic surface in a uniform manner. On the other hand, localized corrosion only removes some specific part of metallic surface, and thus, although some part of metallic surface looks not corroded, some parts of metal are undergoing corrosion process. When two metallic components form a gap between them, the area could form a corrosion cell that has higher rate of corrosion than the possible uniform self-corrosion on the metallic surfaces. This leads to corrosion that attacks only that particular gap area. This corrosion that is induced by crevice or gap is named crevice corrosion. Crack and defects on metallic surface can also serve as location of localized attack. Another example of localized corrosion happens on metals that form protective layer on their

surface, such as stainless steel and aluminum. This protective layer is called passive layer. The passive layer provide barrier between metallic surface and electrolyte that could be in contact with metallic surface, and hence preventing electrochemical reactions to occur on the surface. But when this layer breaks up, and electrolyte comes in contact with the metallic surface, electrochemical reactions may start to occur. Once corrosion cell is formed, the resulting anodic reaction is highly localized that prefer to go in the direction of the depth of metal, forming small holes or pits, because the surrounding area is protected by passive layer. This is called pitting corrosion.

Some corrosion is induced by organic substance or microbes and bacteria. Organic substance that coated metallic surface may fail and start localized attack that results in filiform pattern, thus called filiform corrosion. Some species of bacteria inhabiting metallic surface induce chemical reaction that harms metal. Corrosion carried out by microbes is commonly local in nature.

Metallurgical features of metals can also induce corrosion. For example, the difference of potential between grain boundary and grain could initiate current transfer between the two areas and start what is called intergranular corrosion. Other factor that could cause corrosion is mechanical phenomena such as wear, erosion or fatigue. For example, erosion and wear can remove metallic protective layer such as that on stainless steel surface and make the metal susceptible to corrosion reaction. The combination of specific environmental condition and stress can cause metals that are susceptible to corrosion to initiate crack that is associated with corrosion, called Stress Corrosion Cracking. Pitting that is formed by localized corrosion can act as stress raiser which can be the location of crack initiation in SCC.

All of those corrosion mechanics mentioned above generally involve common mechanism despite some other phenomena such as loading, organic materials or mechanical process such as wear, that is electrochemical reaction between two metals or two parts of a metal. The next section will explain fundamental aspect of electrochemical reaction in related to corrosion in metals.

1.1.2. Rate of Corrosion

Faraday's law relates the charge passes across electrode-electrolyte interface with moles of substance reacting as:

$$Q = n.F.n_i \tag{2.1}$$

where, *F* is Faraday Constant (96,485 C/mol), *n* is the number of electron involved in the reaction, and n_i is moles of substance. The derivative of equation (2.1) with respect to time represents the rate of current exchange in the reaction:

$$I = n.F.\frac{\mathrm{d}n_i}{\mathrm{d}t} \tag{2.2}$$

where *I* is electric current passes across the electrode and electrolyte (Ampere). This expression is commonly used in calculating the rate of corrosion and measurement of current exchanged during corrosion reaction is used to predict the rate of thinning on uniform corrosion.

1.1.3. The Electrode Potential

The current exchange between two electrodes is possible because the difference of electric potential of the electrode, or the electrode potential. In an external circuit, the movement of electrons is from the most negative potential to the most positive, thus the

current is assigned as the opposite direction. A voltmeter is used to measure the potential difference between two electrodes. Because only relative difference between two electrodes can be measured, standard electrodes are used to determine the associated electrode potential for other metals. The most common standard electrode in laboratory is the Standard Hydrogen Electrode (SHE).

Table 1.1 lists examples of electrode potential of some metals based on its reduction reaction.

Table 1.1. Electrode potential of some metals versus SHE

Half Reaction	E (mV)
$Au^+ + e^- \rightarrow Au$	1.68
$Cu^{2+} + 2e^- \rightarrow Cu$	0.3402
$Fe^{2+} + 2e^- \rightarrow Fe$	-0.409
$2H^+ + 2e^- \rightarrow H_2$	0.00
$Mg^{2+} + 2e^- \rightarrow Mg$	-2.375
$Zn^{2+} + 2e^- \rightarrow Zn$	-0.7628

In the table, because the SHE is used, the hydrogen electrode has zero potential. The electrode potentials only show which direction current will flow, thus given the value of electrode potentials of two coupled metals, the anode and cathode of the electrochemical coupling can be determined. For example, it can be seen that iron has lower potential than copper, and thus electron will move from iron to copper and iron acts as anode and will be corroded.

1.1.4. Polarization of Potential

When two metals coupled electrochemically, the electrode potential on the surface of metals changed as the results of various equilibrium potentials of all the anodic and cathodic reactions involved [26]. This change of electrode potential is called

polarization. The anodic polarization refers to the change of potential into more positive value, while cathodic polarization is the change in more negative.

The polarization of electrochemical cell is the sum of activation polarization, concentration polarization and ohmic drop. The activation polarization is related to charge transfer in between electrodes. For example, the rate of electron and ion transfer in a reaction can be varied, and resulting in shift of electrode potential on the surface. The concentration polarization is caused by concentration gradient on the surface. When electrochemical reactions occur, the ions in electrolyte can be depleted such that it forms gradient of concentration. This makes the rate of currents flow varies across the surface. The last component which is ohmic drop is related to resistivity of electrolyte involved.

The polarization of potential occurs on both electrodes in electrochemical cell, but both polarizations will reach same point. The potential at this point is called corrosion potential. By plotting polarization of potential against current at which polarization occurs, the behavior of a electrochemical cell can be further revealed. Since as explained previously that current density represents the rate of reactions involved in corrosion, the current at corrosion potential represents the rate of anodic and cathodic reactions of the corrosion cell, and as such is called corrosion current. This corrosion current is commonly taken as corrosion rate of the whole corrosion cell in practice.

1.2. Pitting Corrosion

Pitting corrosion occurs on a metal that form passive layer that prevent the metal surface to interact chemically with its environment. This layer is supposed to make the

metal resistant to corrosion. However, once the passive layer breaks down, a particular form of corrosion process occurs instead. The corrosion reaction dig into the depth of metal and very localized in nature. The process forms small holes or pits on metal's surface. Hence, it is called pitting corrosion. Figure 2.2 illustrate the mechanism of pitting growth corrosion.

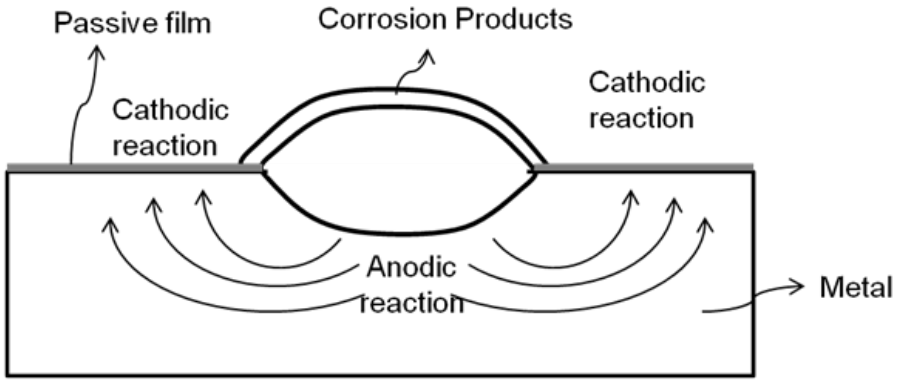

Figure 2.2: A simple representation of pitting corrosion

The mechanism of pitting corrosion phenomenon involves electrochemical corrosion as explained in previous chapter. Once an area of passive layer breaks, a portion of metallic surface is exposed to the environment. If the environment is enough to drive the current exchange, electrochemical reactions occur. Electrons move from the exposed area to its surrounding. However, the surrounding area is highly passive. In case where oxygen reduction on passive film is dominant, the cathodic area will have increased pH and more stabilized passivity [27]. At the same time, the corrosion product gather on the top of pit that already formed as illustrated in Figure 2.2. The corrosion product covers the pit and creates another environment between pit and its surrounding area. This environment is of lower pH and thus increasing corrosion rate. The high contrast between the passive area of the surface and active area inside pit is the cause

of localized attack that tends to go in the direction of depth of metal rather than attacking surface of metal uniformly. This also means that measurement of thickness reduction or representing corrosion rate as mm per year becomes less useful, as pitting corrosion only takes small amount of metallic materials. The danger of pitting corrosion is the defects formed on the metallic body in the form of pits. These pits are stress raisers and reduce the strength of metallic component, thus reducing the age of service. Leaks can also be problem caused by pitting that digs too deep into the metallic component.

The breakdown of passive layer can be caused by different mechanisms and factors. The flaws in coating metallic surface can be the initiation of pit, as well as pore in coating. Outside pre-existing flaws, passive layer is also theorized to break by three mechanisms; penetration of corrosive agent such as chloride ions through the film, local adsorption of corrosive agent and film rupture caused by internal stress in metals. After passive layer breaks down, and pit initiates, the pit may or may not be a stable pit. This state is called metastable pit. Metastable pits formed below a characteristic potential called pitting potential. Once formed, metastable pits can undergo repassivation and thus pitting growth stops. Once potential of pits are above pitting potential, metastable pits continue to grow and form larger stable pits. In this study, these early processes of pitting initiation are not considered. The modeling only considers pit growth after stable pit growth state is reached.

The stable pits growth depends on type of metals, electrolyte and pit-bottom potential (since it is highly localized). As a consequent of highly localized behavior of pitting corrosion, pits take various shapes. The most common pitting shape is

hemispherical shape. Figure 1 gives some examples of common experimentally observed pitting shape, adapted from [10]. The shape of pit depends on condition of the metals and its environment.

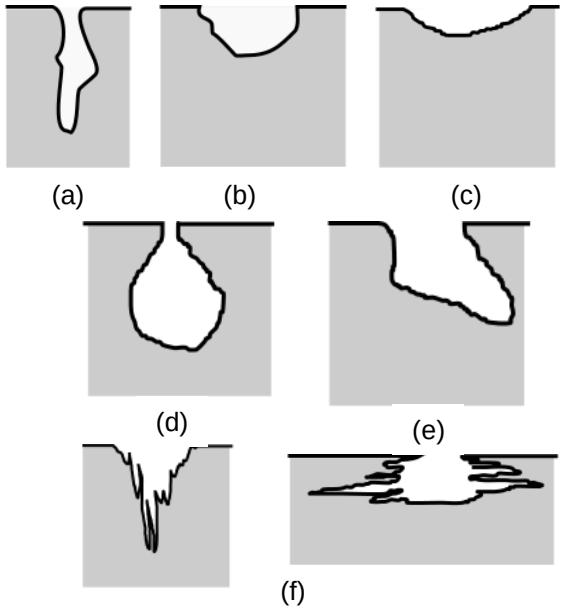

Figure 2.3: Some examples of common experimentally observed pitting shape, adapted from [3], (a) Narrow and deep, (b) Elliptical, (c) wide and shallow, (d) subsurface, (e) undercutting, (f) shapes influenced by microstructural orientation

Pitting corrosion occurs in three steps: initiation, metastable growth, stable growth and repassivation or pit death [10] [28]. The initiation of pits has been treated both as probabilistic [29-35] and mechanistic by considering its electrochemical aspects [36-39] in various study. Some models only consider some aspects of pitting damage such as pit density [33], or pit width and depth [34-35]. Modeling using Cellular Automata (CA) has been done to predict various aspects of pitting corrosion [40-44]. CA is a good tool to use since pitting corrosion can be considered probabilistic phenomenon. However, CA application to pitting corrosion needs improvement since it

either lacks correlation to actual dimension or environmental parameters. Since pitting corrosion involves electrochemical reactions, an attempt to model it using boundary element has been done [45]. In this thesis, pitting corrosion is modeled by assuming its initiation and growth as probabilistic. CA was used to model the initiation and growth of pits. However, to correlate the CA parameters to actual dimensions and environmental parameters, another method called the Boundary Element Method (BEM) was used to model the distribution of currents that flow in a corrosion system. Chapter 3 explains the approach in detail.

Chapter 3 Modeling Approach of Pitting Corrosion

3.1. Electrochemical Corrosion

Previous chapter has described that electrochemical corrosion is driven by electrochemical reaction, caused by potential difference. Therefore, many researchers have suggested [46 – 48] that assuming the electrolyte is homogeneous, potential field around corrosion cell is governed by Laplace's equation. The modeling is illustrated in Figure 3.1.

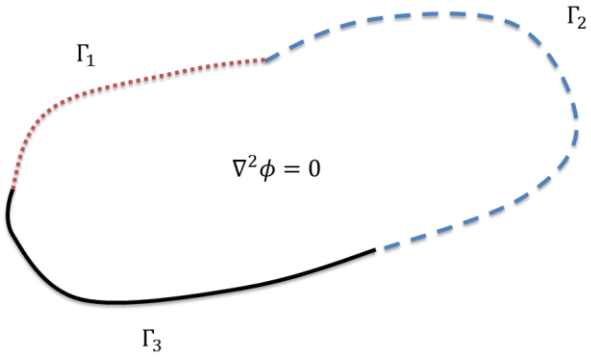

Figure 3.1 A corrosion cell with arbitrary shape, consisted of three types of boundaries. The domain is governed by Laplace's equation

Figure 3.1 shows an arbitrarily shaped corrosion cell, with three types of boundary condition. Boundary Γ_1 and Γ_2 are electrode's surfaces, which are anode and cathode respectively. On this boundary, polarization of potential due to chemical activity happens. At boundary Γ_3, the current density is zero. Therefore the system can be written as,

$$\nabla^2\phi = \frac{\partial^2\phi}{\partial x^2} + \frac{\partial^2\phi}{\partial y^2} + \frac{\partial^2\phi}{\partial z^2} = 0 \qquad (3.1)$$

with boundary conditions,

$\phi = f_1(i)$ at Γ_1 (3.2)

$\phi = f_2(i)$ at Γ_2 (3.3)

$i = 0$ at Γ_3 (3.4)

where ϕ is electrostatic potential, f_1 and f_2 are experimentally determined functions that account for polarization phenomenon that occurs on the surface, and i is current density. The current density is defined as,

$$i = \frac{\partial \phi}{\partial \mathbf{n}} \tag{3.5}$$

where $\mathbf{n}$ is vector normal to direction of ϕ.

The Boundary Element Method (BEM) can be used solve the system governed by Laplace's equation [46-47]. However, boundary conditions (3.2) and (3.3) results in more unknowns in the typical BEM matrix, since values of both potential and current density are not known. To solve the final equation of BEM, a Newton-Raphson scheme as devised by [46] was implemented. The BEM then can be used to obtain potential distribution over a corrosion cell with arbitrary geometry by solving the above Laplace's equation with the above boundary conditions. As an example, a case studied in [46] was considered. The case is illustrated in Figure 3.2.

A piece of SUS304 stainless steel and FC20 gray cast iron are immersed in NaCl solution. The two pieces form a corrosion cell. Gray cast iron as anode corrodes. The polarization of this corrosion cell was measured as in [48] and approximated as [46],

Cathodic Polarization: $\phi_c = -48\ \mathrm{Log}^2(i) - 137\ \mathrm{Log}\ (i) - 372$ (3.6)

Anodic Polarization: $\phi_a = 18\ \mathrm{Log}^2(i) + 35\ \mathrm{Log}\ (i) - 683$ (3.7)

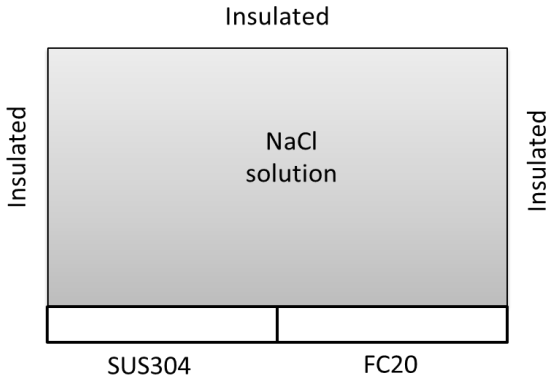

Figure 3.2 Example of a simple corrosion cell

where ϕ is electrostatic potential and i is current density. The units are adjusted accordingly. Figure 3.3 shows the approximated polarization curve using equation (3.5) and (3.6).

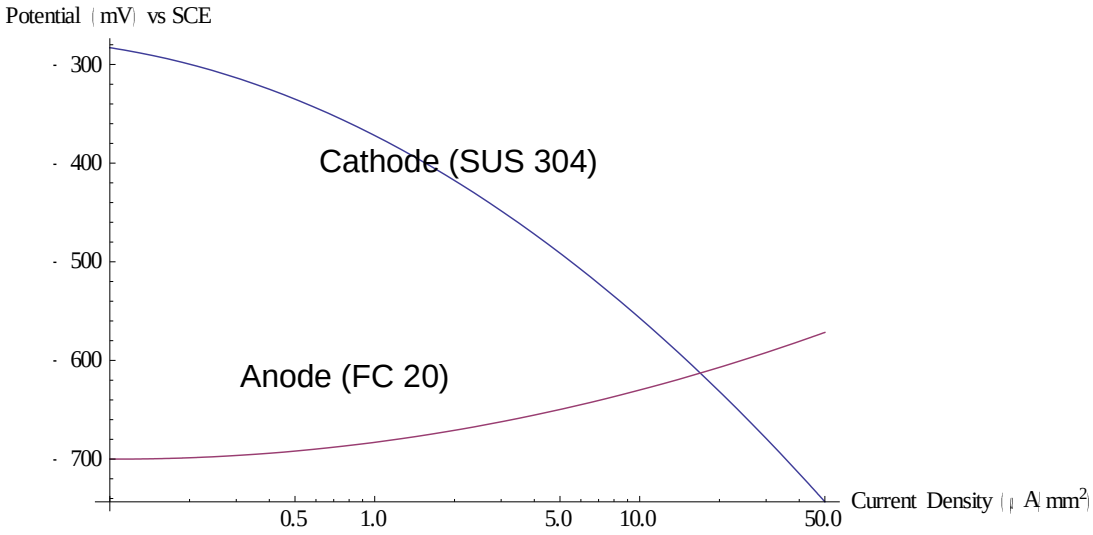

Figure 3.3: Approximation of polarization of the corrosion cell in Figure 3.2, adopted from [18]

The experimental corrosion cell as in Figure 3.2 is modeled for BEM simulation as in Figure 3.4. The model has 80 elements. The cathode and anode elements were assigned with boundary conditions (3.2) and (3.3), with equations (3.5) and (3.6) as the function. The rest of the elements were assigned as insulation, as in equation (3.4). The purpose of the simulation is to predict the distribution of potential over the domain.

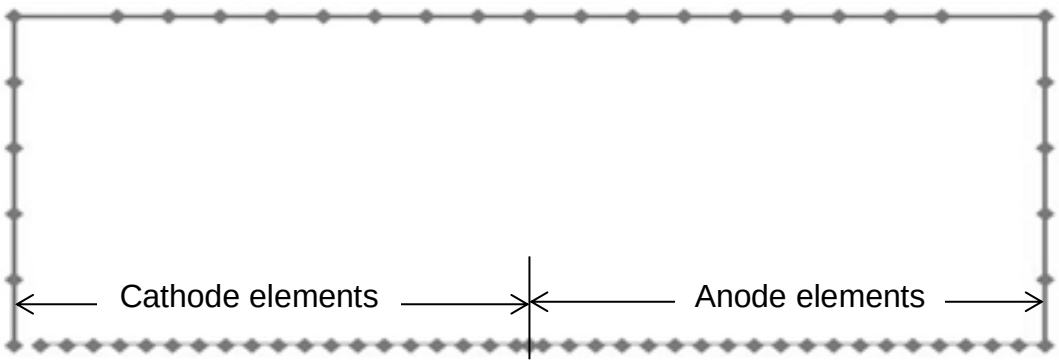

Figure 3.4: BEM model for corrosion cell in Figure 3.2

Among important things in analyzing corrosion system is the distribution of potential and current density on metal's surface as it will provide the behavior of corrosion cell and its corrosion rate. The distribution of potential is also what is needed in this study. The results of this simulation are shown in Figure 3.5.

The results have been compared with experimental results in [46] and show good comparison. In this example, it has been shown that a corrosion cell can be analyzed by obtaining potential and current density distribution.

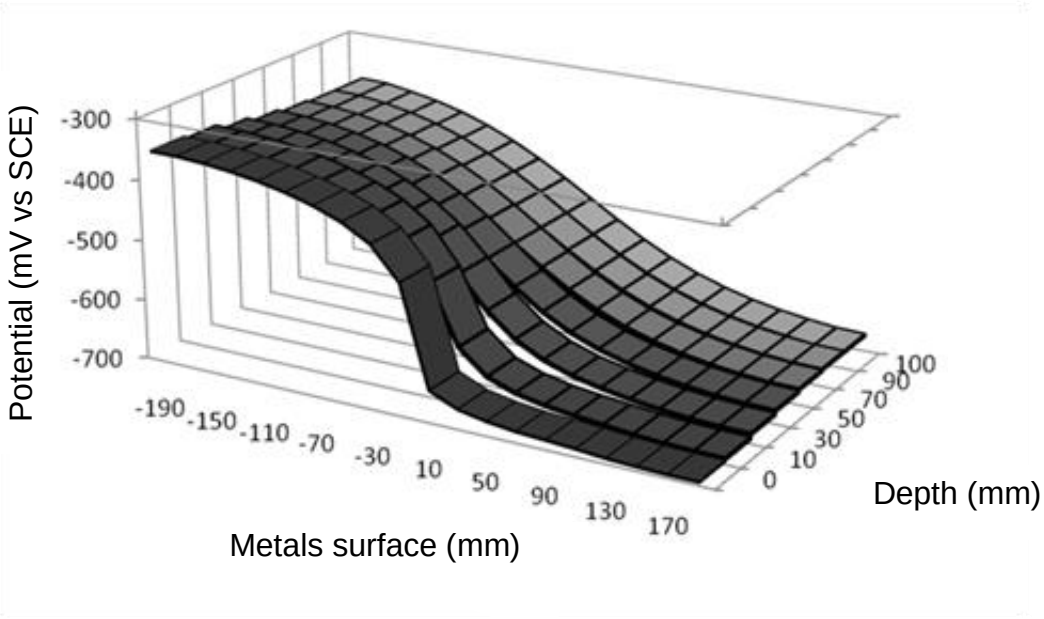

Figure 3.5: Potential distribution of corrosion cell as in Figure 3.2

In this study, it is assumed that pitting corrosion is mainly driven by electrochemical reaction, thus the behavior of the corrosion cell formed when pit exist and actively corrode may be simulated by the same way of the above example. The BEM is used to generate the potential distribution over the metal surface undergoes pitting corrosion once the corroding part and cathodic part are given. In pitting corrosion, the corroding part is the area inside pit itself, while the cathodic part is the area surrounding it. While the cathodic part is protected by supply of currents from the corroding part, the surface of cathodic part is basically susceptible to corrosion after the passive layer is broken and it is exposed to environment, as explained in previous section. The mechanism of passive layer breakdown is not incorporated here, however the initiation of new pits around another pit is simulated by the changing of cathodic-anodic part of the area after a discrete time by Cellular Automata, which will be explained in the next section.

3.2. Cellular Automata

Cellular Automata (CA) is a model that consists of a lattice of discrete, identical finite-state machines that work according to same sets of transition rules [49]. Cells can be in any shape, but the most common shape is square. Each cell has its own state, which is binary state in early development, but can be represented in real numbers as well to allow modeling of physical phenomena such as heat transfer. The state of each cell synchronously evolve in discrete manner, that is from initial time step (at $t = 0$) to specified time step ($t = n + 1$, where n is integer). The evolution of the state of the cell is dictated by transition rules or functions that take into account the cell's current state and its neighboring cell's. The transition rules are the same for all cells and can be deterministic or probabilistic [50]. So the evolution of the lattice is defined by the arrangement of the cells, the cell's state and transition rules. For each discrete time step, the lattice of cells will show development of pattern resulting from cell's state.

The arrangement of cells can take k −dimension [50]. Two dimensional CA has been used to model various dynamical systems, the most common referred ones are modeling heat transfer and diffusion [50] [51]. The transition rules consider the cell's state as well as the neighboring cell's state. The most common neighboring cell's schemes used are Moore and Neumann, as shown in Figure 3.6.

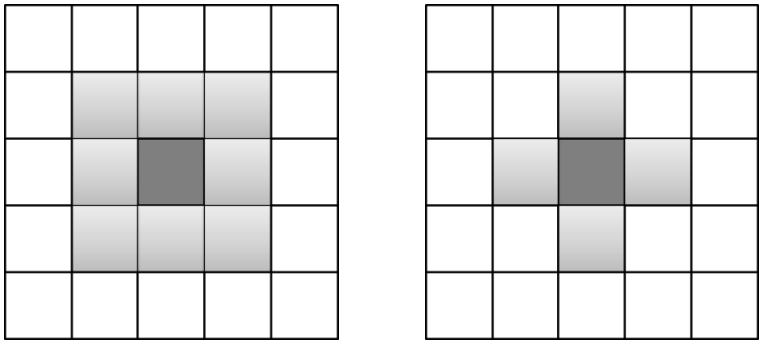

(a) (b)

Figure 3.6: Examples of neighborhood used in CA, (a) Moore, (b) Neumann

Transition rules can take various forms; the fundamental feature is the alteration of cell's state based on its own state and the neighboring cell's. One way to express the transition rules is the summation of cell's state involved,

$$S_{i,t+1} = S_{i,t} + \sum_{k=1}^{N} S_{k,t} \tag{3.7}$$

where $S_{i,t}$ is cell i's state at time t, and N is the number of neighbors.

At the boundary, discontinuity appears. There are three common way to deal with transition of the boundary cells. One can set the boundary cells at one extreme to be the neighbor of the other extreme (such as, a cell on far right is a neighbor to a cell in the same row at the far left). This is called periodic boundary condition. The second method and is called reflective boundary condition is to set the cells at the boundary as having the same state as the cells adjacent to them. The third is fixed boundary condition where the boundary cells have a fixed state. Fixed boundary condition is used in modeling of physical phenomena such as heat transfer.

3.2.1. Applications of CA for Pitting Corrosion

Previous application of CA on pitting corrosion in [40] considers a growth of pit on the surface of metal in relation to pH, corrosive agent concentration and potential developed on the surface. The transition rule of the CA involves summation of cell's state. The cell's state is represented as real numbers from zero to one, representing transition from state of "not corroded" (zero) to "fully corroded" (one). In this study, the objective is to allow for simulation of pitting cavity growth given the environmental condition. In order to take into account the environmental condition, the BEM simulation of electrochemical corrosion is brought into CA. The pitting corrosion model is CA-based where time is discretely taken into account, but the state of cell is represented by simulation of electrochemical corrosion by BEM. The transition rule then is associated by summation of this cell's state. However, pitting corrosion can be seen as having probabilistic nature macroscopically. Hence the transition rule will be based on probability of each cell to continue to corrode based on its state value.

Figure 3.7 shows the structure of the cells. Each cell has two layer of state. One is based on the BEM simulation results called State I, and another represents the status of the cell, as a cathode, anode or the body of metal (non-electrode metal) called State II. The latter type of state is symbolic in nature so it is represented by integer 1, 2 and 0 respectively. This is similar to the state of cells of basic CA as explained in previous section. However, the evolution of these second layers of states is not based on its value, but is driven by the State I. So the results of BEM simulation are used to drive the cell's evolution.

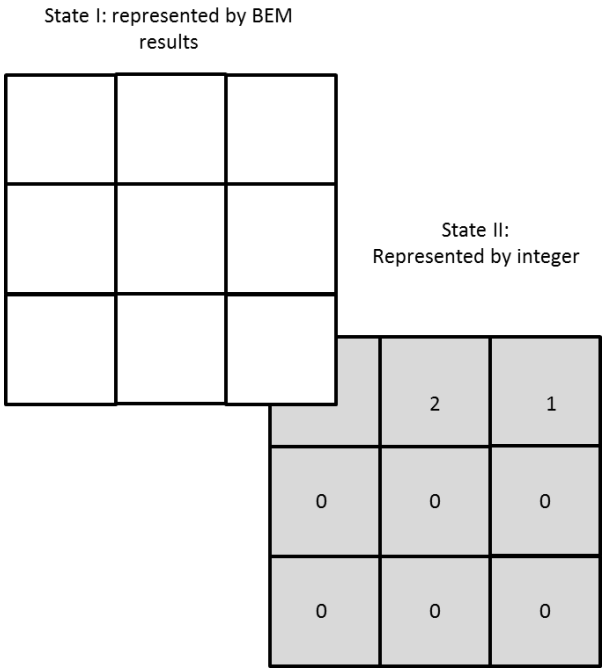

Figure 3.7: The cell's state structure. Each square is a cell.

The surface of metal starts as passive body. Once pitting corrosion initiated, cathode and anode start to form on the surface. The simulation is done once pitting corrosion starts and small pit has started growing in stable manner. Cells that have to be taken under consideration are only cells that represent surface of metals. These cells are divided into cathode and anode cells. For every time step, the transition rules that take place can be summarized as following,

1. The anode cells will always be removed (corroded and converted into corrosion product). If there is any non-electrode cell share boundary with anode cells, then the states of anode cell are transferred into the cell.

2. Cathode and non-electrode cells have chance to change state into anode. The chance is calculated as follow,

Cathode $$S_{i+1} = \frac{\sum_{k,l=1}^{N} S_{i_{k,l}}}{m \times E_{corr} \times N_{cathode}} \quad (3.8)$$

Anode $$S_{i+1} = \frac{m \times E_{corr}}{\sum_{k,l=1}^{N} S_{i_{k,l}}} \quad (3.9)$$

where,

S = Potential value from BEM simulation (V)

E_{corr} = Corrosion potential of cathode or anode (V)

m = number of electrode neighbors

$N\_cathode$ = number of cathode cells

k, l = index of cell and its neighbors

The term $N\_cathode$ reflects the highly passive nature of cathode area and represent the mechanism of breakdown of passive film after a pit initiates. Once pit grows, the cathode area reduces and increases the chance of the area to start corroded and grow pit.

In this study, the discretization of BEM is taken directly to represent the cells. The boundary elements of BEM are taken as boundary of individual cells, and the value that each element holds is taken as State I in CA.

3.3. Example Case

The CA scheme as explained in previous section is now applied for a simple case. This case only considers a small localized site on which a first pitting already

initiated. When pit initiates, it forms a region of cathode and anode as already explained. The anode area is smaller than the cathode ones. It is assumed that the current exchange between anode and cathode takes place uniformly in and on the system. So the corrosion cell formed can be modeled as two dimensional rectangular area as shown in Figure 3.8.

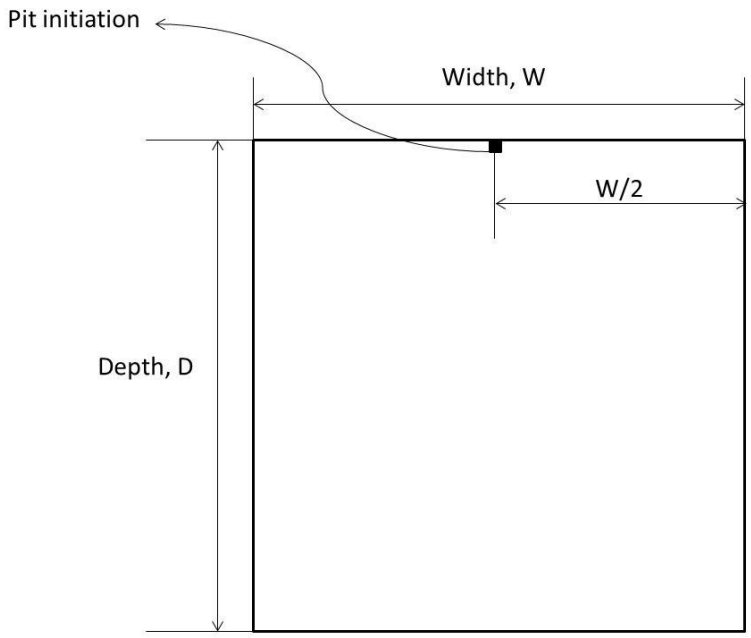

Figure 3.8: Model of pitting corrosion simulation, unit is in mm.

The region of the corrosion cell (the rectangular model) is formed by initiation of pitting. By assuming the flow of electrons and ions are uniform over the corrosion cell, the pit initiation location consequently will be on the middle of the surface of the region. The simulation was done with different polarization functions that represent the corrosion cell behavior in specific environment, and different width, W and depth, D, of the region. The width and depth of the region determine the area that currents will have to travel once corrosion cell is formed. The dimensions are varied into 5x5, 10x10 and

20x20 mm for width x depth. The polarization functions used is as shown in equation (3.10), (3.11) and (3.12).

I
$$\text{Cathodic: } \phi_c = -48\,\text{Log}^2(i) - 137\,\text{Log}\,(i) - 60$$
$$\text{Anodic: } \phi_a = 18\,\text{Log}^2(i) + 35\,\text{Log}\,(i) - 90 \quad (3.10)$$

II
$$\text{Cathodic: } \phi_c = -48\,\text{Log}^2(i) - 137\,\text{Log}\,(i) - 60$$
$$\text{Anodic: } \phi_a = 18\,\text{Log}^2(i) + 35\,\text{Log}\,(i) - 250 \quad (3.11)$$

III
$$\text{Cathodic: } \phi_c = -48\,\text{Log}^2(i) - 137\,\text{Log}\,(i) - 60$$
$$\text{Anodic: } \phi_a = 18\,\text{Log}^2(i) + 35\,\text{Log}\,(i) - 350 \quad (3.12)$$

Polarization function II is an approximation of polarization of pitting corrosion measured in [48]. The rest of polarization functions are modification of polarization function II in order to give variations of polarization in the example case. Figure 3.9 shows plot of the polarization functions. The cathodic polarization function is kept same while the anode polarization is varied so it has larger difference to that of cathode, thus making the corrosion cell more corrosive. It can also be seen that polarization curves I have less corrosion current than the rest.

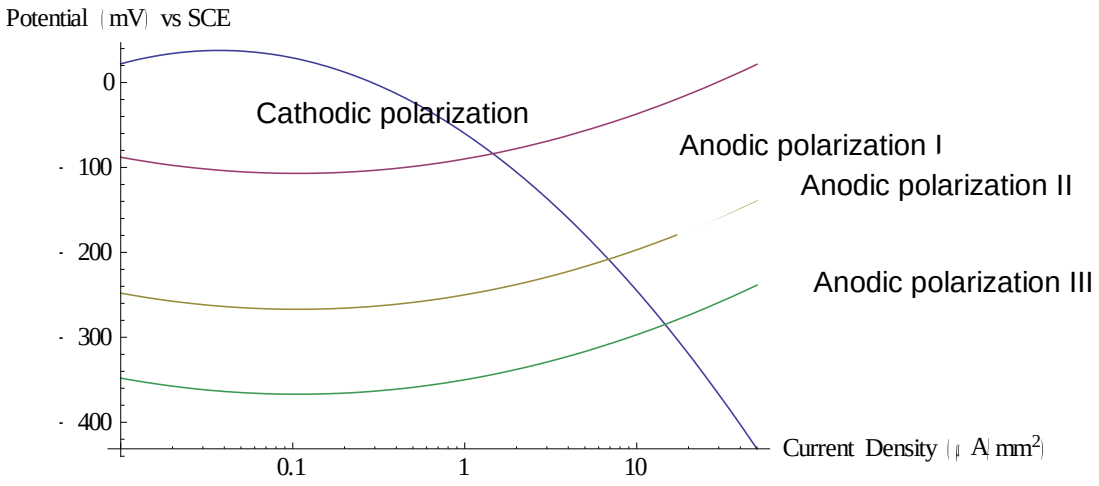

Figure 3.9: Plot of polarization function I, II and III

The simulation for each dimensions and polarization functions variety were run 5 times. The number of pitting and ratio of width over depth obtained from simulation are averaged. Results of simulation are presented in next section.

3.4. Results and Discussion

3.4.1. Shape of pit cavity

The morphologies of pit cavity resulted from different polarization are compared. Figure 3.10 shows comparison of pit growth of corrosion cell with varied dimensions under polarization I after time step 10 and 20.

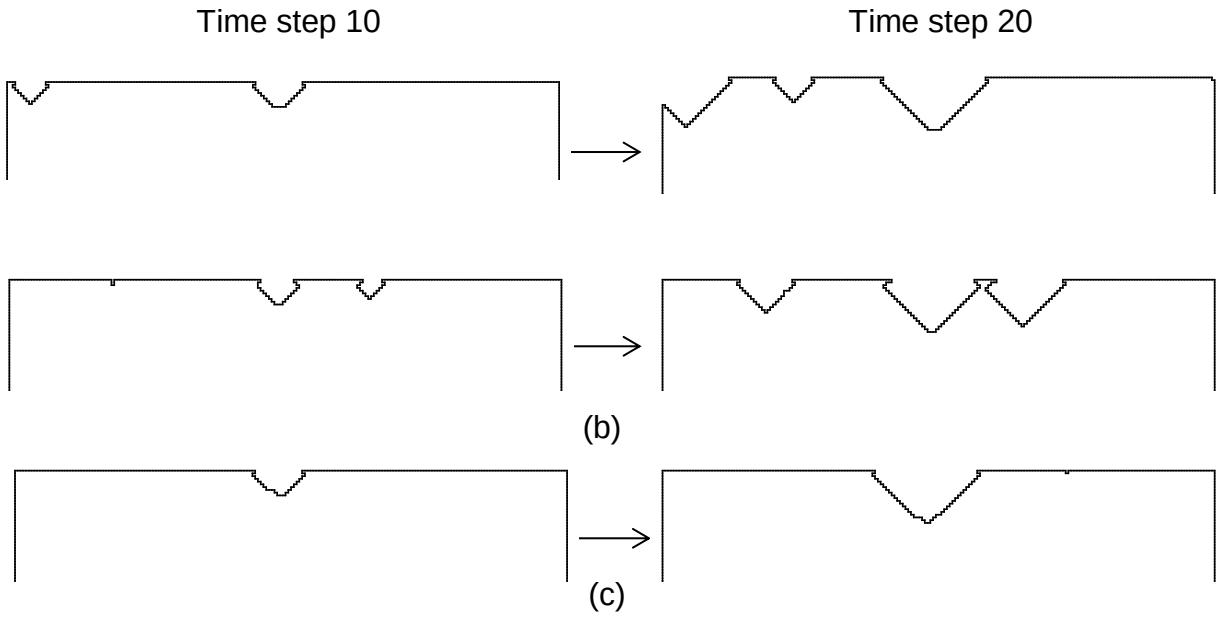

Figure 3.10: Samples of simulation results for corrosion cell with dimension (a) 5x5, (b) 10x10 and (c) 20x20 mm under polarization I.

The resulting pit shape is conical or resembling typical hemispherical pit. This can be explained on basis of electrochemistry of corrosion. Polarization I shows that the difference of electrode potentials is relatively low. Thus the anodic (corroding) reaction is relatively low and currents are distributed more uniformly over the surface. The results also show consistency to the above explanation when dimensions are increased. Figure 3.10 only shows one sample of higher dimensions of corrosion cell (the 10x10 and 20x20 mm dimensions). Figure 3.11 shows some other sample at time step 1. Higher dimensions of corrosion cell means the anodic area on pitting cavity should supply currents to more area. Thus current distribution becomes less uniform, and pitting growth start to show minor roughness and irregularity. Although it shows basic shape of conical or hemispherical pit, the larger the dimensions, the more minor irregularity of feature formed.

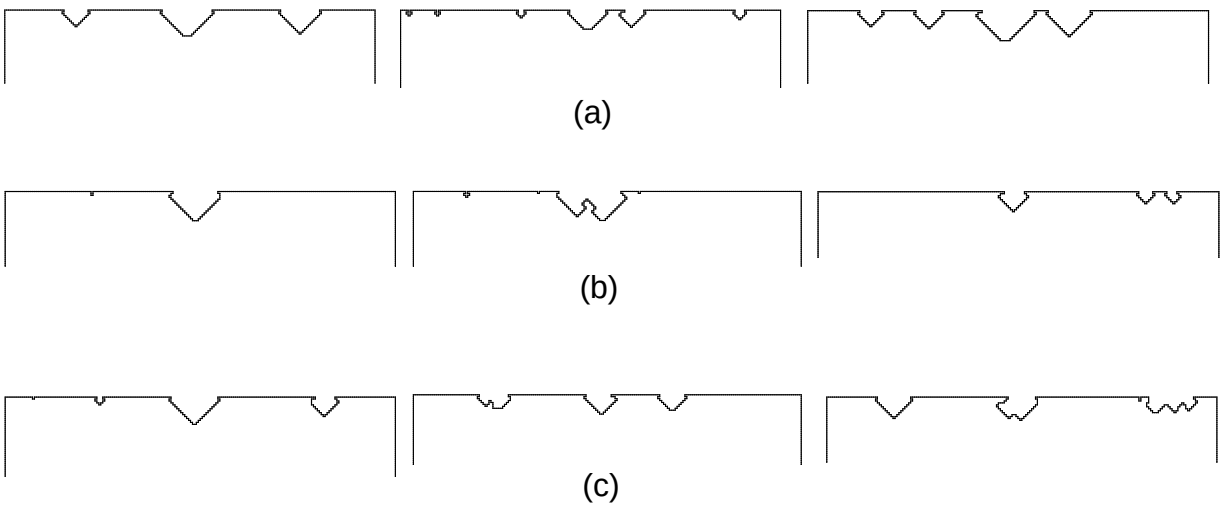

Figure 3.11: Other samples of pitting growth at time step 15 under polarization I for (a) 5x5, (b) 10x10 and (c) 20x20 mm corrosion cell dimensions.

Under polarization II, pit shapes show more variation and deviation from the former shape. Figure 3.12 shows samples of result under this polarization. Polarization II has bigger difference of electrode potentials and thus the corrosion rate of anodic part will be relatively high, as well as reduction reaction on passive surface surrounding pits. This makes the anodic reaction in pit cavity to prefer to remove materials inside pit cavity. Additionally, anode area close to passive surface has higher chance to stop corroding. It then leads to pit shapes that have preference to the right or left, and subsurface pit, such as illustrated in Figure 2.3 (d) and (e). From the results, it can also be seen that at smallest dimensions of corrosion cell of 5x5 mm, the shapes still show some resemblance to conical or hemispherical shape. This is because the anode of the initial pit supplies current to less area and maintain some level of uniformity.

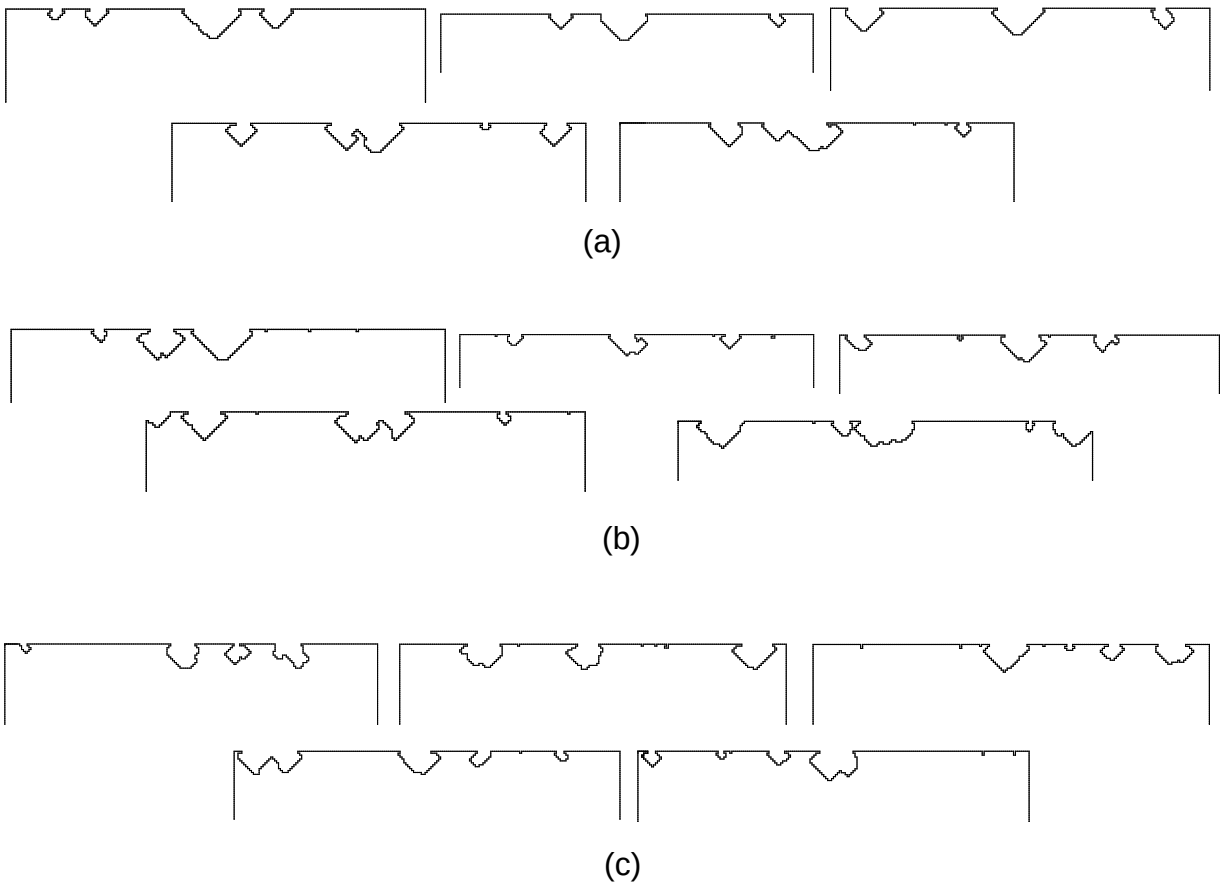

Figure 3.12: Pit shape under polarization II for (a) 5x5, (b) 10x10 and (c) 20x20 mm corrosion cell dimensions.

Polarization III has even higher difference of electrode potential but compared to polarization II, they do not differ too significantly. Results of simulation of pit cavity growth under this polarization show irregularity just like polarization II. Some samples of results are shown in Figure 3.13.

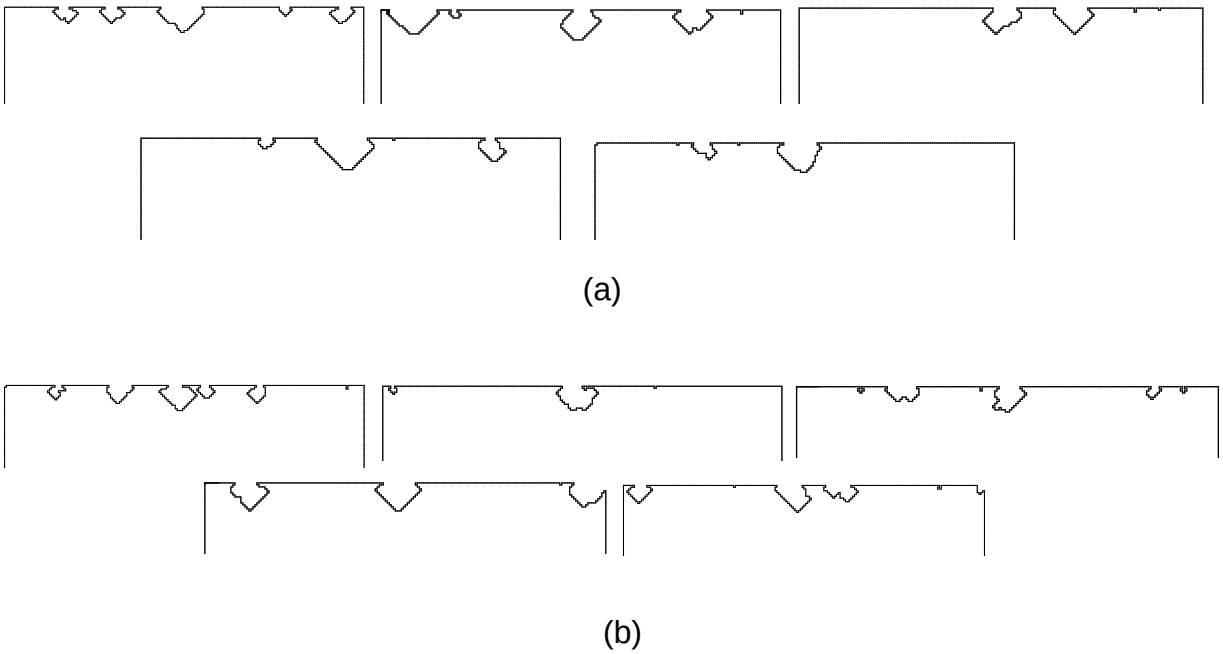

(a)

(b)

Figure 3.13: Pit shape under polarization III for (a) 5x5, (b) 10x10 mm corrosion cell dimensions.

Figure 3.14 shows the growth of individual initial pit under three different polarizations at few time steps. As shown previously, polarization I results dominantly with smooth hemispherical-like pit. Polarization II and III have chances resulting in more varied shape of pits, especially when corrosion cell has larger dimensions. From some result of simulation such as shown in Figure 3.13 (b), some pits develop initially as hemispherical-like shape. After few time steps, the horizontal growth on the surface became less dominant than vertical and subsurface growth.

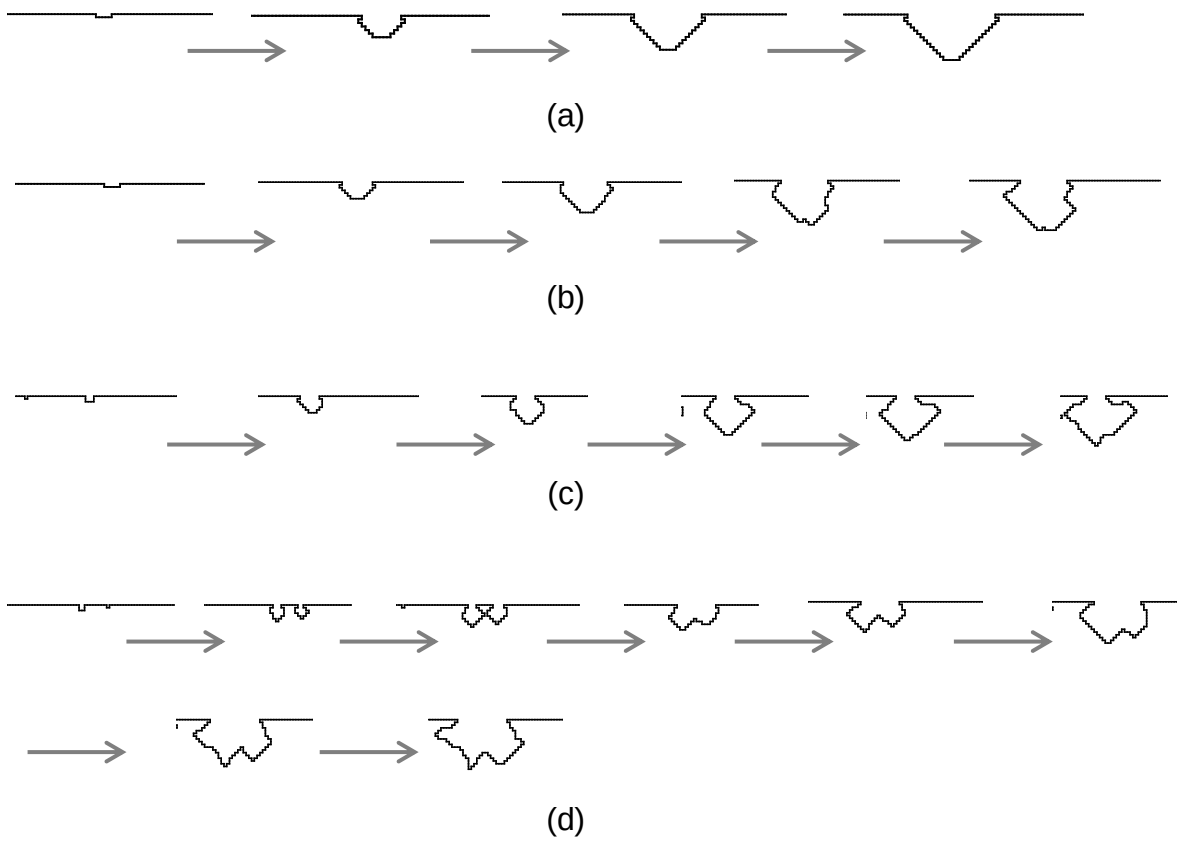

Figure 3.14 Growth of initial pits under (a) polarization I with corrosion cell dimensions of 5x5 mm (b) polarization III with corrosion cell dimensions of 5x5 mm and (c) 10x10 mm, and (d) polarization II with corrosion cell dimensions of 20x20 mm

This is more apparent in Figure 3.13 (c) because the corrosion cell dimensions are larger. This is also consistent with electrochemical principle of corrosion that as dimensions increased, the anodic area on pit becomes more localized (that is, the pit becomes more anodic while surrounding area adjacent to the pits become highly passive/cathodic), then the corrosion attack tends to remove materials inside the pit resulting in subsurface pit cavity as in Figure 3.13 (c).

Some pits assume different shape after merging with other. This can result different shape and change the direction of the shape the pits take. When pit takes shape, the area of corrosion cell becomes larger, thus while pit grows, the nature of the corrosion cell also changes. In Figure 3.13 (d) two pits that grows dominantly in the direction of the depth of materials merge together and thus increasing the anodic area. Notice that this happens under polarization II with corrosion cell dimensions of 20x20 mm, where the anodic area on pit surface becomes more localized. Materials removal still dominantly happens at subsurface.

From some simulation results, it seems that under polarization II and III, pits that grow dominantly into the depth of metal are helped by other additional pits that appear as a result of minimum and non- uniform currents supply onto cathodic surface. Figure 3.14 shows the surrounding area of pit on corrosion cell of Figure 3.13 (d) and pit on corrosion cell of dimensions 20x20 mm under polarization II. After a few time steps, new pits start to grow. These new pits provide additional currents the whole corrosion cell. As the supply of currents to the surface now is supported by multiple pits, the initial pit can continue to expand under the surface, and results in subsurface form and more irregularities under the surface. So the additional pits around initial pits may help the formation of subsurface and deeper pit. Notice also that the two cases happen under polarization II with corrosion cell dimension of 10x10 and 20x20 mm. When corrosion cell dimension is 5x5 mm, the results show fewer tendencies to form subsurface formation as shown by samples of results in Figure 3.12 (a).

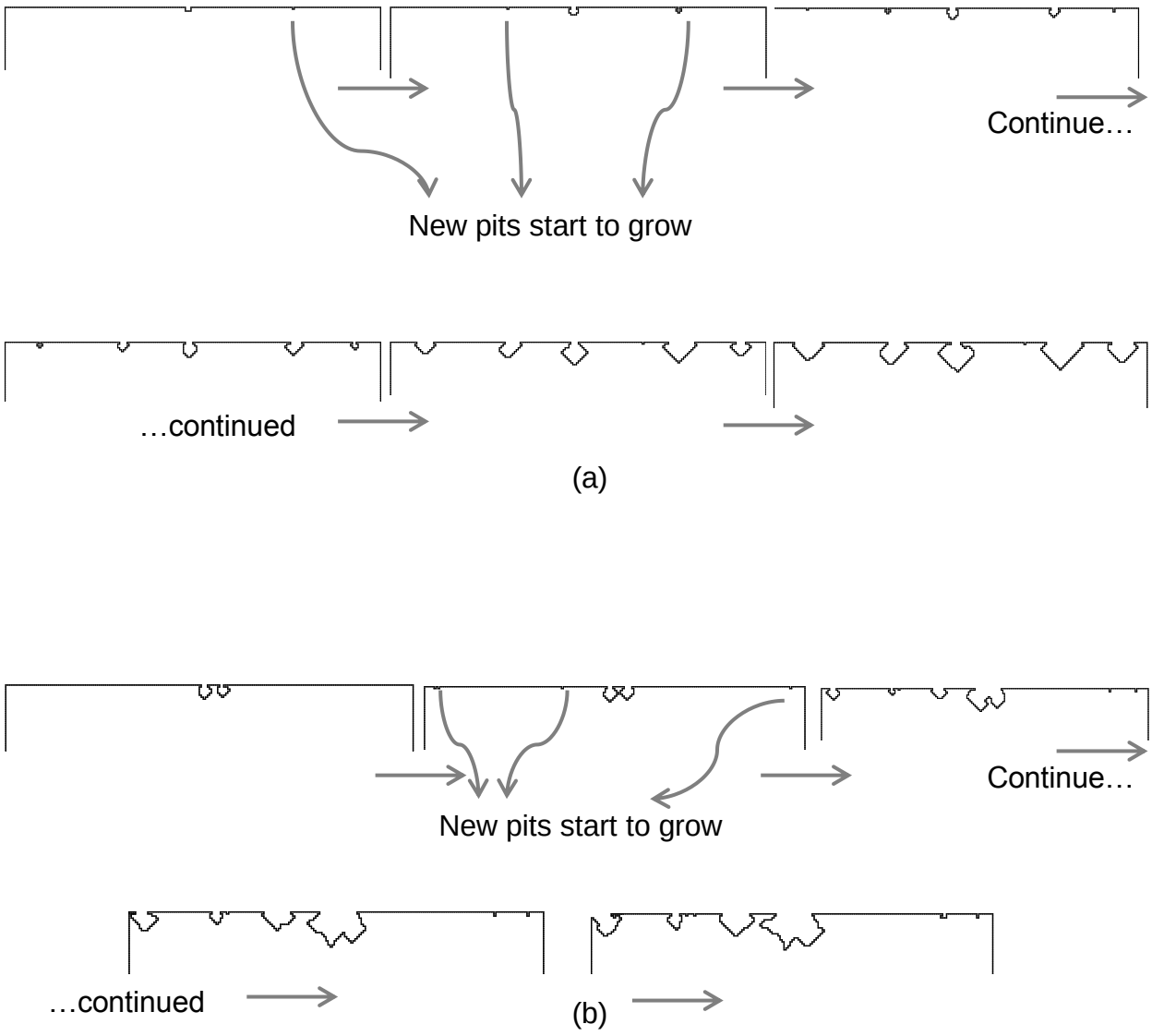

Figure 3.15 the growth of pits on surface of corrosion cell under polarization II with dimension (a) 10x10 mm and (b) 20x20 mm.

Samples of results shown in Figure 3.14 and 3.15 shows the growth of pits that resembles commonly found pit shapes, as shown in Figure 2.3. However, comparison with actual pit growing under controlled environment is not presented in this study. This is due to the lack of comprehensive data for the purpose of this study. The CA

simulation also has limitation. The CA simulation is based on BEM simulation of current exchange in a corrosion cell under certain environment represented by polarization function. It is assumed that the reactions occurring in pit corrosion cell is aggregated in polarization function. However, because pits start at size of few microns, microstructure of metals as well as crystal structure may influence pit growth, as shown in in Figure 2.3 (d) and (e). This is not considered in this study. The dynamics of passive layer breakdown is also simplified into the amount of currents that anodic site on pit can provide to the whole corrosion cell. Passive layer plays important role in pitting corrosion as it is what causes corrosion attack to be highly localized and remove materials exclusively in small area. However, the CA simulation has successfully show different growth of pit under different condition (represented by polarization function) driven by dynamics of number of cathode and anode while the system evolves.

3.4.2. Pit width-depth ratio and number of pits

The simulations were done five times for each dimensions and polarizations. For each result, the number of new pits was counted and ratio of width and depth were calculated. New pit are counted if it has more than one corroded cell in horizontal and vertical direction. The number of pits can change over time, as new pits grow and two or more pits merge. The example of latter can be seen in Figure 3.13 (d). The simulation is terminated at time step 20, so the numbers of pits were taken at time step 10 and 20. The results are shown in Table 3.2. Figure 3.16 shows a plot of width-depth ratio at CA iteration of 20 at different corrosion cell dimensions.

Table 3.2. Average Pit's width-depth ratio and number of pits. T is time step.

Polarization	Dimensions (mm)	Width/Depth		Number of pits	
		T=10	T=20	T=10	T=20
I	5x5	1.82	2.50	4	4
	10x10	1.64	1.84	3	3
	20x20	1.33	2.06	2	2
II	5x5	1.51	1.93	4	4
	10x10	1.07	2.08	3	4
	20x20	1.07	1.18	3	4
III	5x5	1.31	1.49	2	4
	10x10	0.69	1.22	4	4
	20x20	1.63	1.66	2	4

Number of pits for all cases show little differences. This may be caused by limitation of current CA model or insignificant difference of condition under the three polarizations. However, the pit width-depth ratios show that polarization I tends to produce higher ratios, as shown in Figure 3.16. This means that under polarization I, the width of pit tends to be higher than the depth, or the pit tends to grow in horizontal rather than in depth direction.

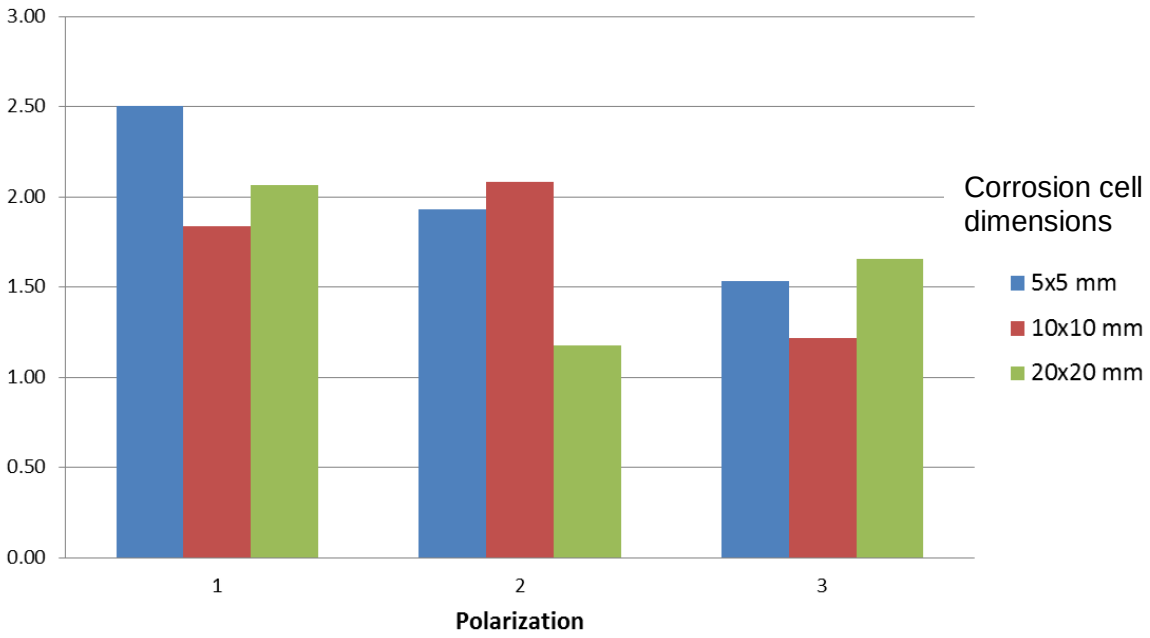

Figure 3.16 Width-depth ratio at CA iteration 20 for each Polarization and corrosion cell dimensions

Chapter 4 Stress Analysis

The analysis on pitting corrosion is extended to simulating distribution of stress given shape of pitting. Ideally, the geometry information from previous data can be transferred to stress analysis tools. However, due to limitation of processing data from CA discretization, image from results of simulation are used to build models for stress analysis. The models were built using Solid Works. The results considered for stress analysis are pit shapes from specific iteration of simulation as described in previous chapter. These results are shown in Figure 4.1.

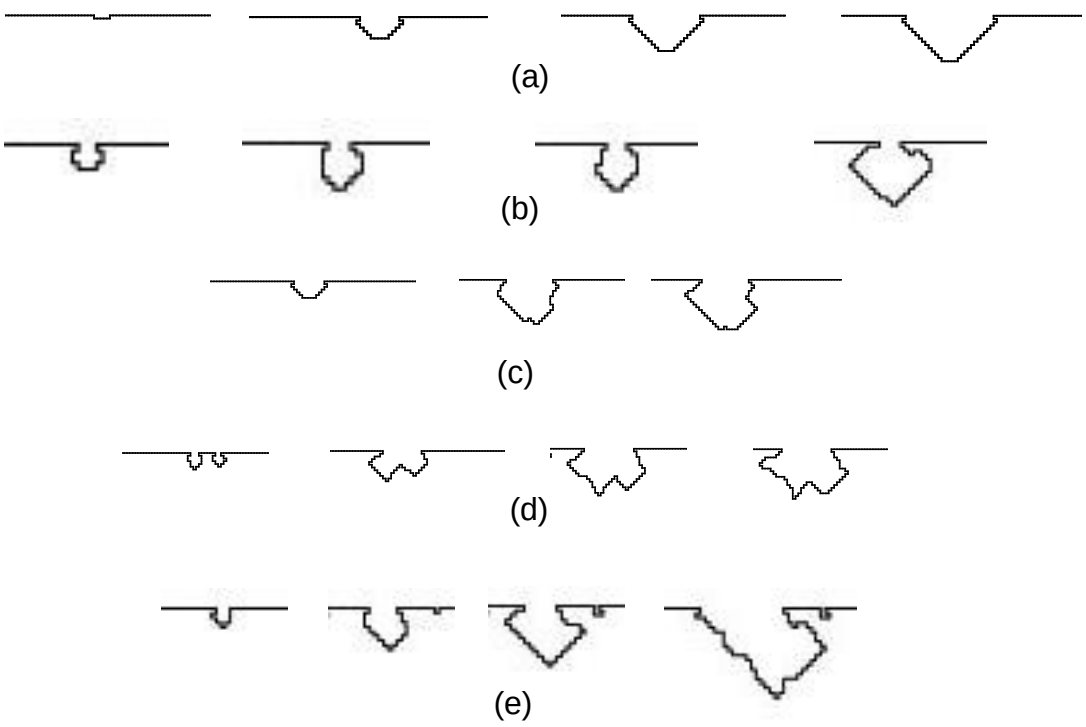

Figure 4.1: Results of simulation that were used to build model for stress analysis. Each set of images show pit growth from initial stage (at the far left) to end of iteration (at the far right).

Figure 4.1 (a) shows one of possible growth of pit under polarization I with corrosion cell dimension of 5x5 mm. Figure 4.2 (b) to (d) are possible growth under polarization II with corrosion cell dimension of 10x10 mm, 5x5 mm and 20x20 mm respectively. Figure 4.1 (e) shows a possible growth of pit under polarization III with corrosion cell dimension of 20x20 mm. These results are selected because they show the growth of hemispherical (early time step of Figure 4.1 (a), conical (later time step of Figure 4.1 (a), and variations of subsurface (Figure 4.1 (b) to (e)) as shown in Figure 2.3 (b), (d) and (e). The purpose of the study is to compare stress concentration factor and stress distribution of each pitting shape. So for each selected pitting shape as shown in Figure 4.1, the dimensions of the body of metal are set to be square with 10 mm for width and height. The model is of two-dimensional plane stress. The model is subjected to loads that pull it to the left and right direction. The top and bottom part where pitting corrosion occurs may freely deform. Figure 4.2 shows the model and boundary conditions for stress analysis.

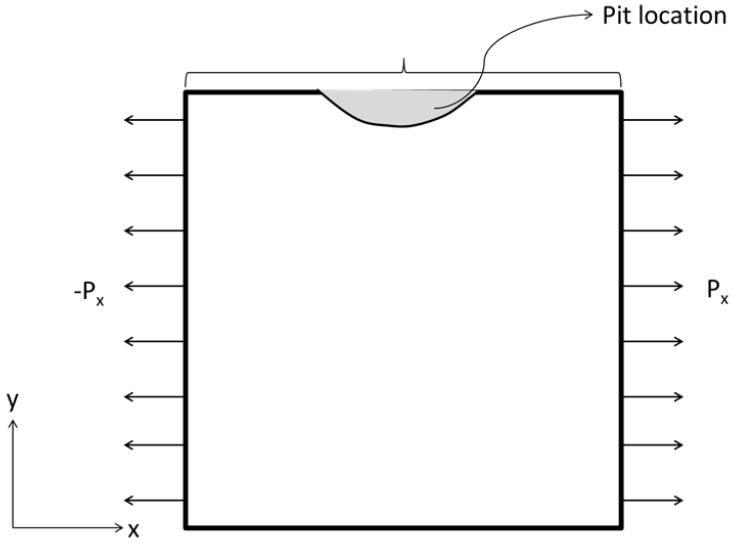

Figure 4.2: Model and boundary conditions for stress analysis

Each model is subjected to load of 100 MPa. The material is taken as Stainless steel with Young's Modulus of 1.93 x 10^{11} Pa. The detail of pit shape had to be taken appropriately. For all pit models, sharp edge on the tip of pit (if any) is avoided. The tip of pit from the CA simulation is made as curvature. Figure 4.3 shows examples of detail on pit tip. All models of pits and meshed models are shown in Appendix I and II.

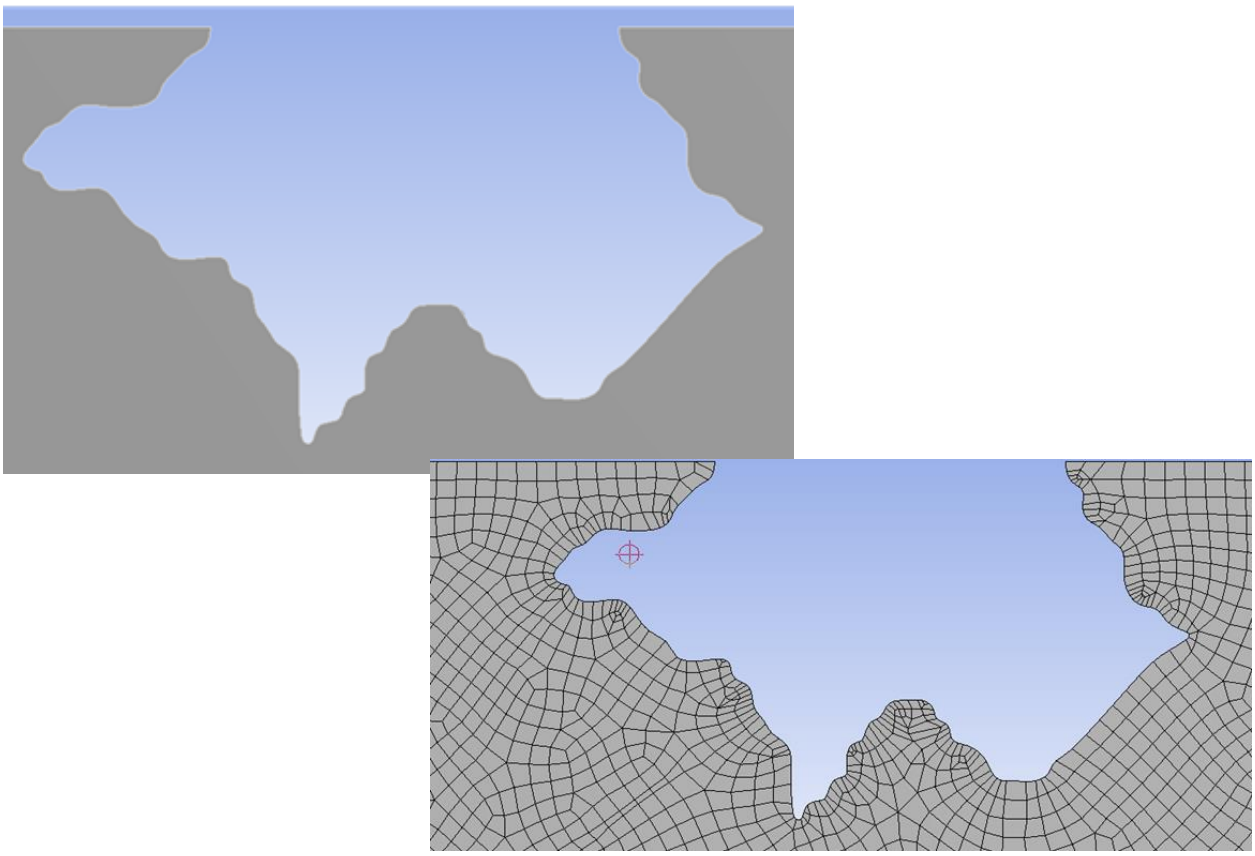

Figure 4.2: Detail of pit in the models

4.1. Results and Discussion

4.1.1. Stress distribution and stress concentration factor

Appendix III shows stress distribution (von Misses) for all cases as in Figure 4.1. For all cases, the lowest stress is always at edge of pit opening on the surface, as shown in Figure 4.3.

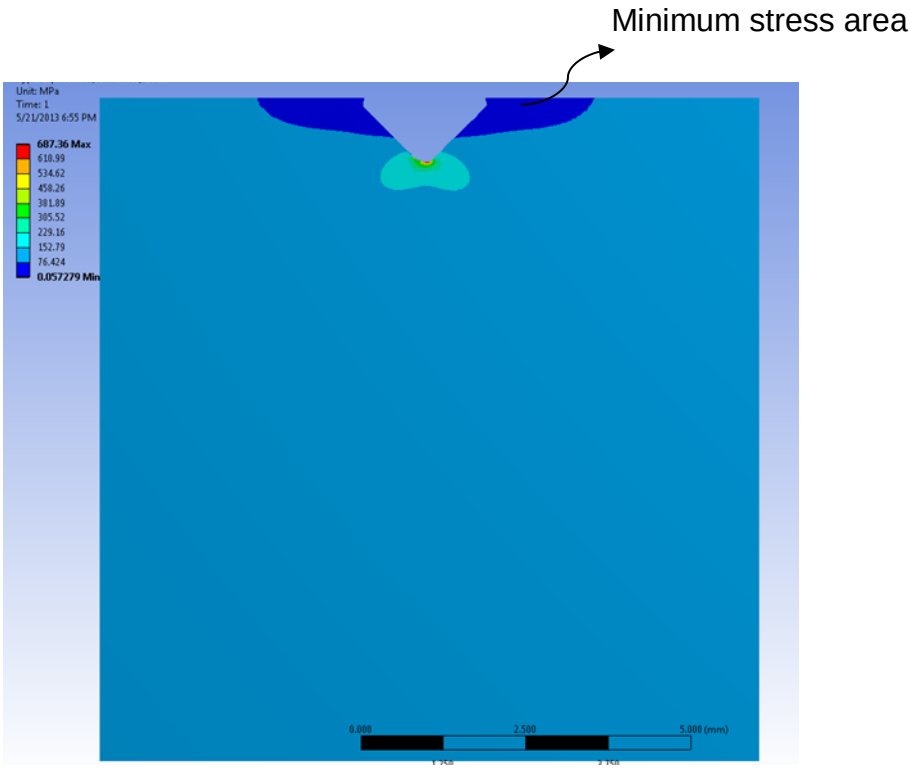

Figure 4.3: Location of minimum stress is always at pit opening

The maximum stress is always found on the tip of deepest part of pit. In Figure 4.3 (b), it is shown that the maximum stress is on a deepest notch of the pit although the pit has other notches that could potentially act as stress raiser. These notches are also potential sites of accumulation of corrosive agent. Additionally, it can be seen from Figure 4.1 (d) or 3.14 (d) that the notches formed as a preferential site for the pit growth.

This means the notches were anodic site. When loads can influence corrosion inside pit such as reported in [53], these pit shapes may influence the rate of corrosion on particular sites of pit and assist in forming deeper pits.

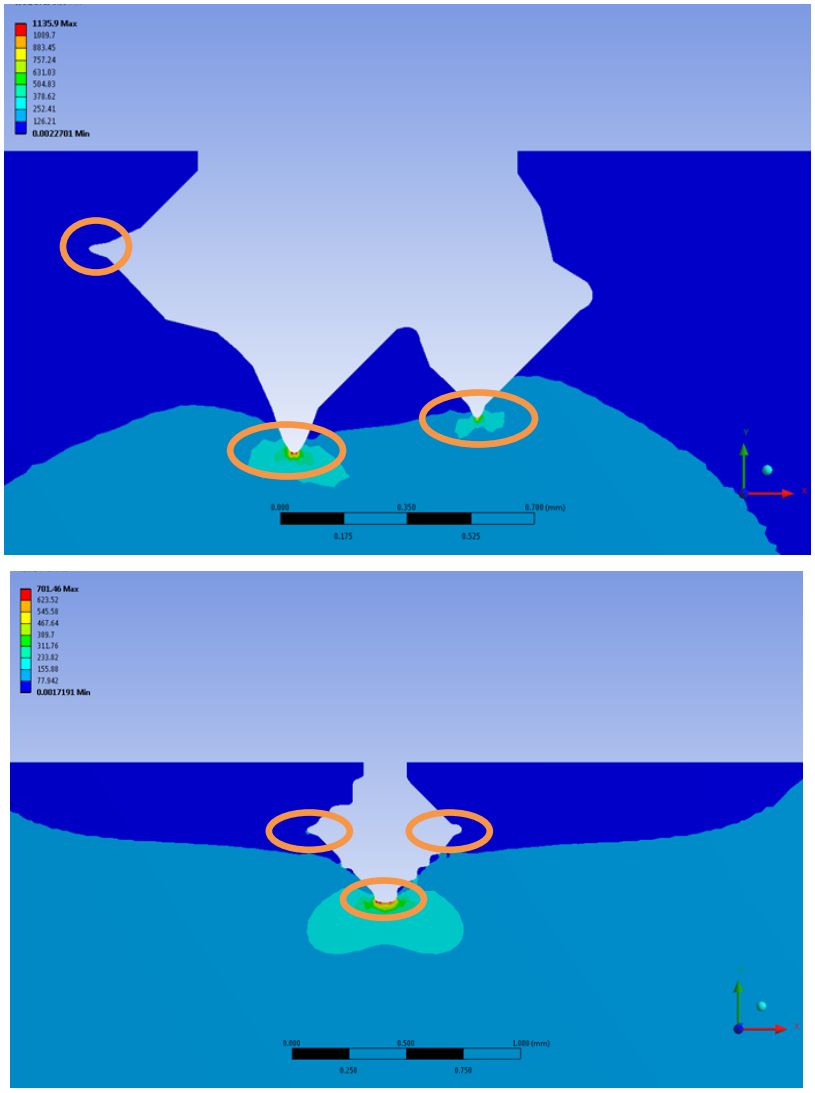

Figure 4.4: Stress distribution on pits with multiple notches.

Stress concentration factors for each case in Figure 4.1 were calculated and plotted as shown in Figure 4.5.

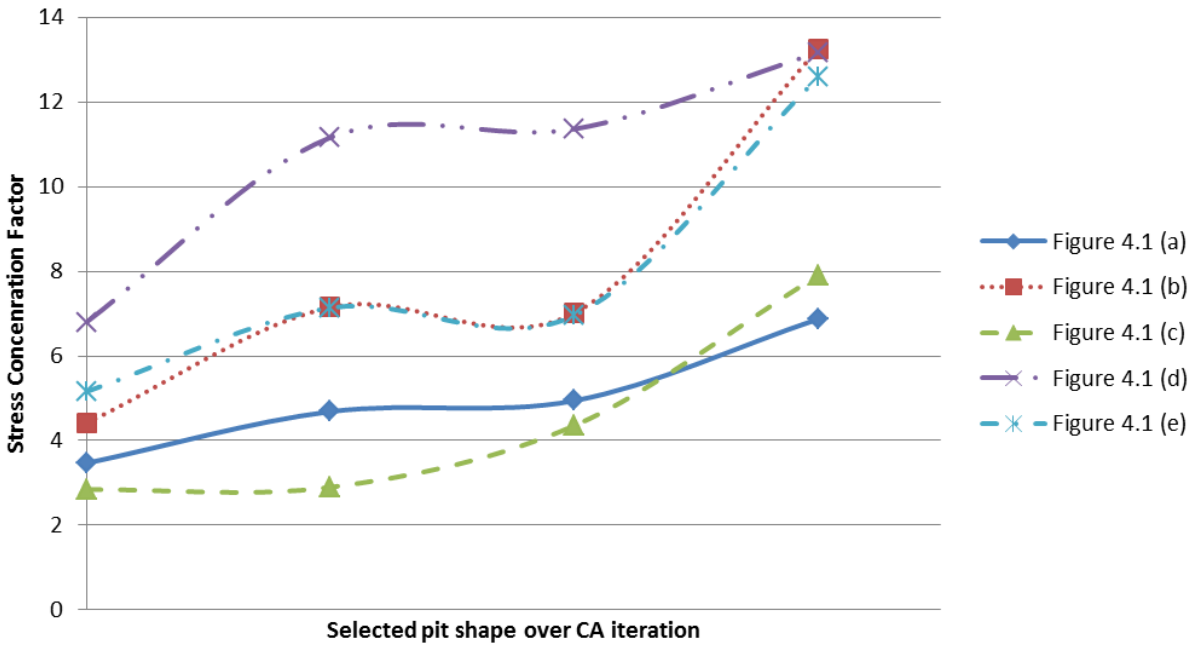

Figure 4.5: Stress concentration factor for every case in Figure 4.1 (a) to (e), plotted versus selected pit shape at selected CA iteration as shown in Figure 4.1 (a) to (e).

It is shown that case in Figure 4.1 (a) has lowest stress concentration factor as well as its increment over time. Pit in case of Figure 4.1 (a) starts as hemispherical shape and its shape does not experience changes too much over time. This shape certainly has less risk in term of stress concentration. Pit shapes formed in case of Figure 4.1 (d) has the most irregular shape and the highest stress concentration factor. Pit that grows in this manner can be the most dangerous since it has high stress concentration and shape that can accumulate more corrosive agent. Pit such as in case of Figure 4.1 (b) and (e) starts initially at low stress concentration but increases significantly over time. Figure 4.1 (b) should be of more concern since its shape could

deceive attempt of visual observation. While the opening looks like it is still in small size, pit under the surface has grown in size.

Figure 4.6 and 4.7 shows stress concentration factor and area of each shape of pit of cases in Figure 4.1 at the end of iteration (end pit shape) respectively.

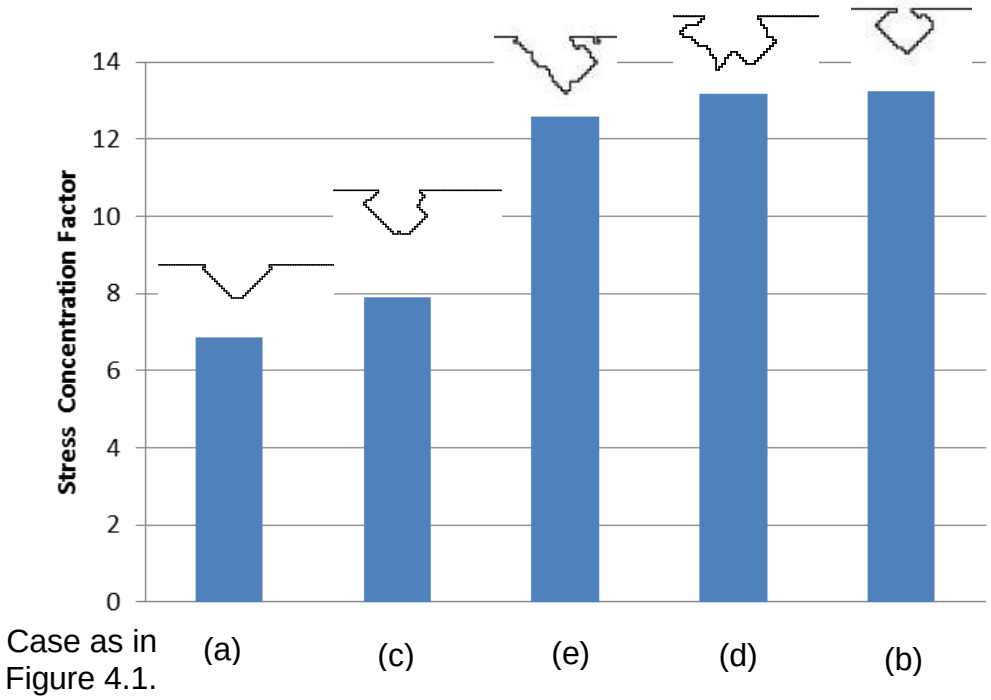

Figure 4.6: Stress concentration for each of end pit shape. Illustrations of pit above graph are not scaled

Pit as in case of Figure 4.1 (a) has the highest area but lowest stress concentration factor. But higher area can also contain higher volume of corrosive agent. Lower area of pits allows lower volume of corrosive agent, however depending on the shape, higher stress concentration may assist in increasing chemical activity at anodic site thus increasing corrosion rate inside pit cavity. The dynamics of load experienced

by object, pit shape and chemical activity are important in the study of pit to crack transition and stress corrosion cracking.

Related to this discussion, discussion in section 3.4.1 and 3.4.2 mentions that under polarization I, the corrosion cell tends to produce pit with conical or hemispherical shape that grows preferentially in horizontal direction (expanding the width). In this section, it has been shown that a sample from pit growth under polarization I shows lowest stress concentration. Therefore, environment that produces polarization of corrosion cell such as in polarization I is the safest when pitting corrosion occurs.

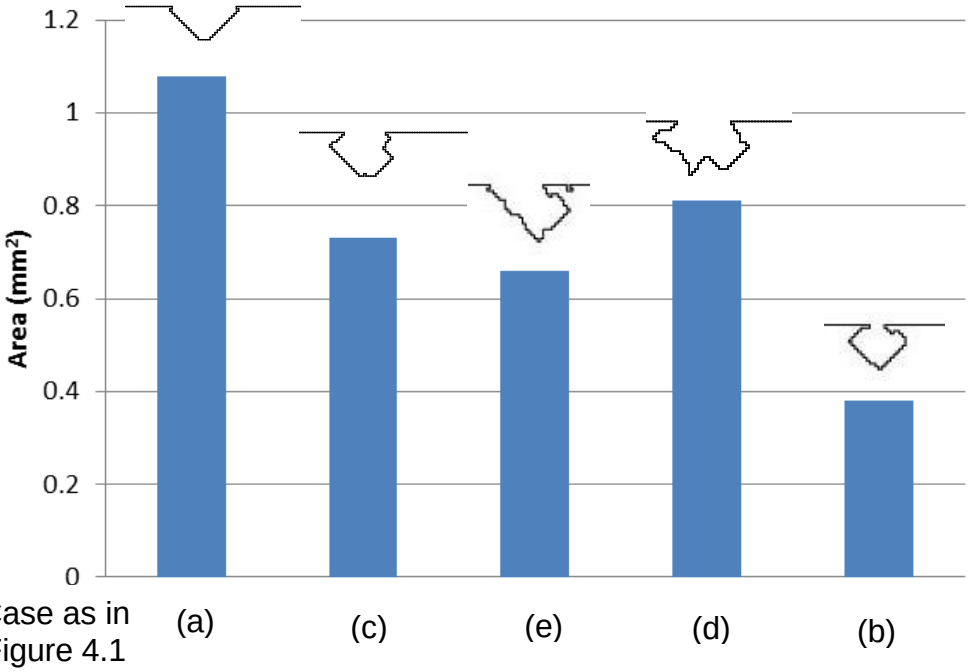

Figure 4.7: Area for each of end pit shape. Illustrations of pit above graph are not scaled

Chapter 5 Conclusions and Future Work

5.1. Conclusion

Modeling of pitting corrosion using combination of BEM and CA has been carried out. The modeling starts by assuming that pitting corrosion can be simplified to typical electrochemical corrosion in metal. The corrosion cell size is assumed to be in constant in this study. The electrode on the surface (top part of the model) in CA simulation remains electrode through the whole iteration of simulation. Results from CA simulation shows that under polarization I, pits grow in more regular conical and hemispherical shapes. It also shows a steady tendency of the pits to grow in this manner. While under polarization II and III particularly with higher dimensions of corrosion cells, the growth of pits can take many irregular form, resembling undercutting and subsurface shapes such as shown in Figure 2.3 (d) and (e). Results also show that smooth conical and hemispherical shapes tend to grow under polarization I and other polarization with smaller dimension of corrosion cell, and some subsurface, undercutting and more irregular shapes tend to grow under polarization II and III particularly with larger corrosion cell. The irregular shapes of pitting that produce notches and subsurface cavity are to be avoided because they can lead to false impression on visual observation. Subsurface cavity can further increase barrier between surface of cavity and the rest of metal's surface, creating another environment inside pit that can lead to more severe corrosion attack.

Stress analysis was carried out for certain cases. Results from CA simulation were taken and modeled. The FEM stress analysis was done using ANSYS

Workbench12. Results obtained show that irregular shapes of pit produced under polarization II and III lead to higher stress concentration factor. A sample of pit that grows under polarization I show steady increase of stress concentration factor, while some samples from polarization II and III can lead to sharp increase of stress concentration factor as pits grow irregularly.

Combining results from CA simulation and stress analysis, it can be concluded that under polarization I, the possible pits that may appear are the safest in terms of stress concentration factor and shapes. Environment that produces polarization such as polarization I on a metal is favorable in order to reduce the risk of pitting corrosion. The shapes of pit under polarization I are more open and thus can accumulate less corrosive agents. Lower stress concentration factor means lower risk for the pits to initiate crack. Polarization I has lowest corrosion potential and difference between anode and cathode electrode potential. Local corrosion cell that may appear on surface of metals are rather hard to predict, but local electrochemical probes [52] can be used to determine distribution of potential occurring on a pitting site. A study can be conducted to determine the behavior of local corrosion cells that may appear on a metal.

5.2. Future Work

Current model has limitations. The size of initial corrosion cell depends on microstructure of materials itself, such as distribution of grains, defects and composition of alloys. These factors are not carried out in this study. Also, the mechanism of passive film breakdown in pitting corrosion is not carried out in detail.

Future work will include microstructure properties and the changing dimension of corrosion cell that may lead to more variation of pit shapes and gives more insight on relation of environment to pit growth. This study does not include real comparison with a specific metal corroded under determined environment. Further work is needed to set a controlled environment that produces pitting corrosion on a specific metal and measure pit shapes and geometry, polarization, chemical activity, pH and other environmental parameters. These data can be used to improve current CA model.

In this study, the CA discretization is directly translated from BEM. Future study is needed to minimize either one of the discretization in order to reduce computation time. A further work to directly bring the discretization of geometry from CA to stress analysis is also considered.

References

[1] C.M. Hansson, The Impact of Corrosion on Society, Metallurgical and Materials Transaction A, 42A, (2011) 2952-2962.

[2] Z. Szklarska-Smialowska, Pitting and Crevice Corrosion, NACE International, (2005)

[3] S.I. Rokhlin, J.-Y. Kim, H. Nagy, B. Zoofan, Effect of pitting corrosion on fatigue crack initiation and fatigue life, Engineering Fracture Mechanics, 62, Issues 4–5, (1999), 425–444

[4] A.M Heyes, Oxygen pitting failure of a bagasse boiler tube, Engineering Failure Analysis, Volume 8, Issue 2, (2001), 123–131

[5] Effects of pitting corrosion on the fatigue behavior of aluminum alloy 7075-T6: modeling and experimental studies, Materials Science and Engineering: A, Volume 297, Issues 1–2, (2001), 223–229

[6] A Turnbull, S Zhou, Pit to crack transition in stress corrosion cracking of a steam turbine disc steel, Corrosion Science, Volume 46, Issue 5, (2004), 1239–1264

[7] S. Ishihara, Z.Y. Nan, A.J. McEvily, T. Goshima, S. Sunada, On the initiation and growth behavior of corrosion pits during corrosion fatigue process of industrial pure aluminum, International Journal of Fatigue, Volume 30, Issue 9, (2008), 1659–1668

[8] G. Pantazopoulos, A. Vazdirvanidis, G. Tsinopoulos, Failure analysis of a hard-drawn water tube leakage caused by the synergistic actions of pitting corrosion and stress–corrosion cracking, Engineering Failure Analysis, Volume 18, Issue 2, (2011), 649–657

[9] S.I. Rokhlin, J.-Y. Kim, H. Nagy, B. Zoofan, Effect of pitting corrosion on fatigue crack initiation and fatigue life, Engineering Fracture Mechanics, Volume 62, Issues 4–5, (1999), 425–444

[10] Frankel, G.S., Corrosion: Fundamentals, Testing, and Protection, ASM Handbook, Vol. 13A, ASM International, (2003), 236–241.

[11] Pidaparti, Ramana M., Patel, Ronak R., Correlation between corrosion pits and stresses in Al alloys, Materials Letters, 62, (2008), 4497-4499.

[12] Ramana M. Pidaparti, Appajoysula S. Rao, Analysis of pits induced stresses due to metal corrosion, Corrosion Science, Volume 50, Issue 7, (2008), 1932–1938

[13] A. Turnbull, L. Wright, L. Crocker, New insight into the pit-to-crack transition from finite element analysis of the stress and strain distribution around a corrosion pit, Corrosion Science, Volume 52, Issue 4, (2010), 1492–1498

[14] M. Cerit, K. Genel, S. Eksi, Numerical investigation on stress concentration of corrosion pit, Engineering Failure Analysis, Volume 16, Issue 7, (2009), 2467–2472

[15] Xiaoli Jiang, C. Guedes Soares, Ultimate capacity of rectangular plates with partial depth pits under uniaxial loads, Marine Structures, Volume 26, Issue 1, (2012), 27–41

[16] N. Acuña, J. González-Sánchez, G. Kú-Basulto, L. Domínguez, Analysis of the stress intensity factor around corrosion pits developed on structures subjected to mixed loading, Scripta Materialia, Volume 55, Issue 4, (2006), 363–366

[17] Jeom Kee Paik, Jae Myung Lee, Man Ju Ko, Ultimate shear strength of plate elements with pit corrosion wastage, Thin-Walled Structures, Volume 42, Issue 8, (2004), 1161–1176

[18] D. A. Jones, B. E. Wilde, Galvanic Reactions During Localized Corrosion On Stainless Steel, Corrosion Science, 18, (1978), 631-643.

[19] V. Vignal, et al, The Use Of Local Electrochemical Probes And Surface Analysis Methods To Study The Electrochemical Behaviour And Pitting Corrosion Of Stainless Steels", Electrochimica Acta, 52, (2007), 4994–5001.

[20] C.A. Brebbia, R. Magureanu, The boundary element method for electromagnetic problems, Engineering Analysis, Volume 4, Issue 4, (1987), 178–185

[21] Shigeru Aoki, Kenji Amaya, Optimization of cathodic protection system by BEM, Engineering Analysis with Boundary Elements, Volume 19, Issue 2, (1997), 147–156

[22] O. Abootalebi, A. Kermanpur, M.R. Shishesaz, M.A. Golozar, Optimizing the electrode position in sacrificial anode cathodic protection systems using boundary element method, Corrosion Science, Volume 52, Issue 3, (2010), 678–687

[23] Jong-Min Lee, Numerical analysis of galvanic corrosion of Zn/Fe interface beneath a thin electrolyte, Electrochimica Acta, Volume 51, Issue 16, (2006), 3256–3260

[24] Luiz C Wrobel, Panayiotis Miltiadou, Genetic algorithms for inverse cathodic protection problems, Engineering Analysis with Boundary Elements, Volume 28, Issue 3, (2004), 267–277

[25] Douglas P. Riemer, Mark E. Orazem, A mathematical model for the cathodic protection of tank bottoms, Corrosion Science, Volume 47, Issue 3, (2005), 849–868

[26] Pierre R Roberge, Corrosion engineering principles and practice, McGraw-Hill, New York, (2008)

[27] H. Kaesche, Corrosion of metals : physicochemical principles and current problems, Springer, New York, (2003)

[28] Corrosion Mechanisms in Theory and Practice, Third Edition, Edited by Philippe Marcus, CRC Press, (2011)

[29] G. Engelhardt, M. Urquidi-Macdonald, D.D. Macdonald, A simplified method for estimating corrosion cavity growth rates, Corrosion Science, Volume 39, Issue 3, (1997), 419–441

[30] M. Ahammed, R.E. Melchers, Probabilistic analysis of pipelines subjected to pitting corrosion leaks, Engineering Structures, Volume 17, Issue 2, (1995), 74–80

[31] A. Valor, F. Caleyo, L. Alfonso, D. Rivas, J.M. Hallen, Stochastic modeling of pitting corrosion: A new model for initiation and growth of multiple corrosion pits, Corrosion Science, Volume 49, Issue 2, (2007), 559–579

[32] R.E. Melchers, R.J. Jeffrey, Probabilistic models for steel corrosion loss and pitting of marine infrastructure, Reliability Engineering & System Safety, Volume 93, Issue 3, (2008), 423–432

[33] X.-X. Yuan, D. Mao, M.D. Pandey, A Bayesian approach to modeling and predicting pitting flaws in steam generator tubes, Reliability Engineering & System Safety, Volume 94, Issue 11, (2009), 1838–1847

[34] F. Caleyo, J.C. Velázquez, A. Valor, J.M. Hallen, Markov chain modelling of pitting corrosion in underground pipelines, Corrosion Science, Volume 51, Issue 9, (2009), 2197–2207

[35] F. Caleyo, J.C. Velázquez, A. Valor, J.M. Hallen, Probability distribution of pitting corrosion depth and rate in underground pipelines: A Monte Carlo study, Corrosion Science, Volume 51, Issue 9, (2009), 1925–1934

[36] J.C. Walton, G. Cragnolino, S.K. Kalandros, A numerical model of crevice corrosion for passive and active metals, Corrosion Science, Volume 38, Issue 1, (1996), 1–18

[37] N.J. Laycock, J.S. Noh, S.P. White, D.P. Krouse, Computer simulation of pitting potential measurements, Corrosion Science, Volume 47, Issue 12, (2005), 3140–3177

[38] Howard W. Pickering, The role of electrode potential distribution in corrosion processes, Materials Science and Engineering: A, Volume 198, Issues 1–2, (1995), 213–223

[39] John Newman, D.N. Hanson, K. Vetter, Potential distribution in a corroding pit, Electrochimica Acta, Volume 22, Issue 8, (1977), 829–831

[40] R. M. Pidaparti, M. J. Palakal, and L. Fang, Corrosion Pit Growth Model using Cellular Automata, AIAA Journal, 42 (12), (2004), 2562-2569

[41] B. Malki, B. Baroux, Computer simulation of the corrosion pit growth, Corrosion Science, Volume 47, Issue 1, (2005), 171–182

[42] Ramana M. Pidaparti, Long Fang, Mathew J. Palakal, Computational simulation of multi-pit corrosion process in materials, Computational Materials Science, Volume 41, Issue 3, (2008), 255–265

[43] Lei Li, Xiaogang Li, Chaofang Dong, Yizhong Huang, Computational simulation of metastable pitting of stainless steel, Electrochimica Acta, Volume 54, Issue 26, (2009), 6389–6395

[44] D. di Caprio, et al, “Morphology Of Corroded Surfaces: Contribution Of Cellular Automaton Modelling”, Corrosion Science, 53,(2010), 418-425.

[45] Sunil Kumar Thamida, Modeling and simulation of galvanic corrosion pit as a moving boundary problem, Computational Materials Science, Volume 65, (2012), 269–275

[46] S. Aoki, K. Kishimoto, “Prediction of galvanic corrosion rates by the boundary element method”, Mathematical and Computer Modelling, Volume 15, Issues 3–5, (1991), 11–22

[47] CA Brebbia, SM Niku, Computational applications of boundary element methods for cathodic protection of offshore structures, Proceedings of the OMAE conference, Houston, USA, (1988).

[48] Jimmy X. Jia, Guangling Song, Andrej Atrens, Influence of geometry on galvanic corrosion of AZ91D coupled to steel, Corrosion Science, Volume 48, Issue 8, (2006), 2133–2153

[49] M. Kutrib, R Vollmar, Th. Worsch, Introduction to Special Issue on Cellular Automata, Pararell Computing 23, (1997), 1567-1576

[50] J.L. Schiff, “Cellular Automata, A Discrete View of The World”, Wiley Interscience, (2007)

[51] Tommaso Toffoli, Norman Margolus, Cellular automata machines : a new environment for modeling, MIT Press, Cambridge, Mass, (1987)

[52] Roland Oltra, Bruno Vuillemin Probing and Modelling of Galvanic Coupling Phenomena in Localized Corrosion, Progress in Corrosion Science and Engineering II, Modern Aspects of Electrochemistry Volume 47, Springer, US, (2012), 243, 296

[53] E.M. Gutman, G. Solovioff, D. Eliezer, The mechanochemical behavior of type 316L stainless steel, Corrosion Science, Volume 38, Issue 7, (1996), 1141–1145

Appendix

1. Models of Pits

1.1. Model for case in Figure 4.1 (a) and zoomed-in of the area around pit

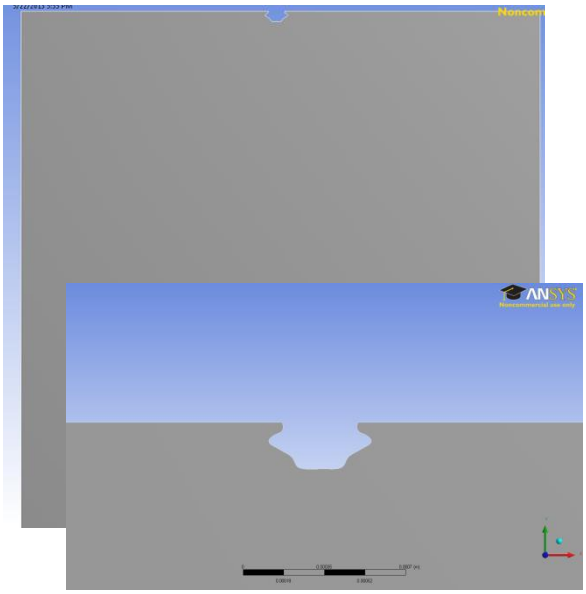

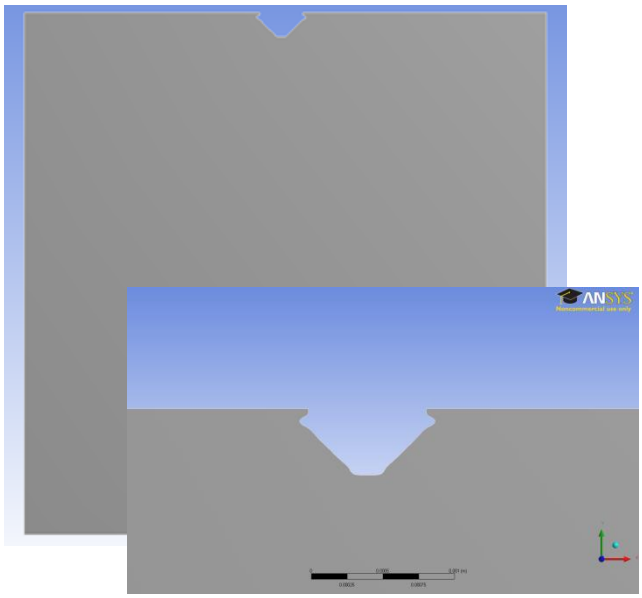

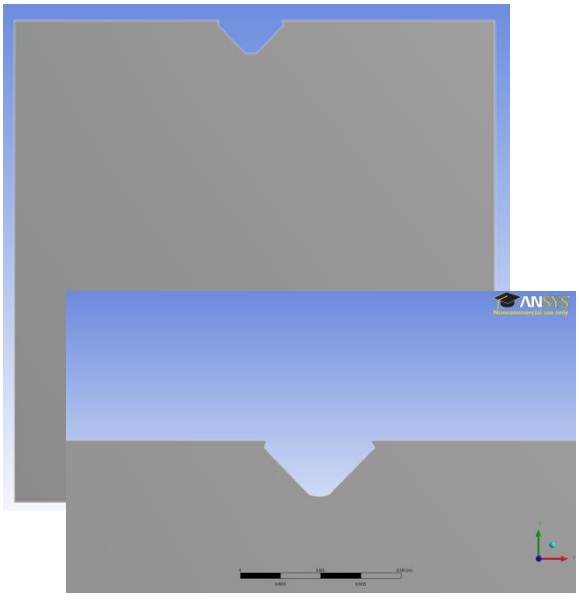

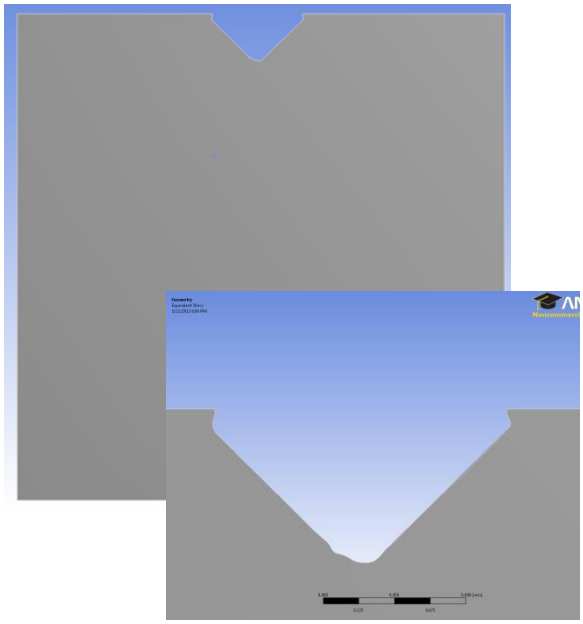

1.2. Model for case in Figure 4.1 (b)

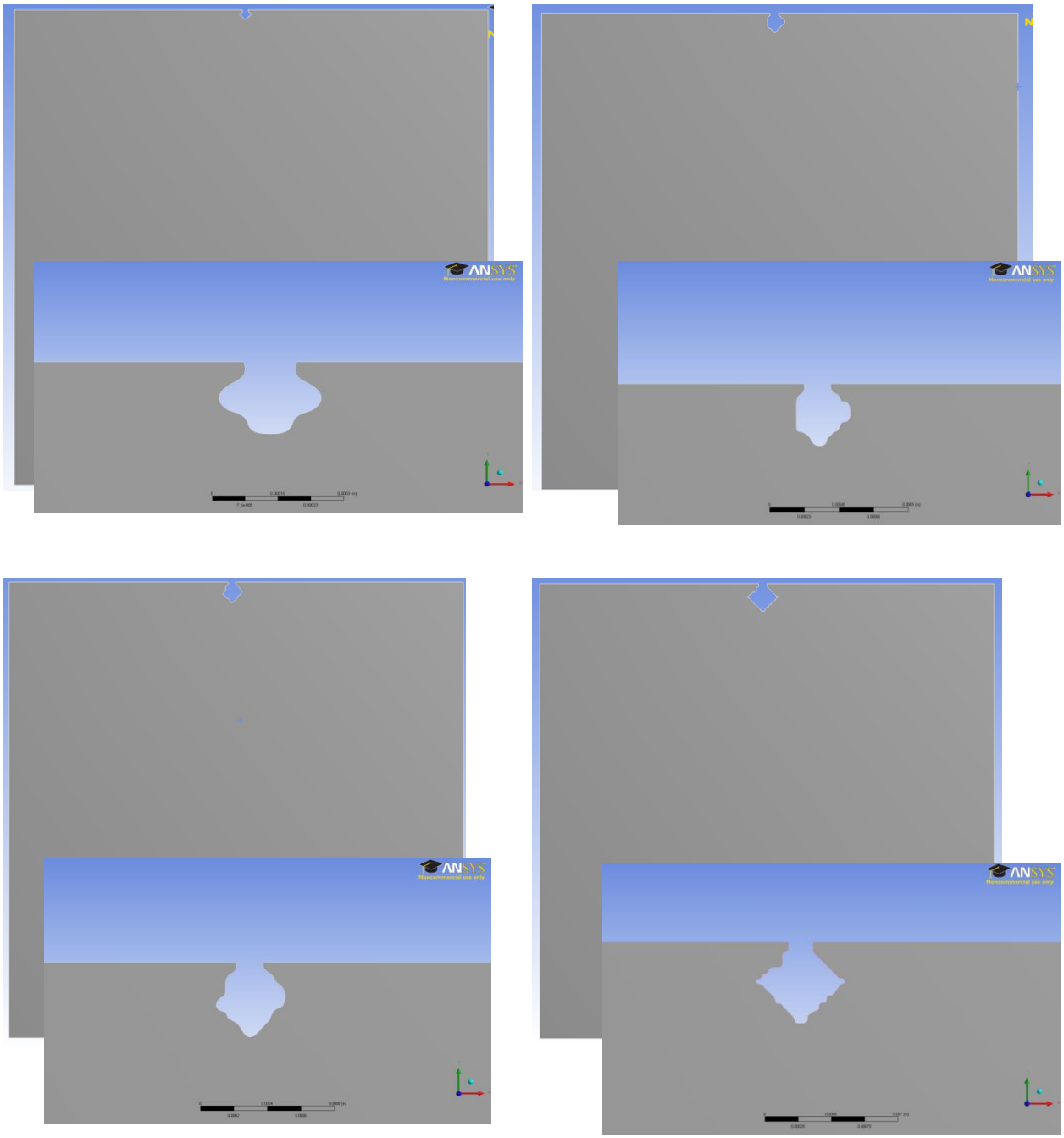

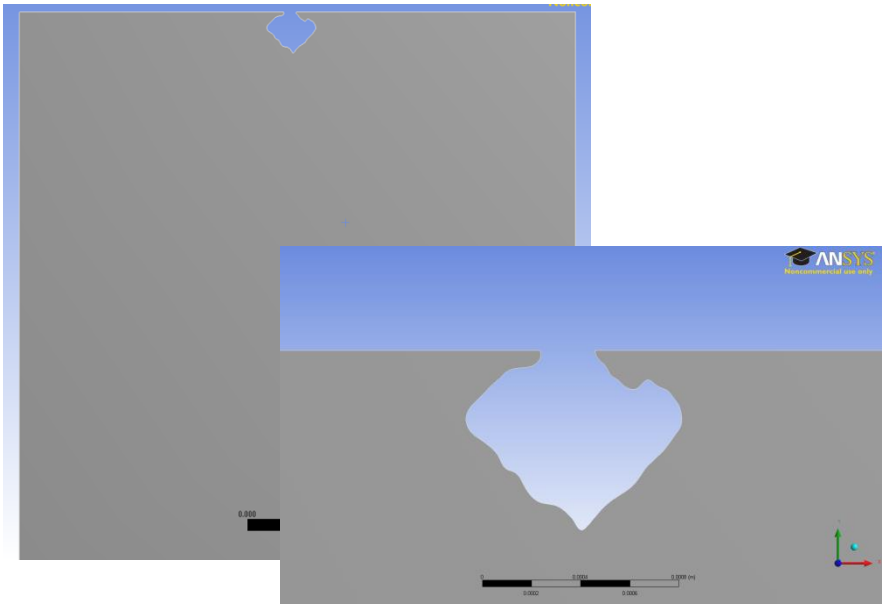

1.3. Models for case in Figure 4.1 (d)

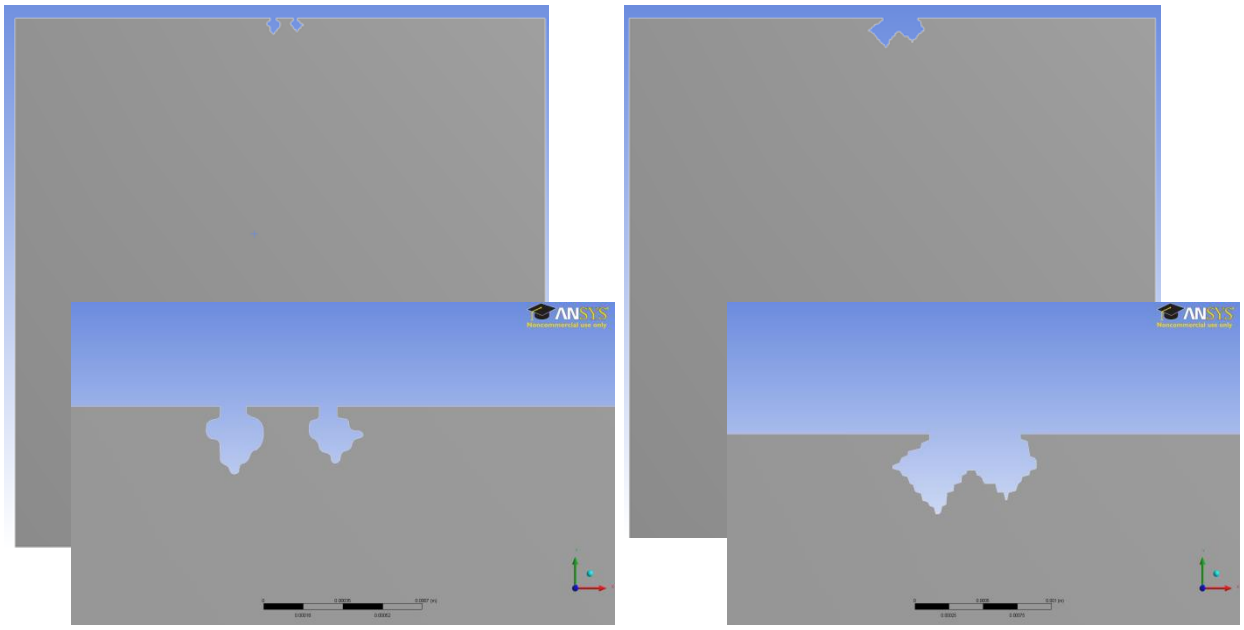

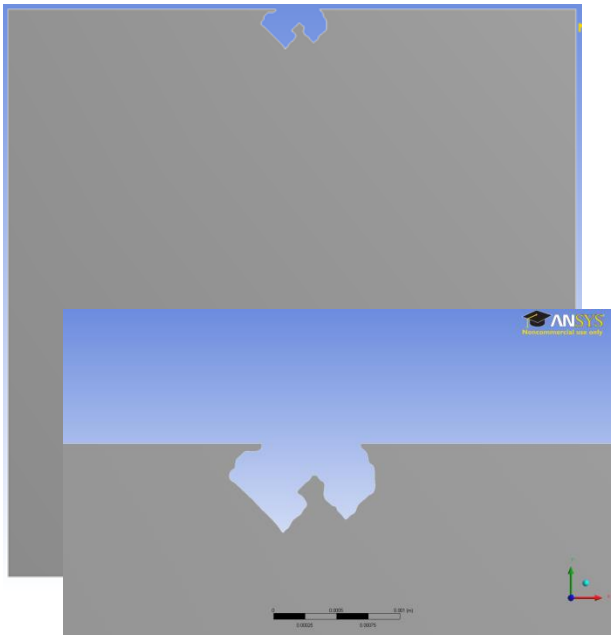
ANSYS
Noncommercial use only

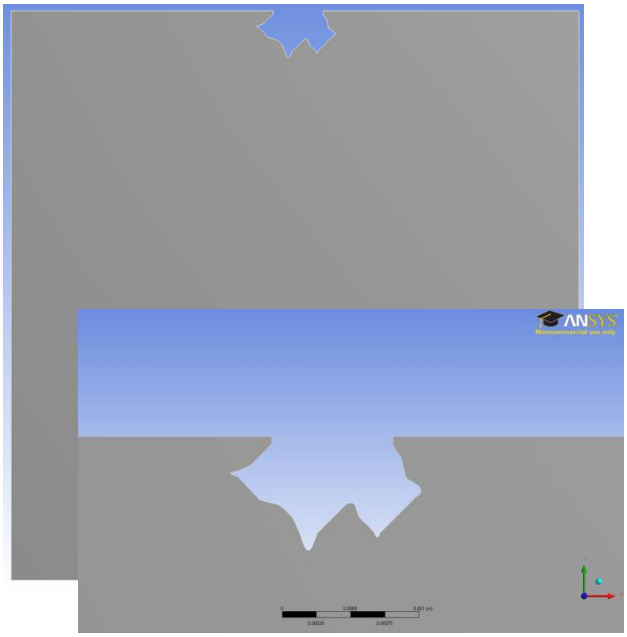
ANSYS
Noncommercial use only

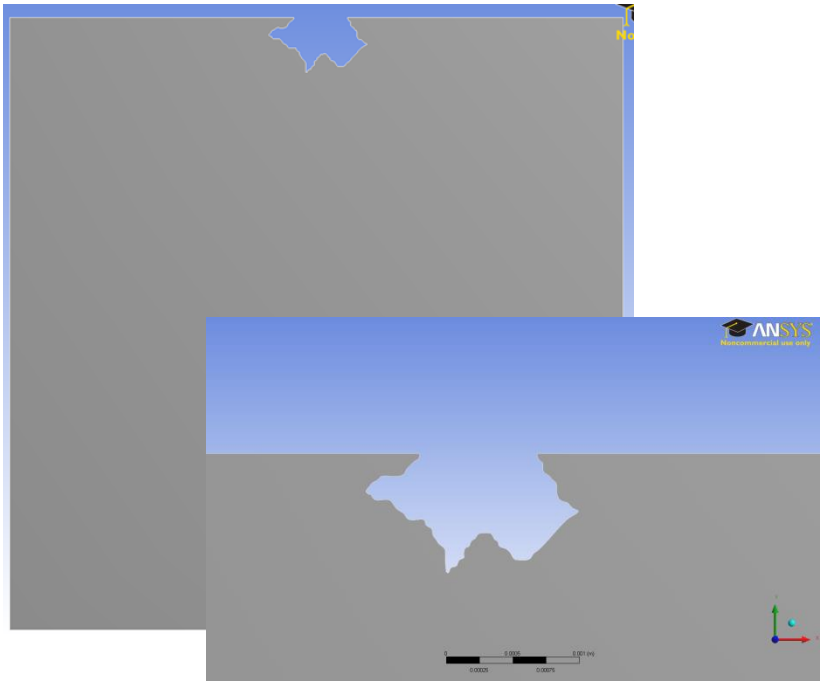
ANSYS
Noncommercial use only

1.4. Model of case in Figure 4.1 (c)

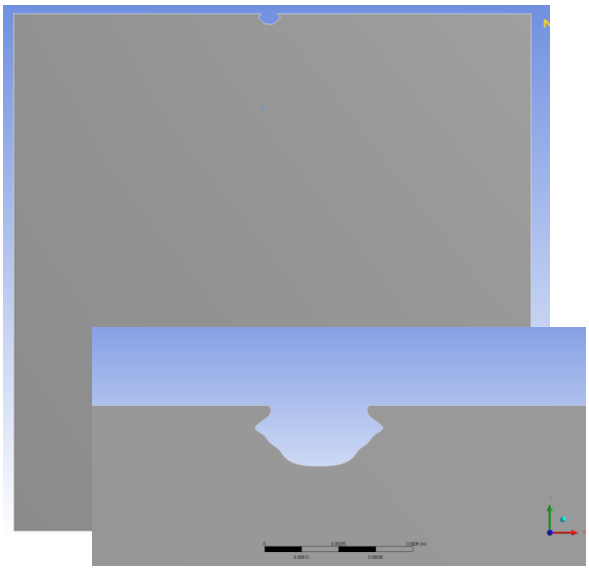

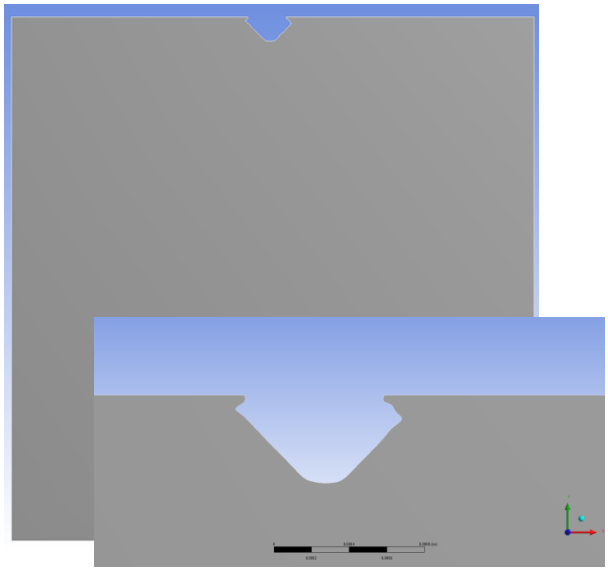

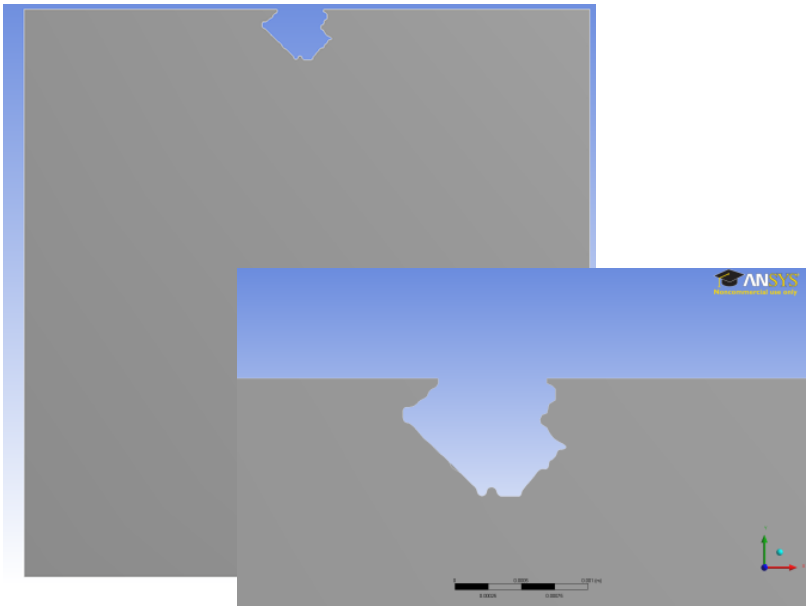

1.5. Model of case in Figure 4.1 (e)

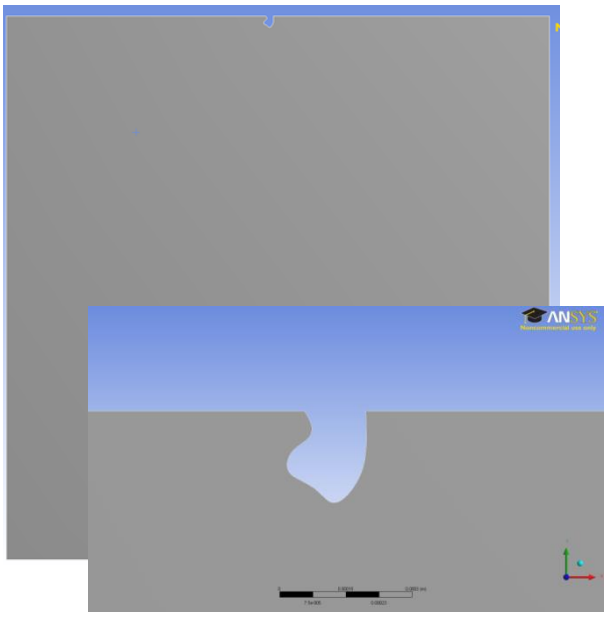

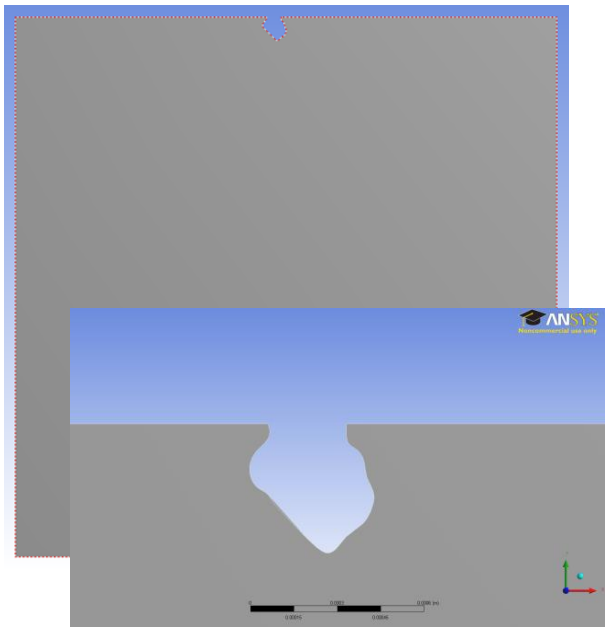

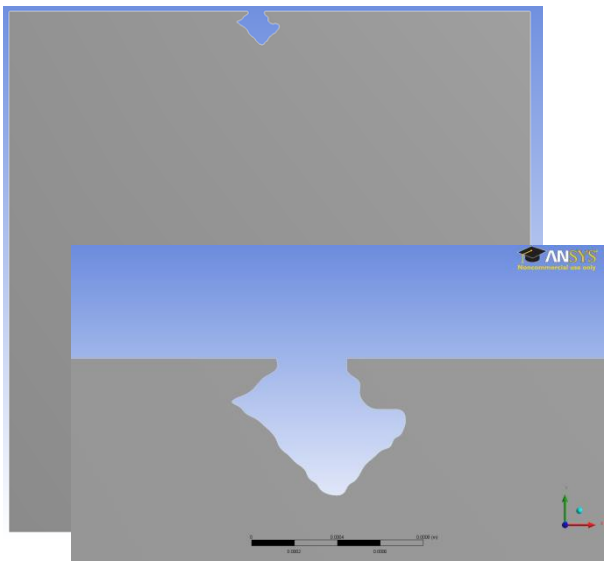

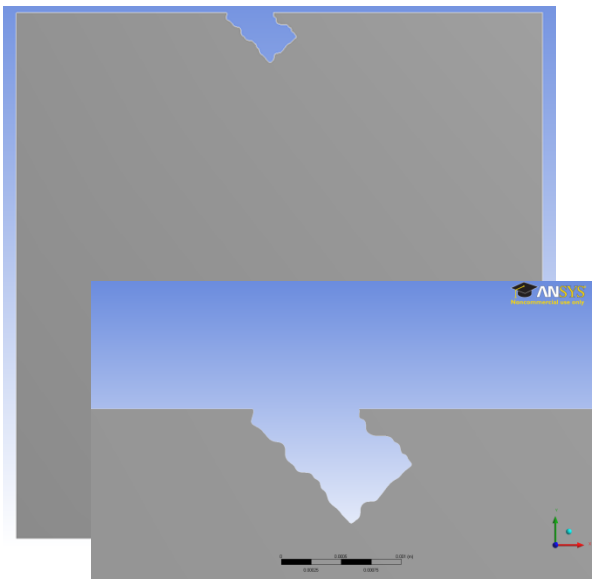

2. Mesh of The Models

2.1. Mesh of models of case in Figure 4.1 (a)

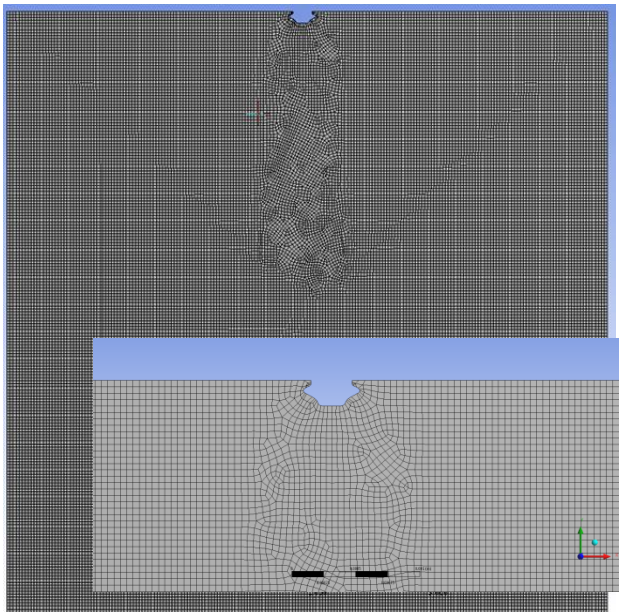

Number of elements: 40381

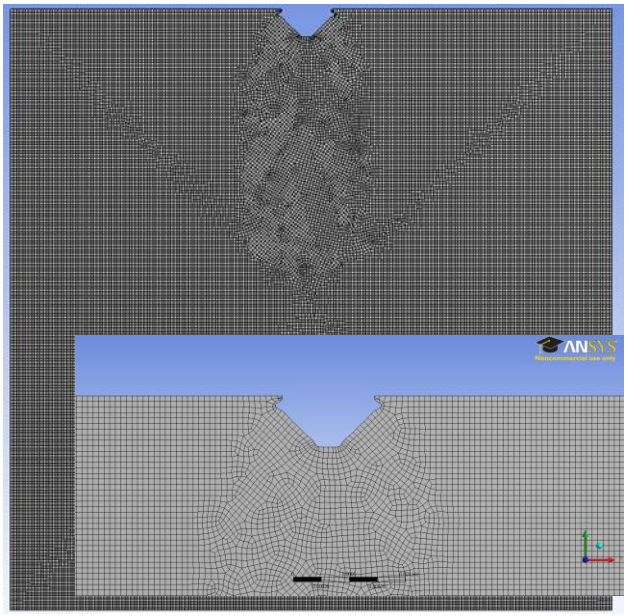

Number of elements: 41004

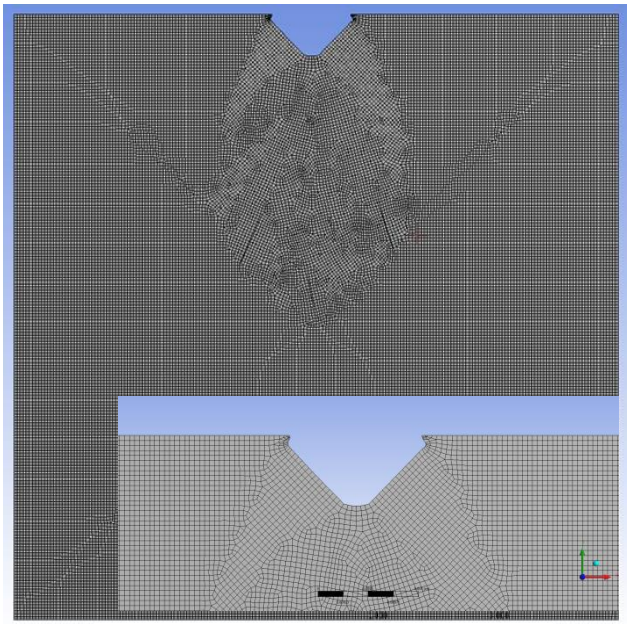

Number of elements: 40910

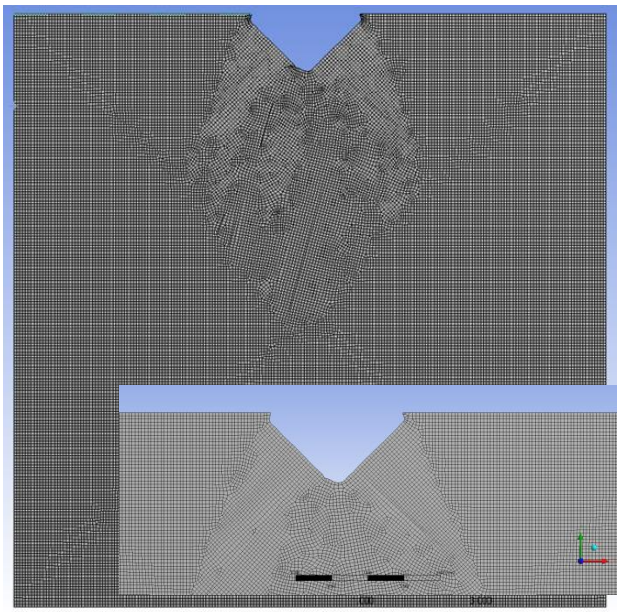

Number of elements: 40905

2.3. Mesh of models of case in Figure 4.1 (b)

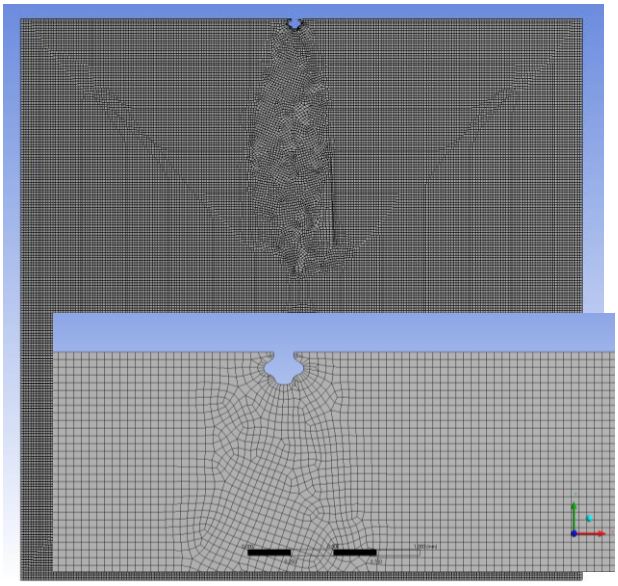

Number of elements: 56986

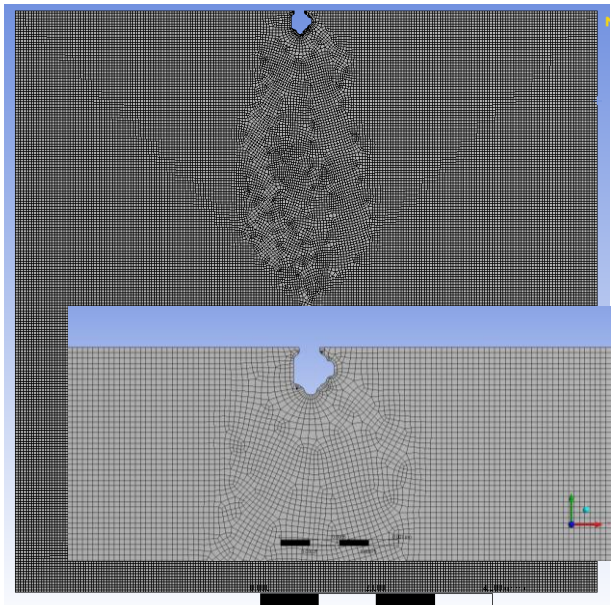

Number of elements: 50172

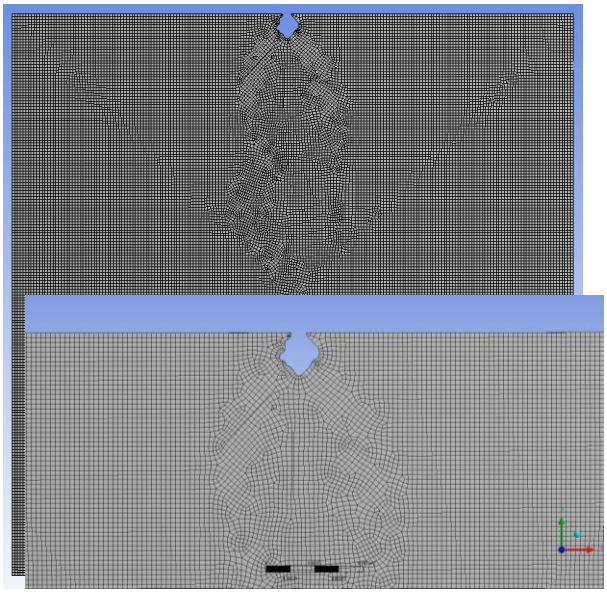

Number of elements: 41379

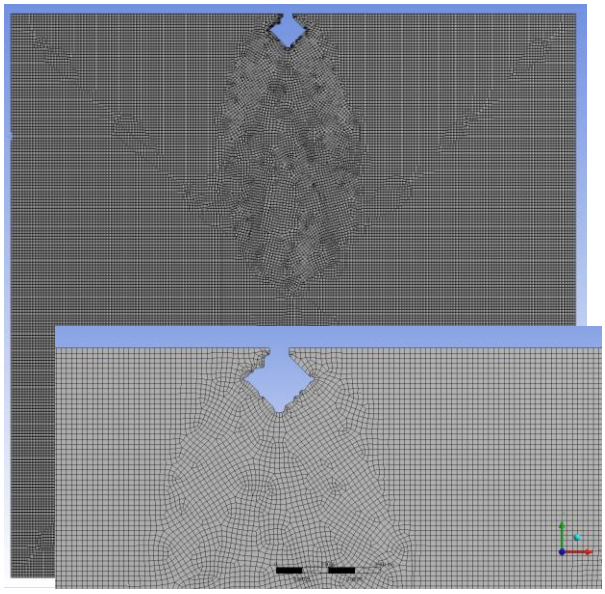

Number of elements: 42369

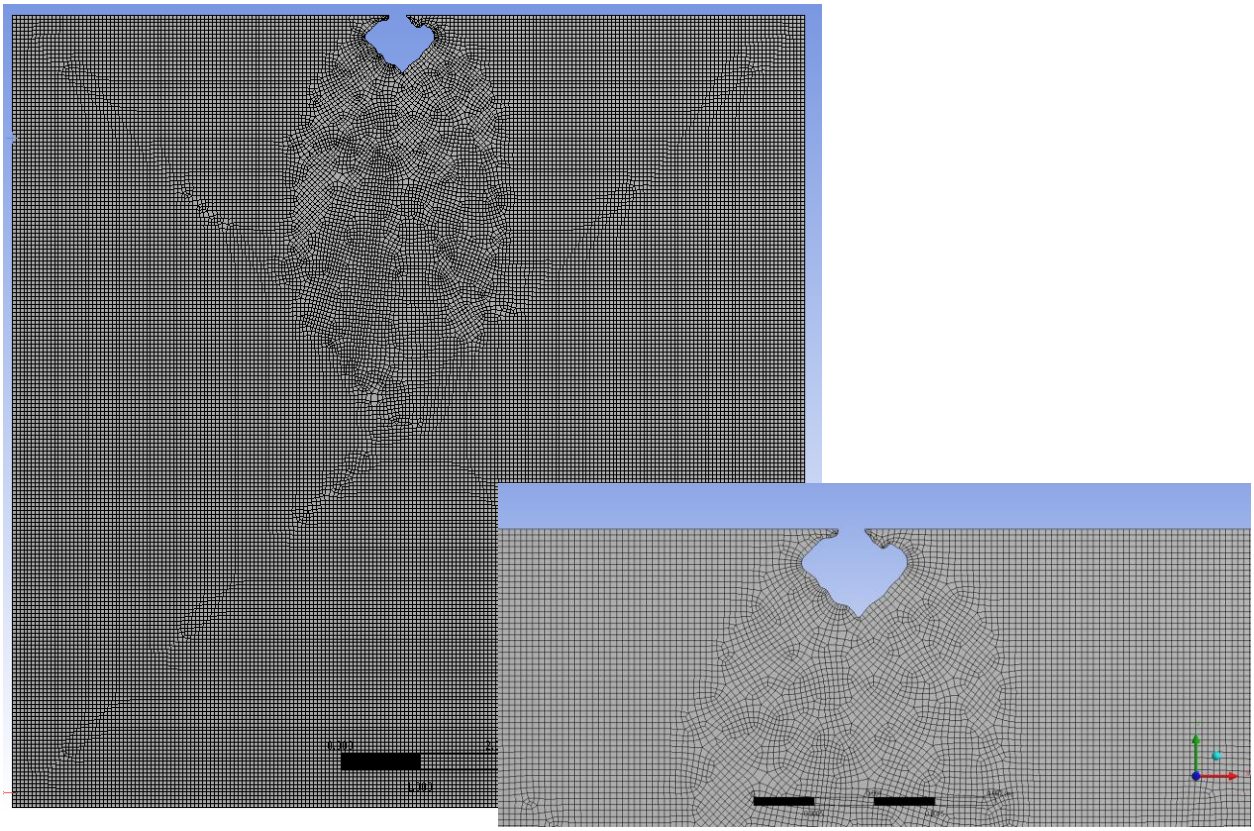

Number of elements: 42063

2.3. Mesh of models of case in Figure 4.1 (c)

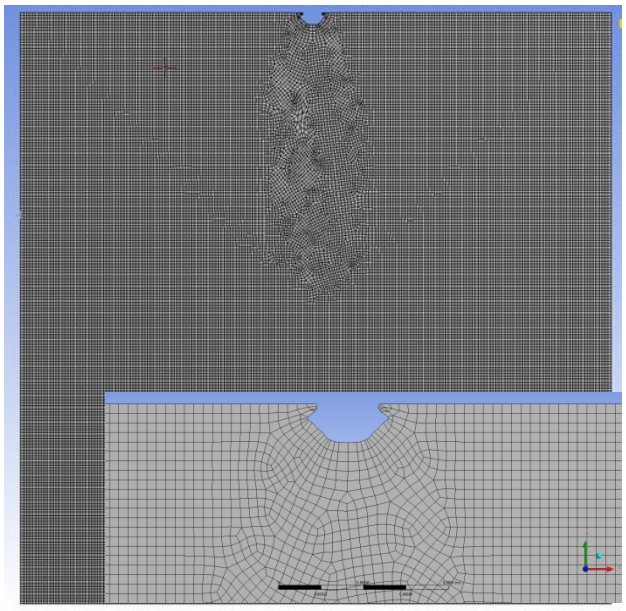

Number of elements: 40350

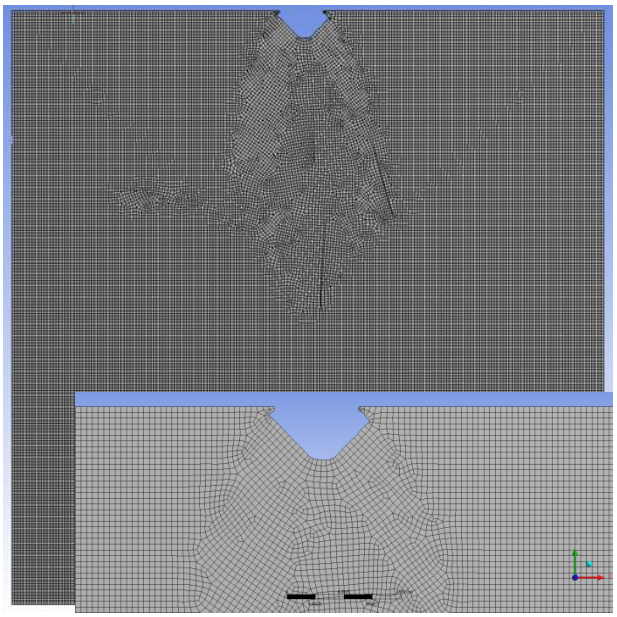

Number of elements: 40380

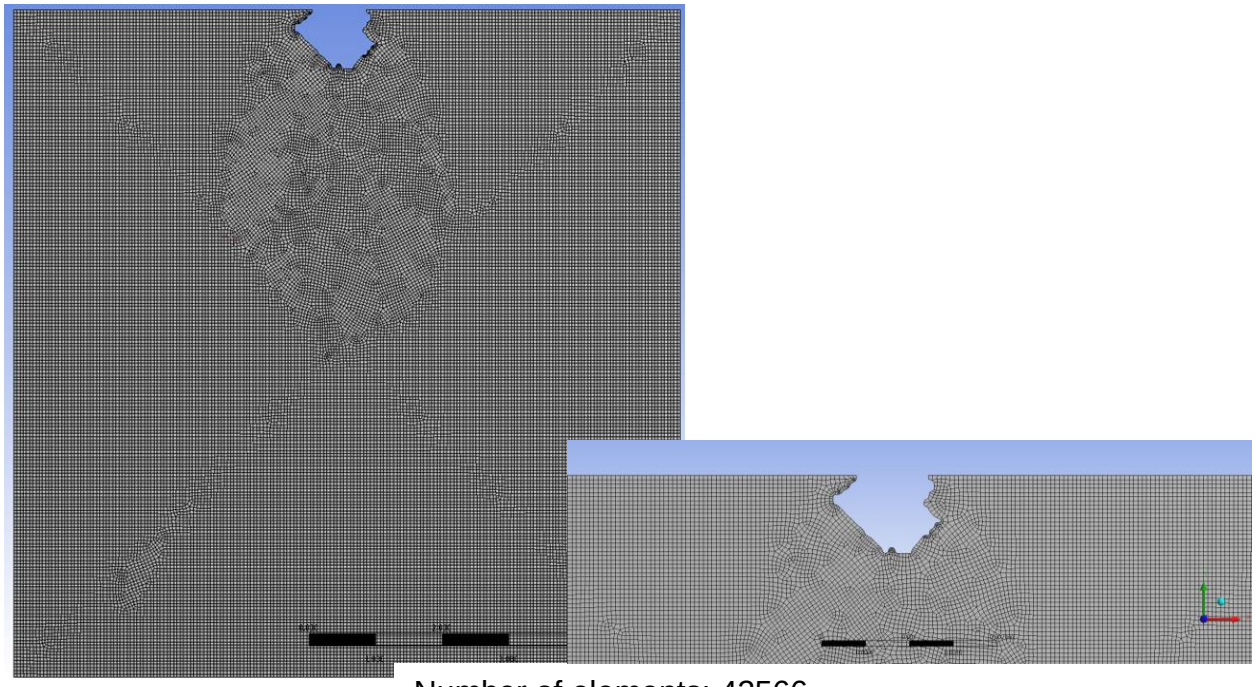

Number of elements: 42566

2.3. Mesh of models of case in Figure 4.1 (d)

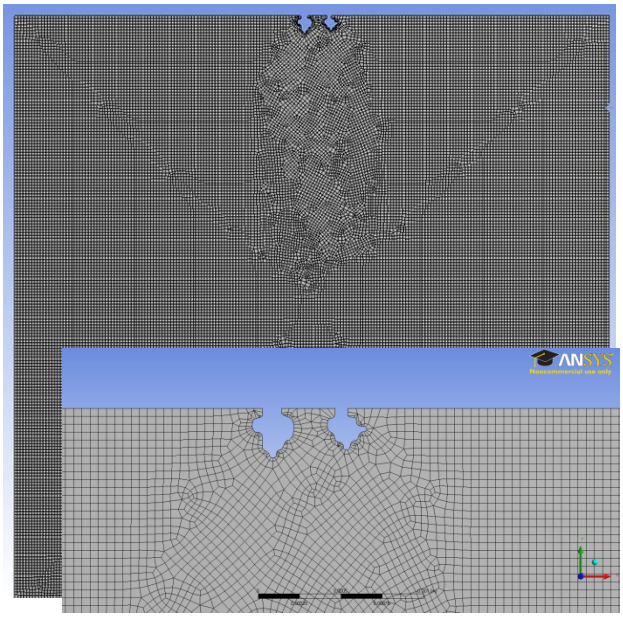

Number of elements: 42770

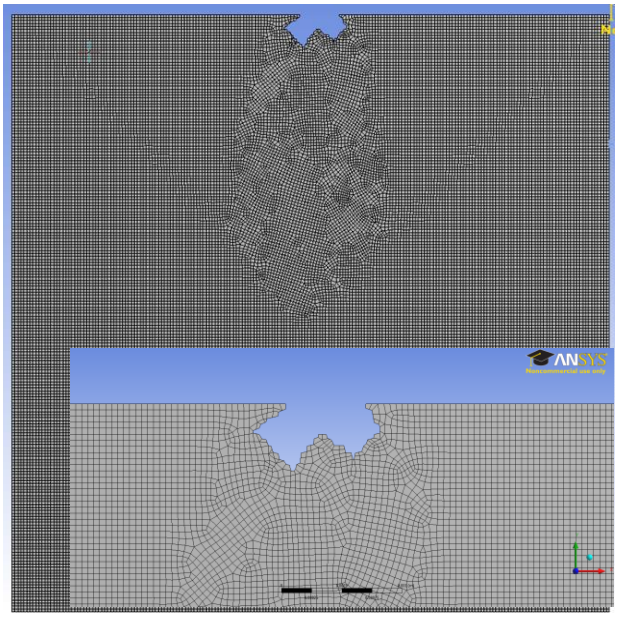

Number of elements: 40381

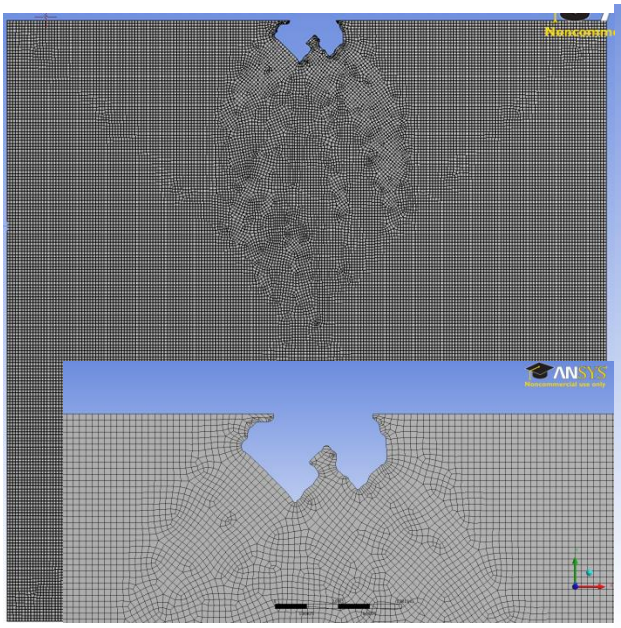

Number of elements: 42814

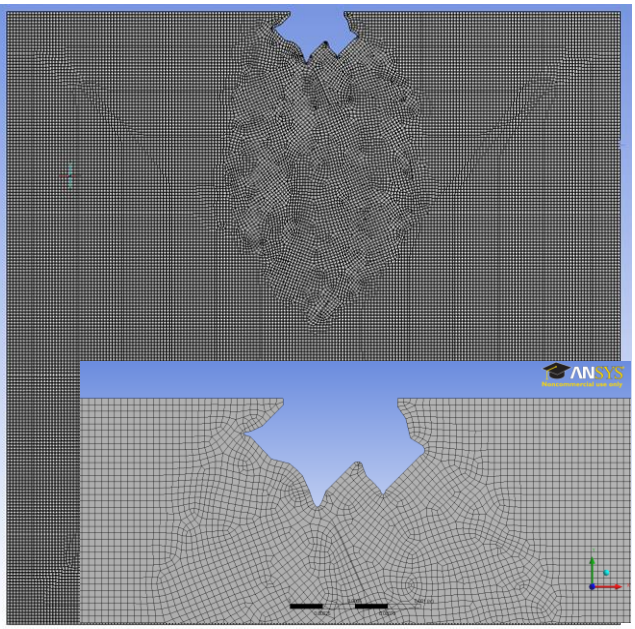

Number of elements: 41459

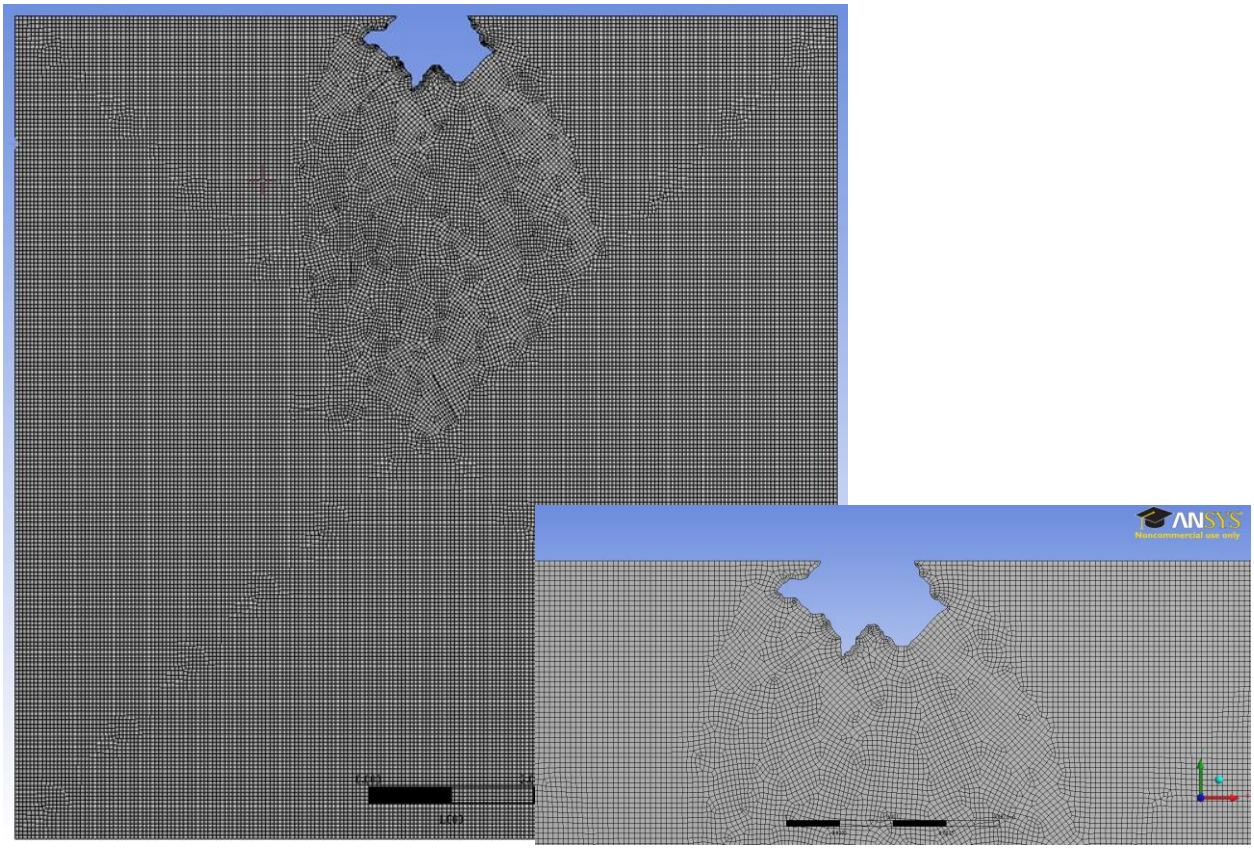

Number of elements: 43336

2.4. Mesh of models of case in Figure 4.1 (e)

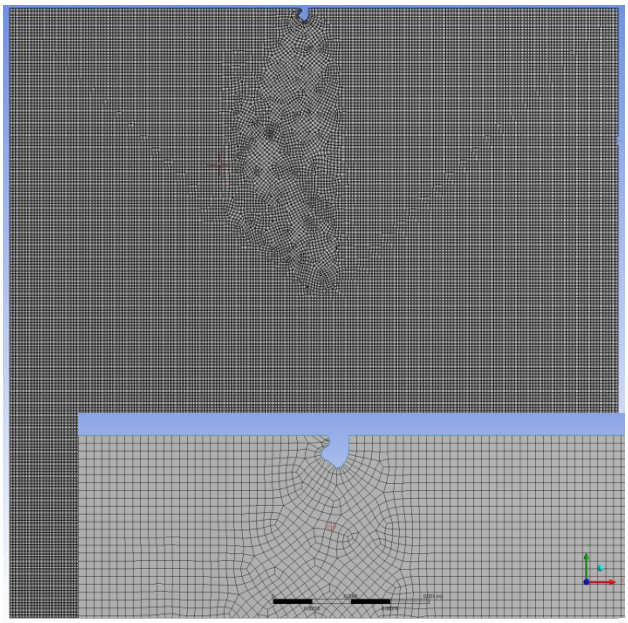

Number of elements: 40353

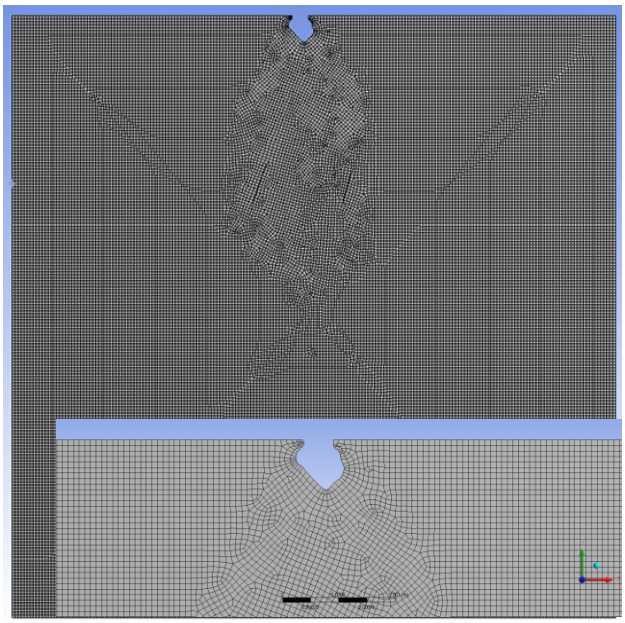

Number of elements: 41125

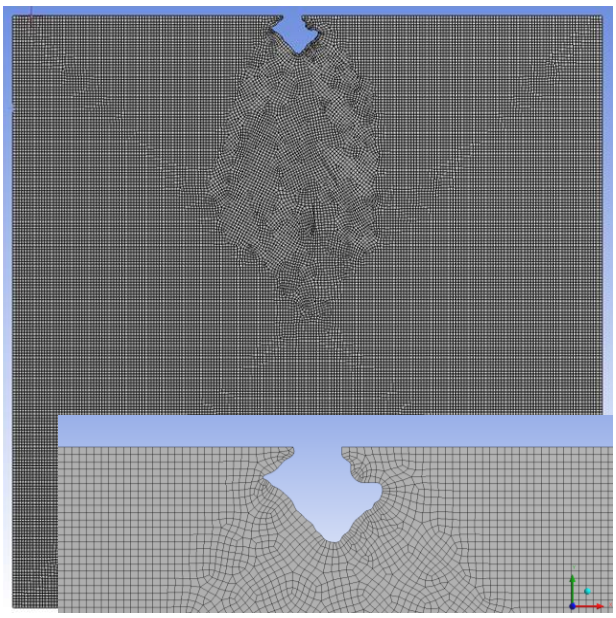

Number of elements: 41805

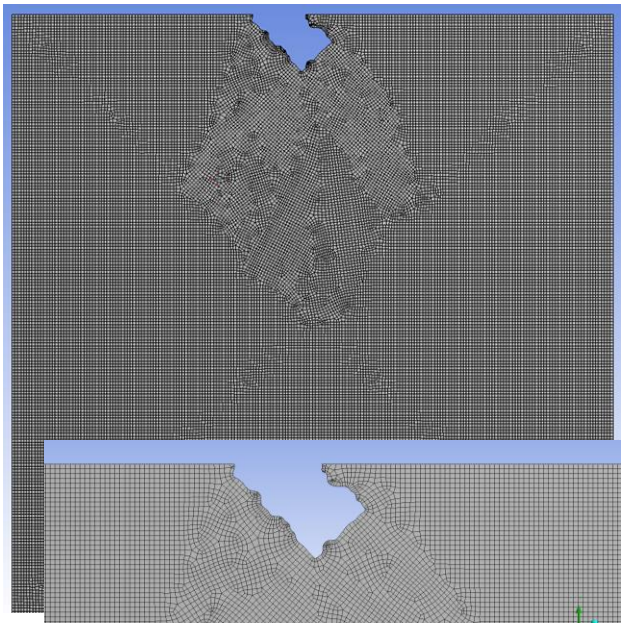

Number of elements: 42367

3. Stress Distribution (Von Misses)

3.1. Stress distribution for case in Figure 4.1 (a)

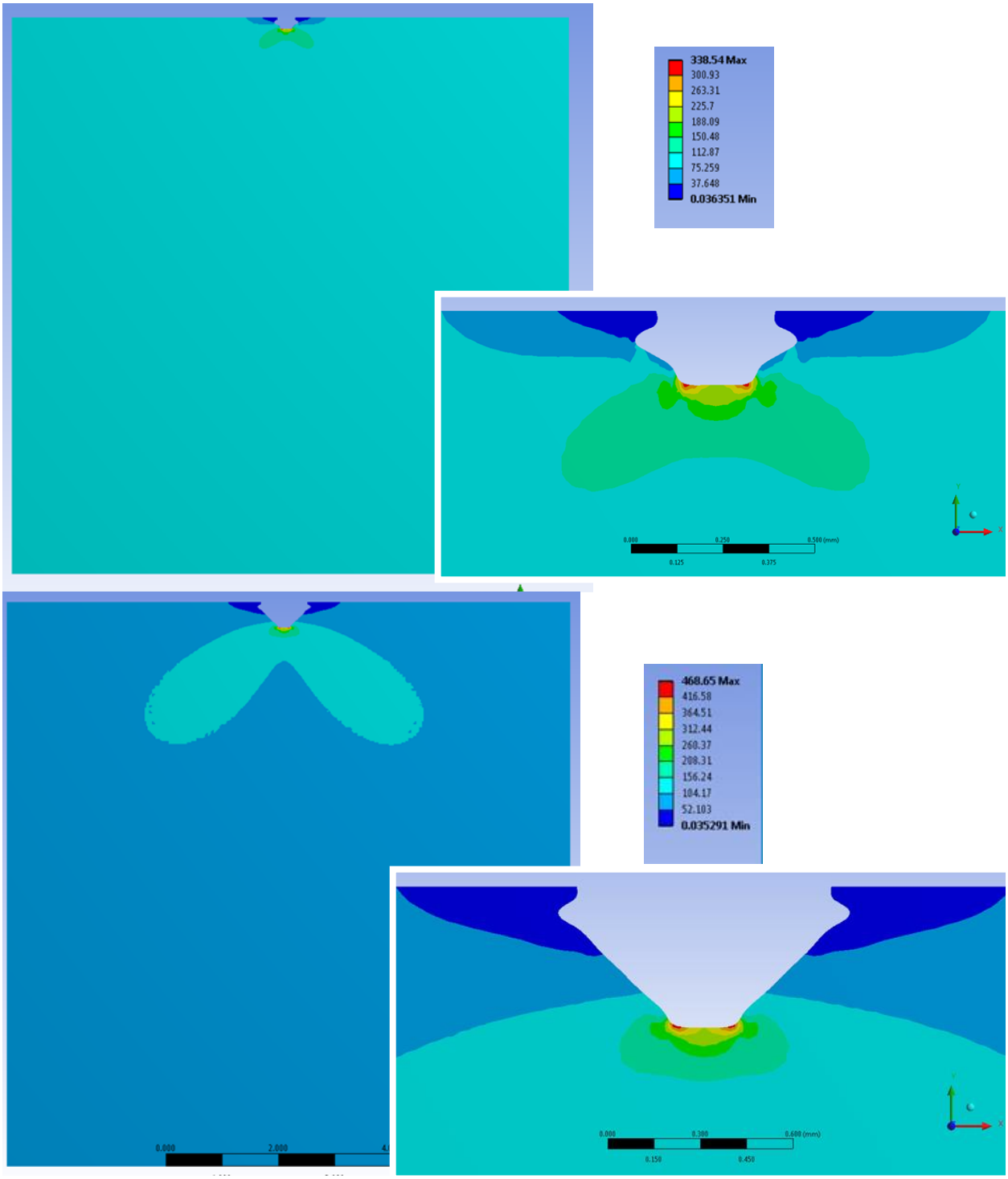

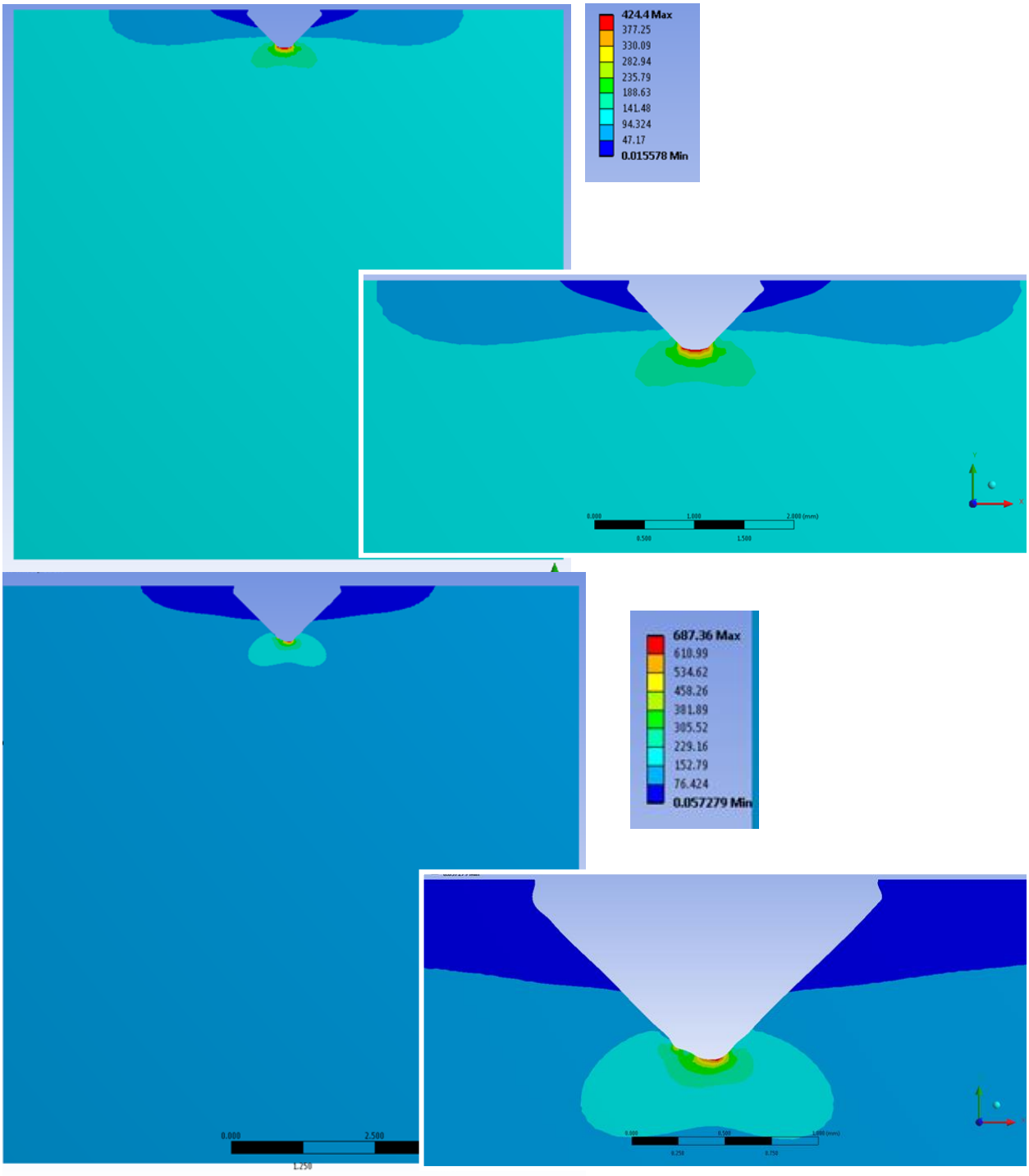
424.4 Max
377.25
330.09
282.94
235.79
188.63
141.48
94.324
47.17
0.015578 Min
687.36 Max
610.99
534.62
458.26
381.89
305.52
229.16
152.79
76.424
0.057279 Min

3.2. Stress distribution for case in Figure 4.1 (b)

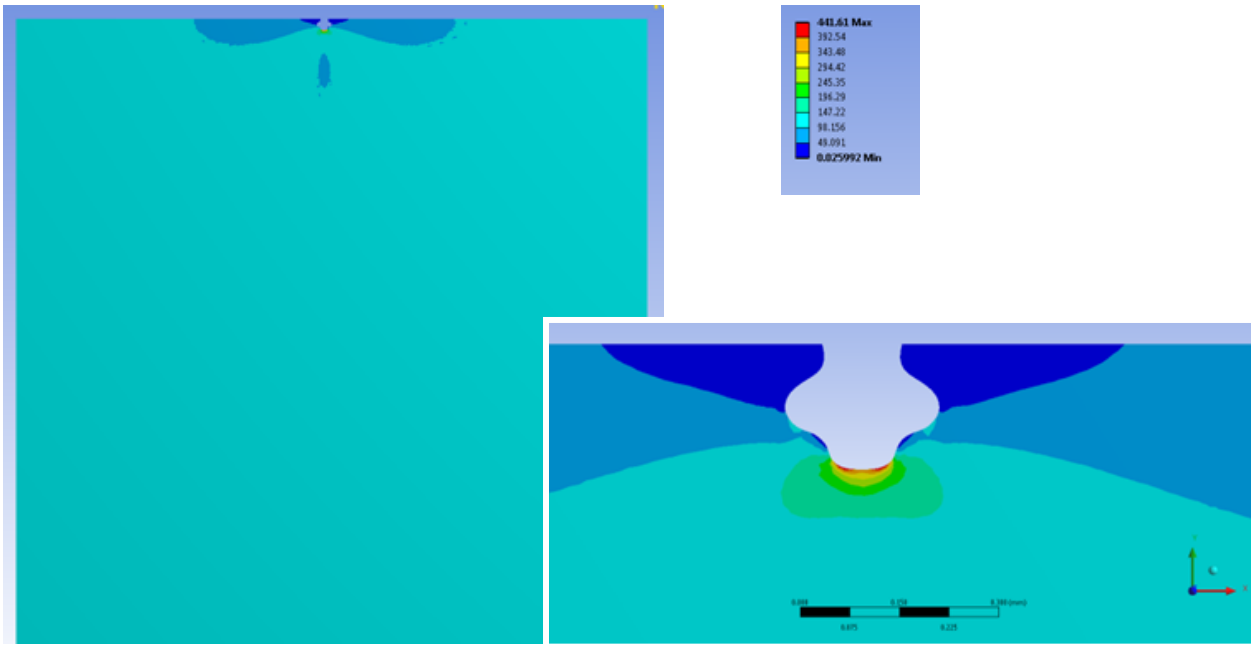

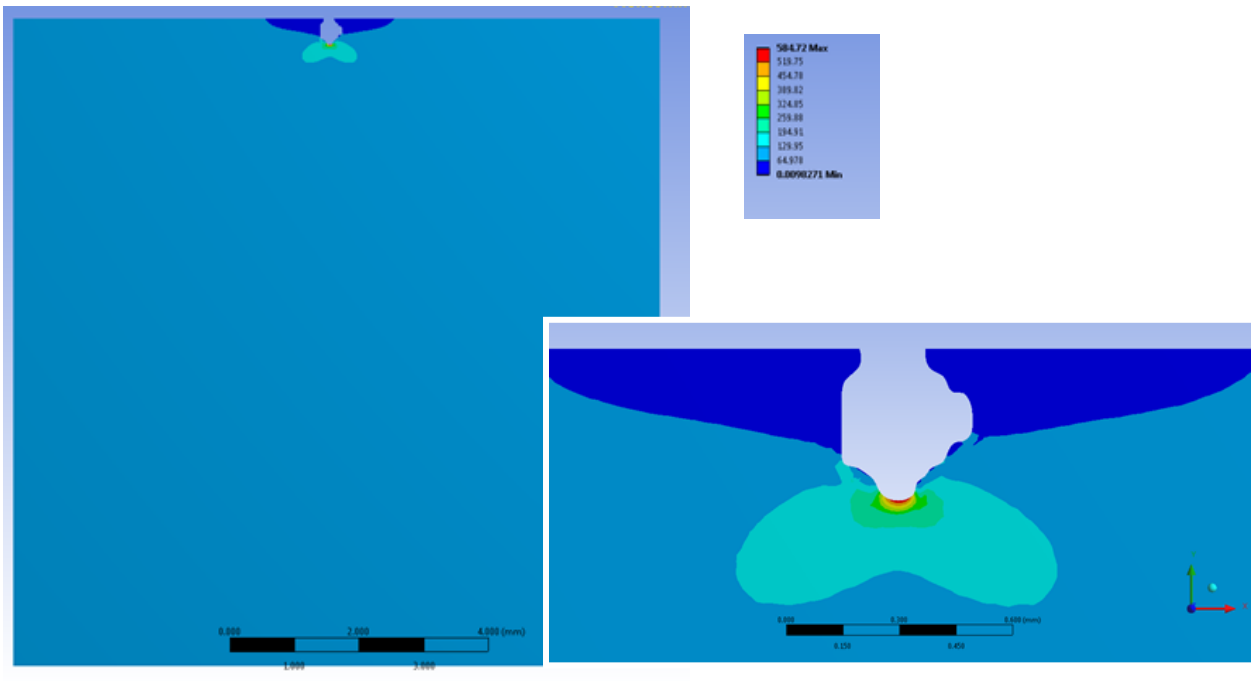

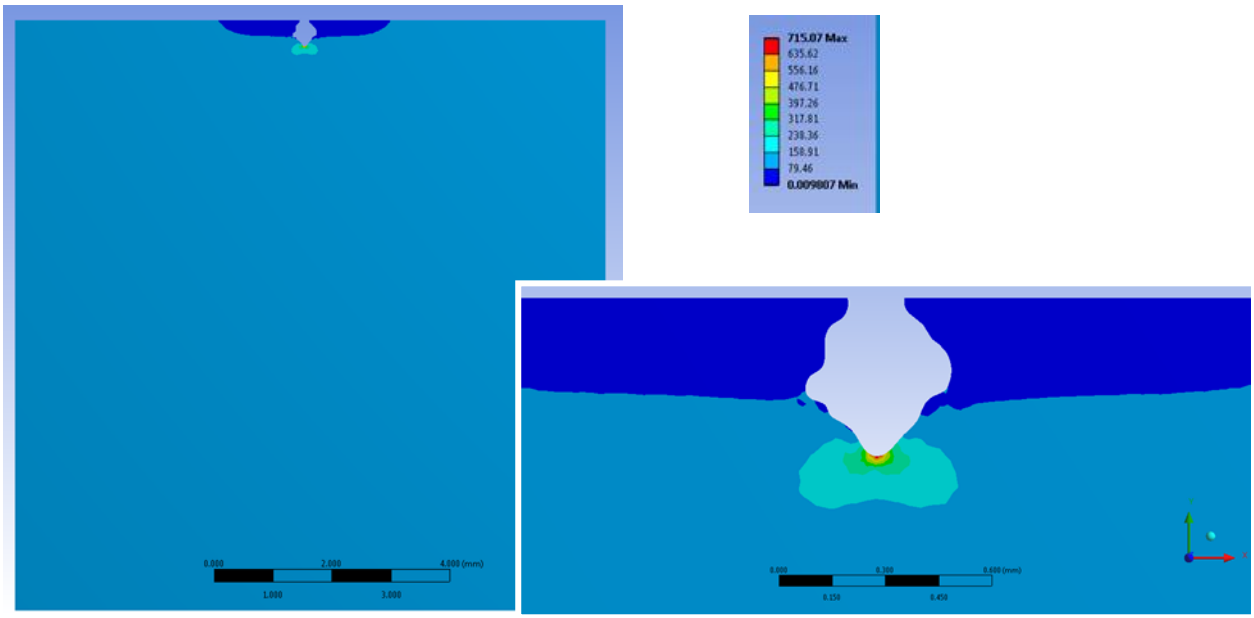
715.07 Max
635.62
556.16
476.71
397.26
317.81
238.36
158.91
79.46
0.009807 Min

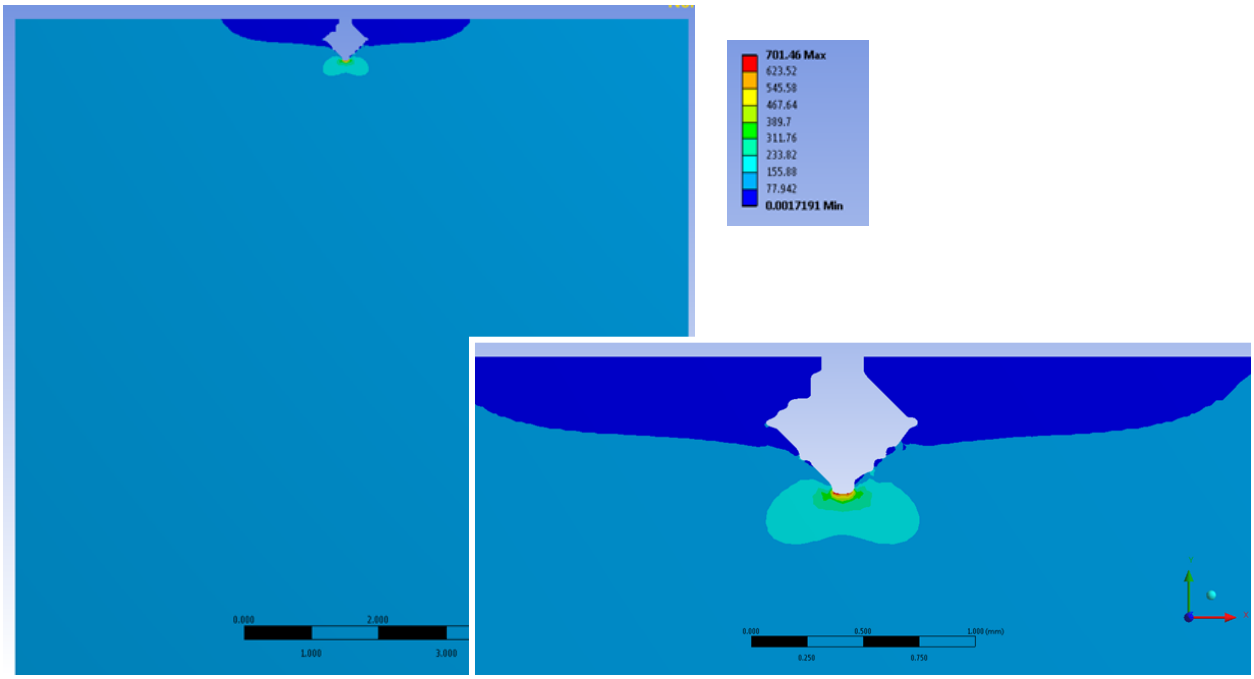
701.46 Max
623.52
545.58
467.64
389.7
311.76
233.82
155.88
77.942
0.0017191 Min

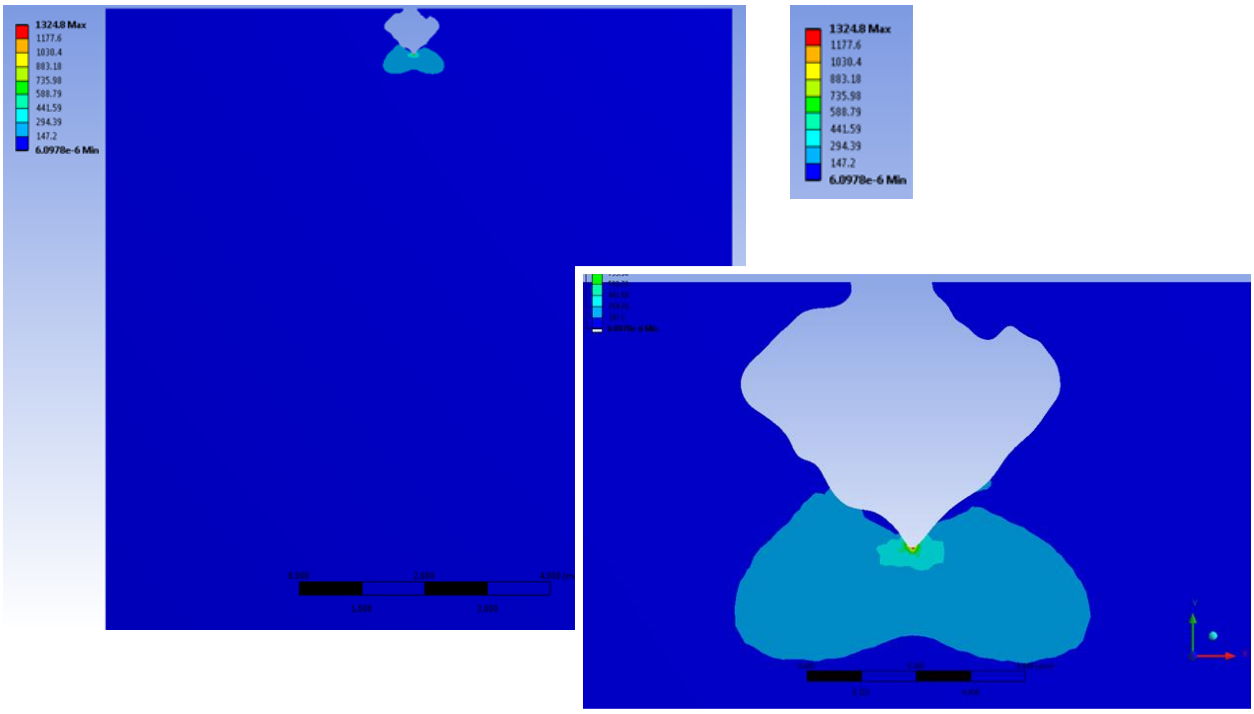

3.3. Stress distribution for case in Figure 4.1 (c)

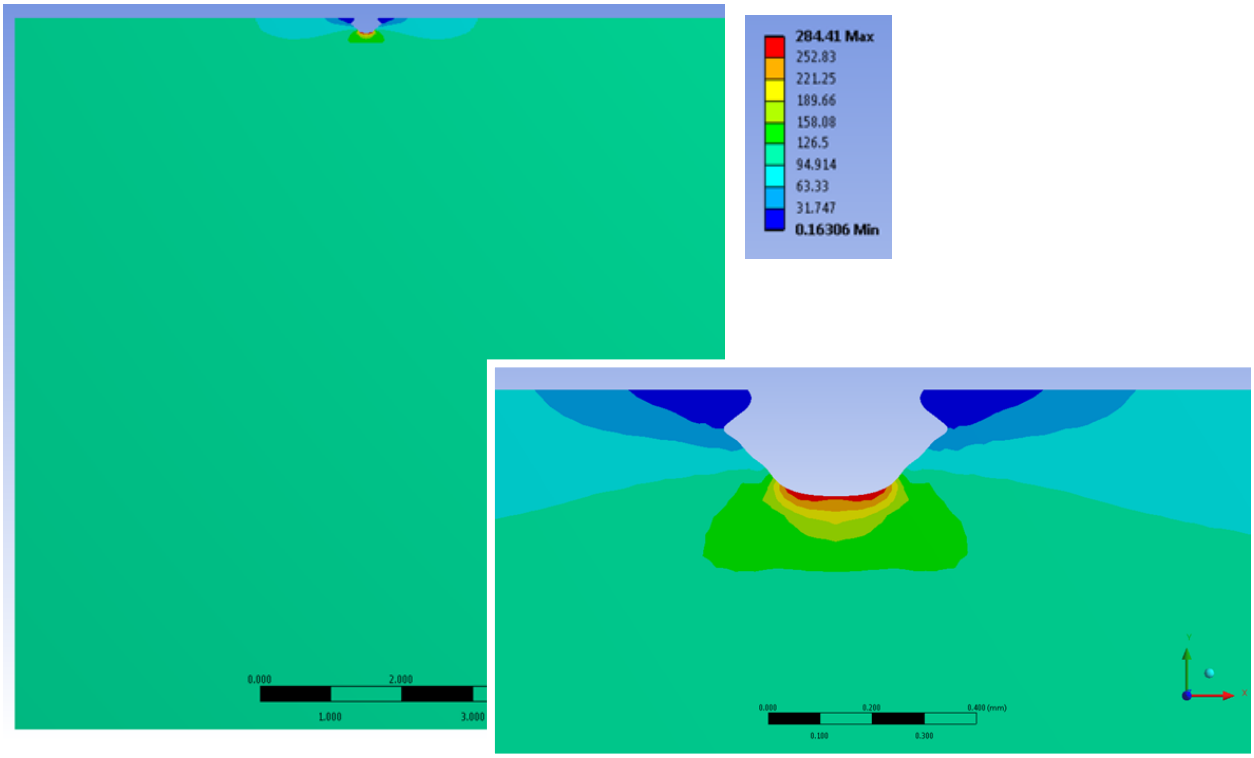

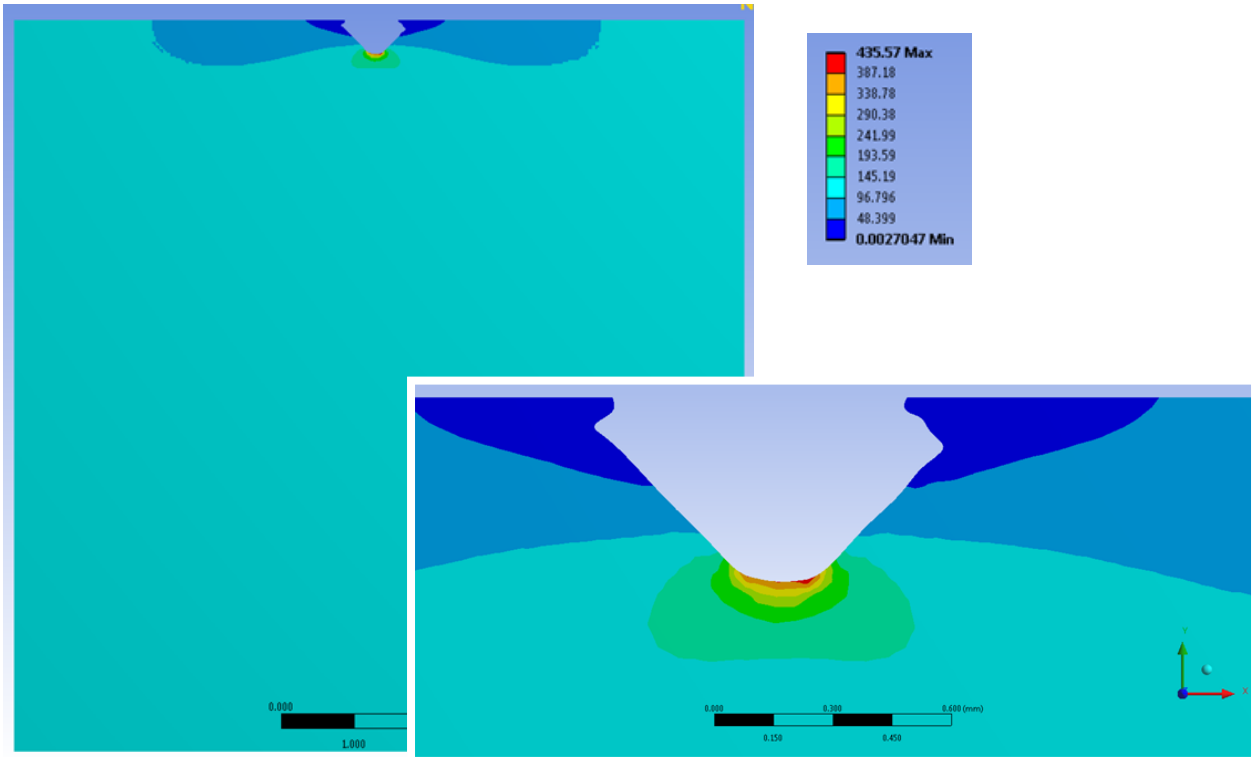
435.57 Max
387.18
338.78
290.38
241.99
193.59
145.19
96.796
48.399
0.0027047 Min

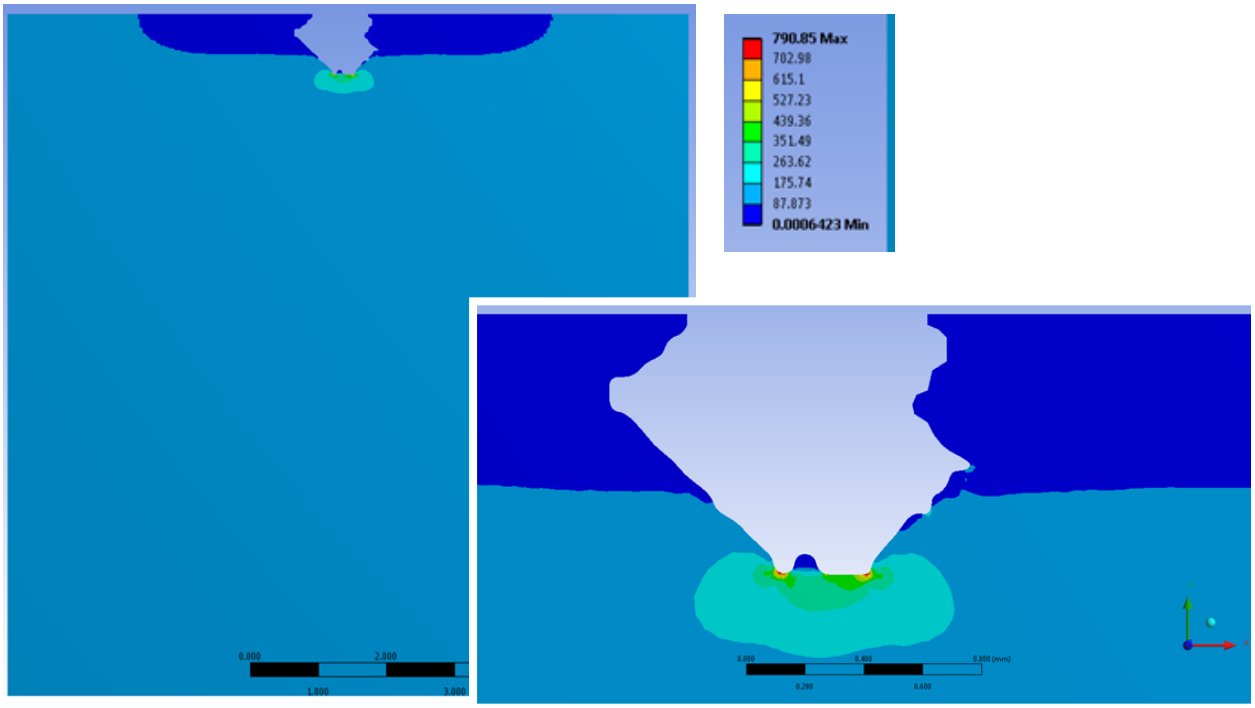
790.85 Max
702.98
615.1
527.23
439.36
351.49
263.62
175.74
87.873
0.0006423 Min

3.4. Stress distribution for case in Figure 4.1 (d)

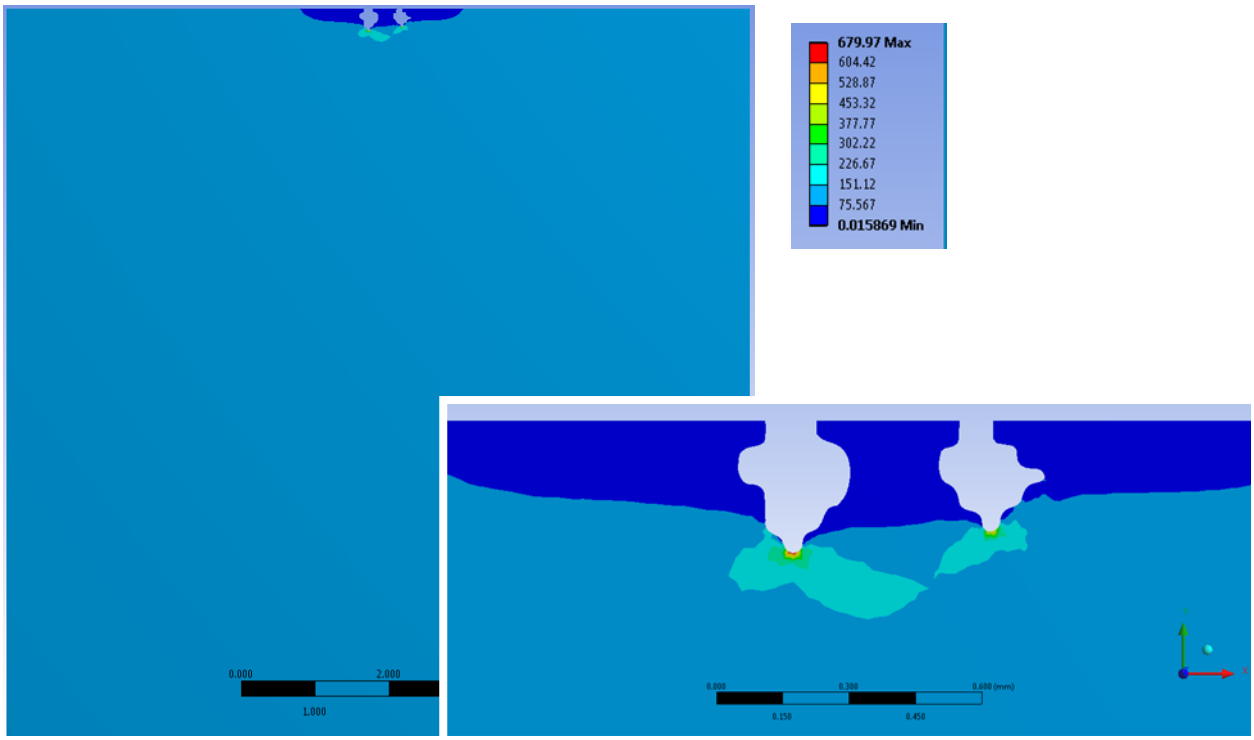

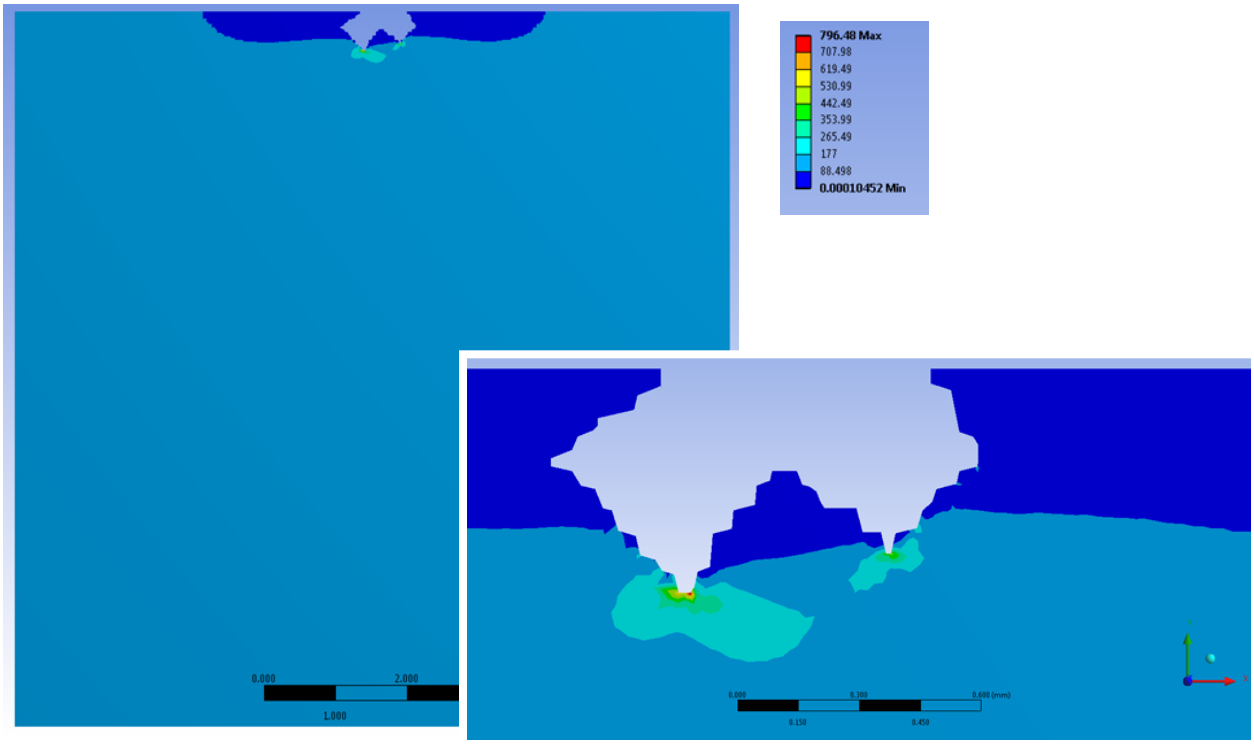

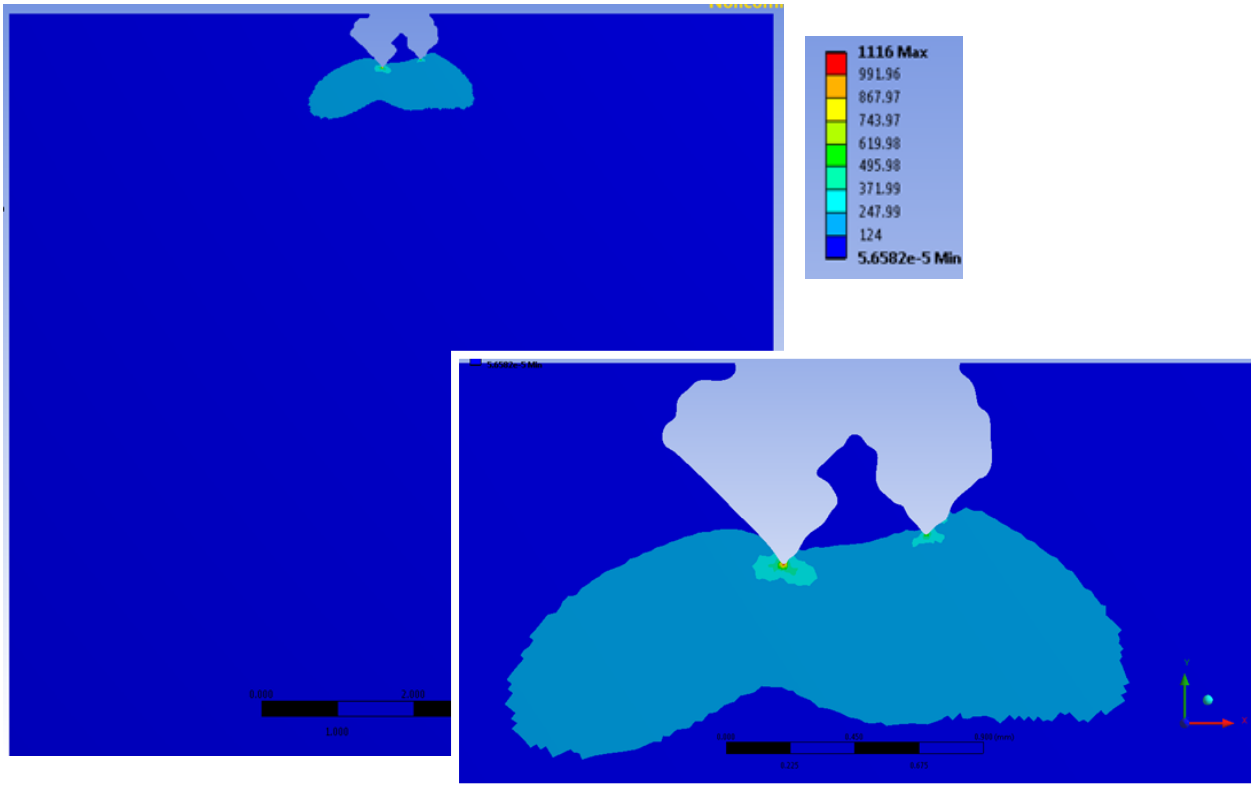
1116 Max
991.96
867.97
743.97
619.98
495.98
371.99
247.99
124
5.6582e-5 Min

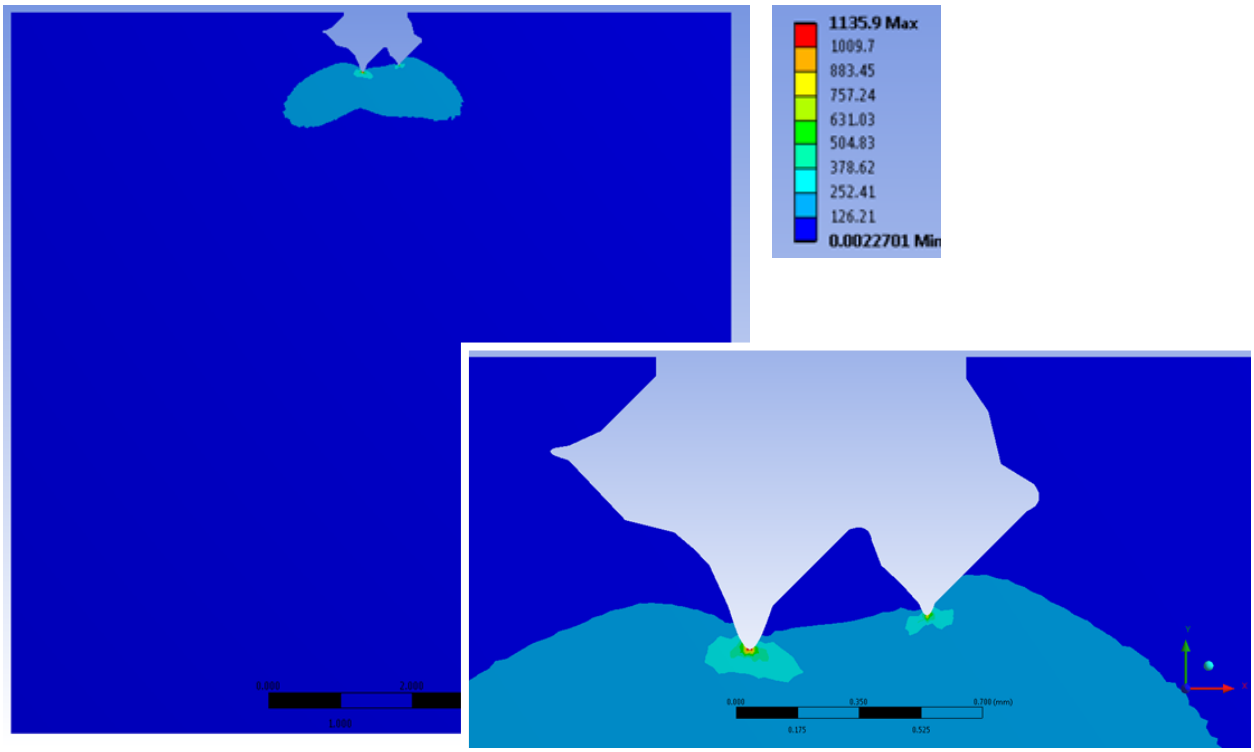
1135.9 Max
1009.7
883.45
757.24
631.03
504.83
378.62
252.41
126.21
0.0022701 Min

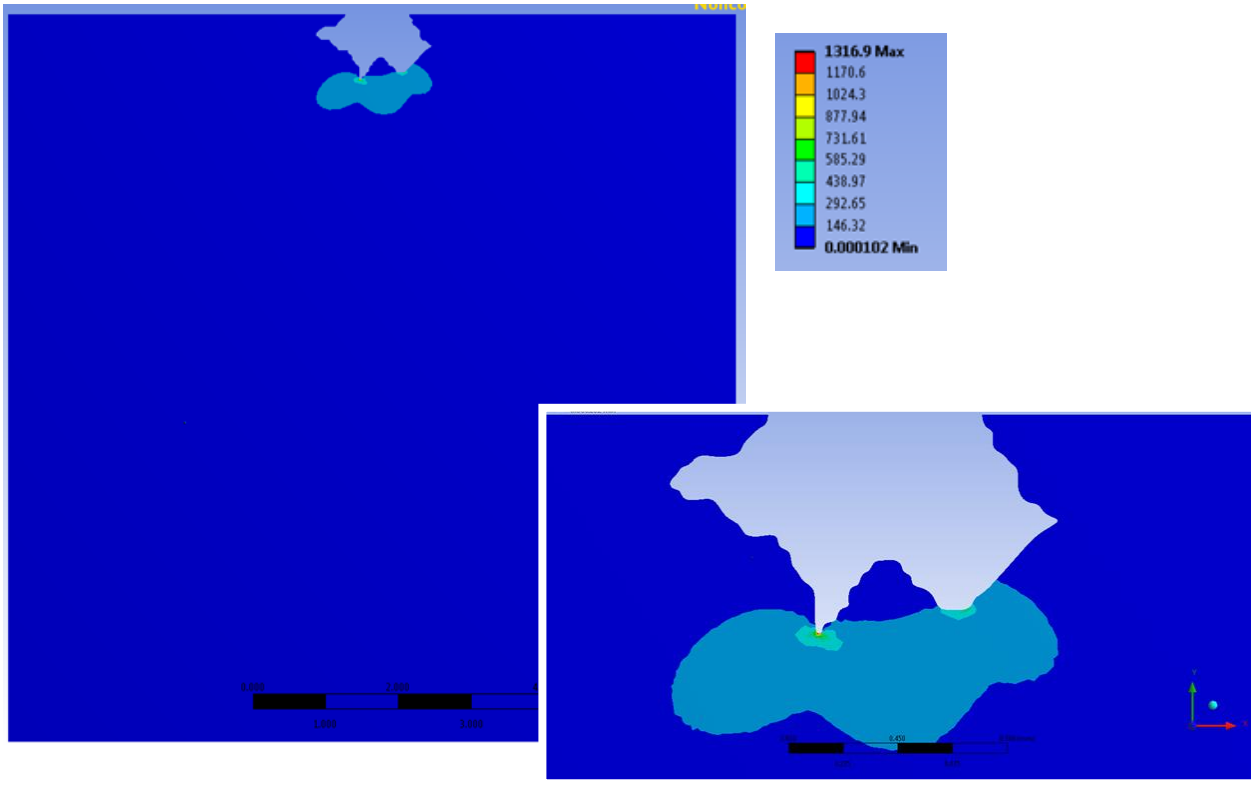

3.5. Stress distribution for case in Figure 4.1 (e)

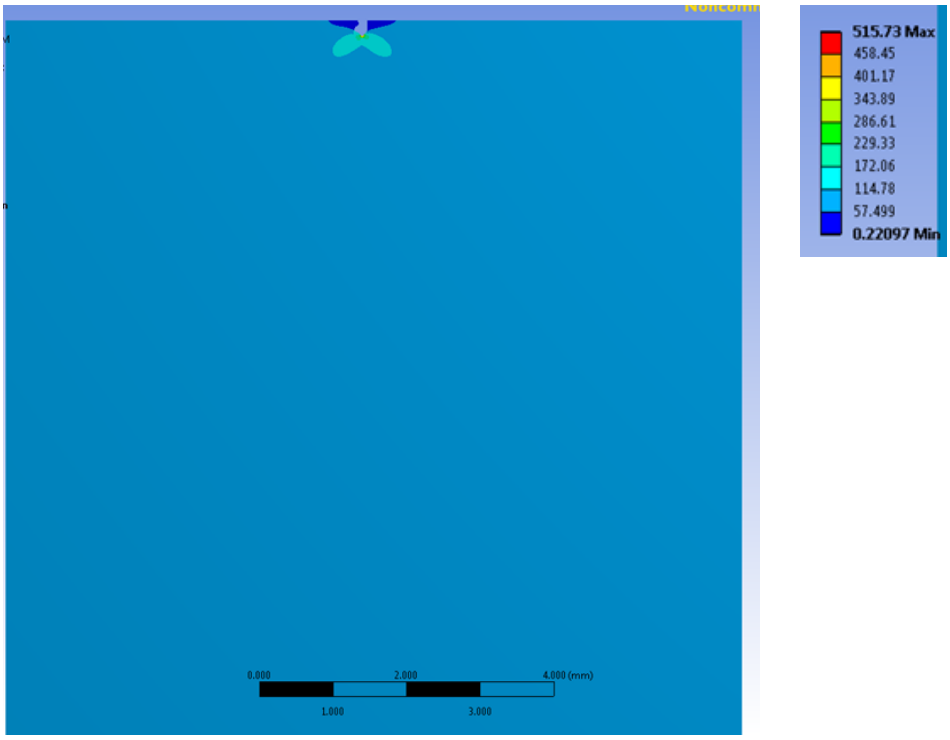

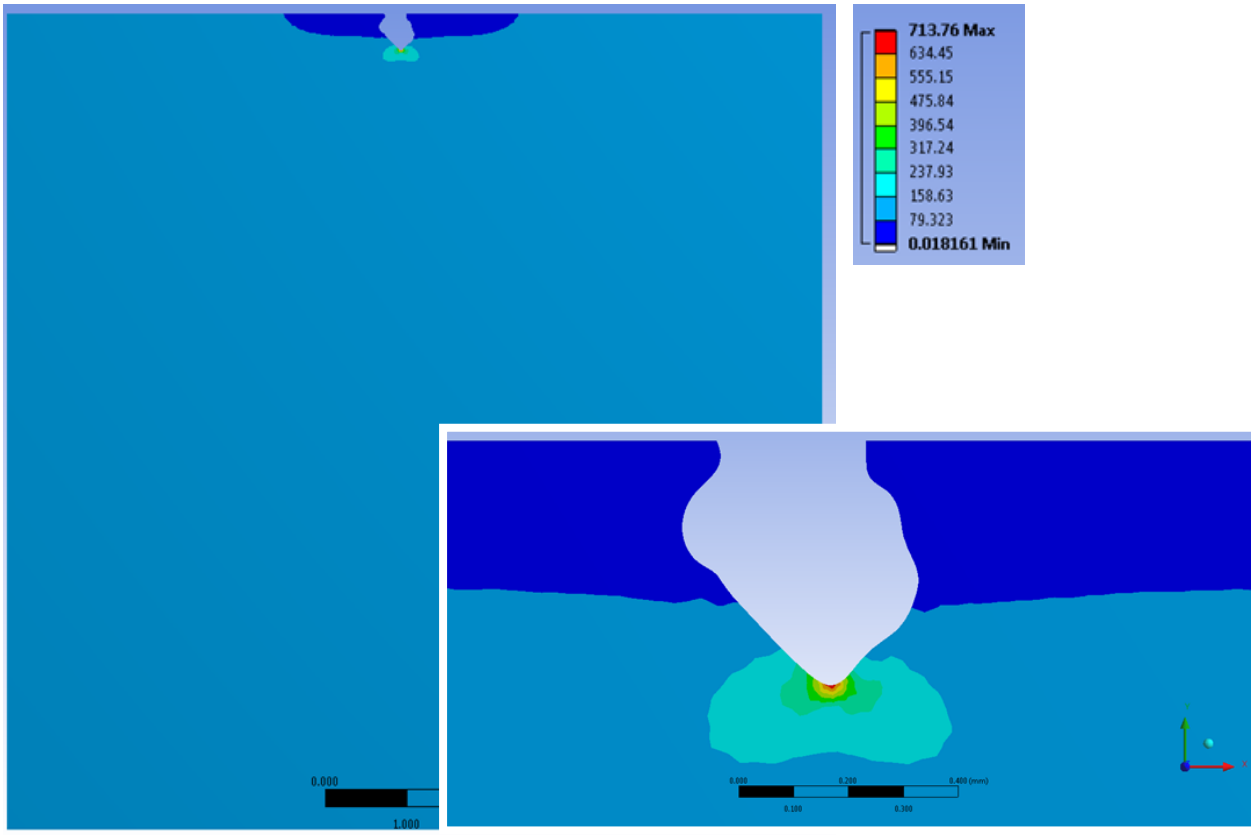
713.76 Max
634.45
555.15
475.84
396.54
317.24
237.93
158.63
79.323
0.018161 Min
0.000
1.000

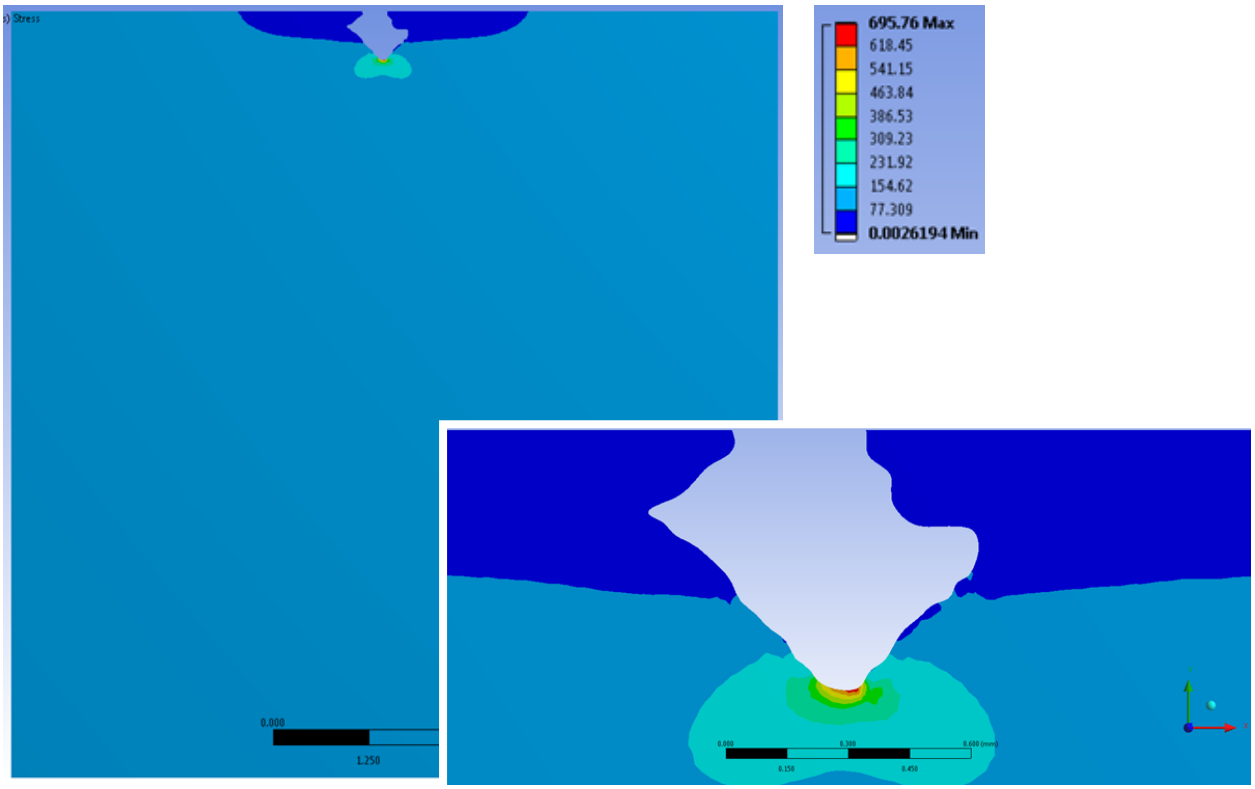
695.76 Max
618.45
541.15
463.84
386.53
309.23
231.92
154.62
77.309
0.0026194 Min
0.000
1.250

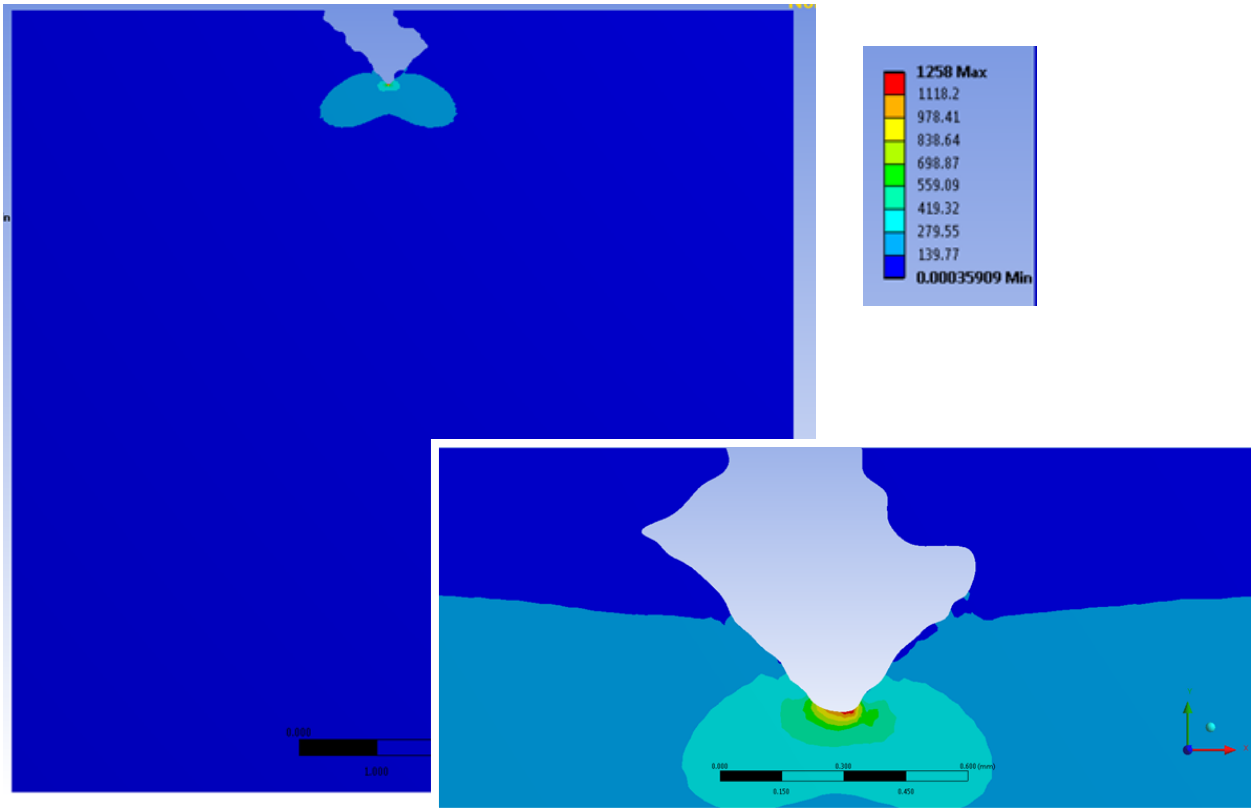
1258 Max
1118.2
978.41
838.64
698.87
559.09
419.32
279.55
139.77
0.00035909 Min

VITA

PERSONAL INFORMATION

Date of Birth: June 21, 1985

Birthplace: Banda Aceh, Indonesia

Nationality: Indonesia

Email: israr.np@gmail.com

EDUCATION

2011-2013 **Virginia Commonwealth University**, Richmond, VA

Master of Science

Field of study: Mechanical Engineering

Current GPA: 3.24/4.00

Thesis topic: “Computational Modeling of Pitting Corrosion”

Expected graduation: August 2013

2003–2009 **Syiah Kuala University**, Indonesia

Bachelor of Engineering

Field of study: Mechanical Engineering

GPA: 3.25/4.00

WORK EXPERIENCE

March 2009 – November 2010

Syiah Kuala University, Corrosion Lab

Research Assistant of a research project under National Strategic Research Fund (Indonesia) entitled “Application of Boundary Element Method for Analysis of Public Building Corrosion Risk Associated with 2004 Tsunami Disaster”

PUBLICATION

- Syarizal Fonna, M. Ridha, Syifaul Huzni, Israr I., Ahmad Kamal Ariffin, Boundary Element Inverse Analysis by Using Particle Swarm Optimization for Reinforced Concrete Corrosion Identification, Advanced Materials Research Vol 339 (2011), 171-175
- Israr BM Ibrahim, Ramana Pidaparti, Simulation Of Pitting Cavity Growth Using Cellular Automata, ASME Early Career Technical Conference, Georgia, USA, (2012)